Cláudia Marisa Monteiro Saraiva

Mestre em Bioquímica

MicroRNA-124-loaded nanoparticles as a new promising therapeutic tool for neural stem cell-based brain repair strategies

Dissertação para obtenção do Grau de Doutor
em Bioengenharia (MIT)

Orientador: Professora Doutora Liliana Bernardino, Universidade da Beira Interior
Co-orientadores: Professor Doutor Lino Ferreira, Universidade de Coimbra; Professor Doutor Manuel Nunes da Ponte, Universidade Nova de Lisboa.

Júri:

Presidente: Professor Doutor Fernando Santana, Universidade Nova de Lisboa.
Arguente(s): Professor Doutor Luís de Almeida, Universidade de Coimbra;
Doutor Ricardo Pires das Neves, Investigador CNC, Universidade de Coimbra.
Vogal(ais): Professora Doutora Liliana Bernardino, Universidade da Beira Interior;
Doutora Teresa Casimiro, investigadora principal – LAQV/REQUIMTE, Universidade Nova de Lisboa;
Doutor Karsten Ruscher, Invesigador BMC, Universidade de Lund, Suécia;
Professora Doutora Paula Alves, Universidade Nova de Lisboa.

FACULDADE DE CIÊNCIAS E TECNOLOGIA
UNIVERSIDADE NOVA DE LISBOA

Julho, 2017

Direitos de cópia • Copyright

Agradecimentos • Acknowledgements

Após uma longa (por vezes atribulada) caminhada dou como concluída mais uma etapa da minha vida profissional e, não poderia deixar de agradecer a todos os que de uma forma directa ou indirecta contribuíram para o sucesso deste projecto.

Começo por agradecer ao MIT-Portugal por me dar a oportunidade de integrar o Programa Doutoral em Bioengenharia de Sistemas, por todos os ensinamentos que me transmitiu sempre de olhos postos no futuro e na inovação sustentável, mas acima de tudo pela rede de contactos que me permitiu estabelecer. Obrigada a todos e, em especial ao Doutor Manuel Nunes da Ponte pela sua co-orientação, disponibilidade e, auxílio sempre que necessário.

À Profª. Doutora Liliana Bernardino, que um pouco "às cegas" me aceitou como sua orientanda, o meu mais sincero obrigada. Obrigada por todos os ensinamentos que me transmitiste, por todo o tempo que me dispensaste, pela confiança que me depositaste no laboratório e, pelos incentivos ao meu crescimento profissional e pessoal. Se hoje me posso chamar investigadora a muito o devo a ti! Tenho muito orgulho de te ter como orientadora e és para mim um exemplo de sucesso. Obrigada ainda por todos os momentos não laborais e aos muitos risos que tornaram esta minha jornada mais agradável!

Ao Doutor Lino Ferreira agradeço a sua co-orientação, a sua pronta disponibilidade, todo o seu apoio, amabilidade e, sentido crítico que em muito contribuíram para o sucesso deste trabalho. Obrigada!

Doctor Karsten Ruscher thank you for the supervision, for making me more critical about research, for the support, for all the time you dedicated helping me and above all to open my scientific horizons. I have learned a great deal of teachings from you!

I am also grateful to Doctor Tadeusz Wieloch for accepting me in his Laboratory as well as all the members of the Laboratory for Experimental Brain Research Group, who were always very friendly and supportive. Thank you for making my passage in Lund very enjoyable, it was a pleasure to meet you all. And of course, I must thank the ones you made my staying in Lund more entertaining and not only worked related.

Agradeço à Doutora Graça Baltazar e a todo o seu grupo que sempre demonstraram disponibilidade para me ajudar nas alturas em que precisei.

Thank you José Miguel Paiva and Doctor Akhilesh Rai for all the help regarding the production and characterization of the nanoparticles. Your help was essential to the success of this work.

À Doutora Francisca Eiriz agradeço a disponibilidade e toda a ajuda aquando da determinação do método analítico usado para os estudos *in vivo*.

O meu muito obrigada à Profª. Doutora Raquel Ferreira e ao Doutor Tiago Santos que acompanharam quase toda a minha caminhada durante a aventura que foi o Doutoramento. Obrigada por tudo o que me ensinaram, ambos contribuíram em muito para o meu crescimento no mundo da investigação. Obrigada também por toda a ajuda laboratorial, pelo apoio, pelas críticas construtivas e, por todos os conselhos/dicas. Muita energia matinal (por vezes tanta que cansava só de olhar), extrema organização, um pouco de agilidade e perfecionismo, uma pitada de conversa (ou queixas), risos até as lágrimas nos caírem dos olhos, azeitonas qb, ingredientes perfeitos de um dia bem passado no CICS. Obrigada!

Agradeço também à Sandra Rocha, à Marta Esteves, à Patrícia Lindeza, à Doutora Ana Clara Cristóvão e, a todos os elementos do Brain Repair Group, quer os membros actuais quer os que por ele passaram nos últimos 5 anos. Todos vocês me ajudaram a percorrer este caminho!

Aos meus amigos começo por agradecer a sua presença constante na minha vida, apesar de ser uma desnaturada. Muito obrigada por ouvirem os meus queixumes e desabafos; por me animarem e encorajarem nas "derrotas" e, celebrarem comigo as vitórias. Sou muito grata por todos os momentos que passo convosco. Momentos sempre repletos de boas aventuras, muitas gargalhadas e que me enchem o coração! Muito obrigada! Agora, deixemo-nos de lamechices e vamos mas é beber um copo, pago eu ;)

Agradeço a toda a minha família e, aos amigos que são como família por todo o apoio incondicional, em especial à Jessica, à Emma, ao Rafael, ao Filipe, à Elsa, à Ilze e ao Pedro. Por último, agradeço de forma muito especial aos meus pais por todo o amor e suporte que me têm dado ao longo da minha vida e, por todos os ensinamentos. Vocês construíram os pilares por que me rejo na vida profissional e pessoal. Tenho muito orgulho em ser vossa filha! Obrigada.

Support and financial acknowledgements

Publications

The work developed during the PhD and herein described resulted in the publication or submission of two original research articles and one commentary article in international peer-review journals:

C. Saraiva, J. Paiva, T. Santos, L. Ferreira, L. Bernardino, MicroRNA-124 loaded nanoparticles enhance brain repair in Parkinson's disease., J. Control. Release. 235 (2016) 291–305. doi:10.1016/j.jconrel.2016.06.005. **– Chapter 3**

Comment in:

C. Saraiva, L. Ferreira, L. Bernardino, Traceable microRNA-124 loaded nanoparticles as a new promising therapeutic tool for Parkinson's disease, Neurogenesis. 3 (2016) e1256855. doi:10.1080/23262133.2016.1256855. **– Chapter 3**

C. Saraiva, D. Talhada, A. Rai, R. Ferreira, L. Ferreira, L. Bernardino, K. Ruscher, MicroRNA-124-loaded nanoparticles increase survival and neuronal differentiation of neural stem cells in vitro but do not contribute to stroke outcome in vivo., Experimental Neurology (submitted). – **Chapter 4**

Additionally, three review articles and one book chapter were published or submitted:

T. Santos, C. Boto, C.M. Saraiva, L. Bernardino, L. Ferreira, Nanomedicine Approaches to Modulate Neural Stem Cells in Brain Repair, Trends Biotechnol. 34 (2016) 437–439. doi:10.1016/j.tibtech.2016.02.003.

C. Saraiva, C. Praça, R. Ferreira, T. Santos, L. Ferreira, L. Bernardino, Nanoparticle-mediated brain drug delivery: Overcoming blood–brain barrier to treat neurodegenerative diseases, J. Control. Release. 235 (2016) 34–47. doi:10.1016/j.jconrel.2016.05.044.

C. Saraiva, M. Esteves, L. Bernardino, MicroRNA: basic concepts and implications for regeneration and repair of neurodegenerative diseases, Biochemical Pharmacology (2017). 10.1016/j.bcp.2017.07.008.

C. Saraiva, T. Santos, L. Bernardino, Stem cell-based therapeutic approaches for brain repair., Springer (submitted).

Abstract

The subventricular zone (SVZ) represents the major neurogenic niche of the rodent brain and its modulation upon brain injury may enhance brain repair. Herein, we used biocompatible and traceable polymeric nanoparticles (NPs) to deliver microRNA-124 (miR-124) into SVZ cells. miR-124 is a key neuronal fate determinant and was recently described as anti-inflammatory and neuroprotective. Therefore, the efficiency of NPs to deliver miR-124 and prompt SVZ neurogenesis and brain repair in Parkinson's disease (PD) and stroke models was evaluated.

Firstly, we showed that miR-124 NPs were efficiently internalized by neural stem/progenitors cells and neuroblasts and promoted their differentiation into matured neurons by targeting Sox9 and Jagged1 (two stemness-related proteins) *in vitro*. Likewise, intracerebral administration of miR-124 NPs increased the number of migrating neuroblasts reaching the olfactory bulb, both in control mice and in mice subjected to a 6-hydroxydopamine (6-OHDA), a model for PD. Moreover, miR-124 NPs increased the levels of new neurons in the lesioned striatum of 6-OHDA-challenged mice, correlating with functional improvement.

Interestingly, miR-124 NPs also demonstrated the ability to decrease cell death and enhance neuronal differentiation of SVZ cultures after oxygen and glucose deprivation, suggesting a potential beneficial role in stroke. Therefore, miR-124 NPs were intravenously injected in mice subjected to photothrombotic (PT) stroke. In contrast to intracerebral administration, miR-124 NPs were unable to promote recovery of lost neurological function in PT mice. miR-124 NPs did not affect SVZ neurogenesis nor post-stroke inflammation.

We conclude that miR-124 NPs treatment modulates PD outcome *in vivo*, while in stroke it improves survival and neuronal differentiation of SVZ cells. However, the promising *in vitro* data from stroke could not be verified *in vivo*. Thus, we provide evidence supporting that miR-124 NPs are well tolerated and positive modulators of endogenous SVZ neurogenesis as well as their potential application in brain repair strategies.

Keywords: Neural Stem Cells; MicroRNA-124-loaded nanoparticles; Neurogenesis; Parkinson's disease; Stroke; Brain repair.

Resumo

A região subventricular (SVZ) representa o maior nicho neurogénico do cérebro de roedores e, a sua modulação após lesão pode promover a reparação cerebral. Neste trabalho, usámos nanopartículas (NPs) poliméricas biocompatíveis e rastreáveis como veículos de entrega de microRNA-124 (miR-124), um promotor essencial da neurogénese, recentemente descrito como anti-inflamatório e neuroprotector. A eficiência das NPs na entrega de miR-124 e, o seu consequente efeito neurogénico e reparador foram avaliados em modelos animais da doença de Parkinson (PD) e acidente vascular cerebral (AVC).

Inicialmente provámos que as miR-124 NPs foram internalizadas por células estaminais/progenitoras neurais e neuroblastos, promovendo a sua diferenciação e maturação neuronal através da diminuição da expressão das proteínas Sox9 e Jagged1. Posteriormente, mostrámos que a administração intracerebroventricular de miR-124 NPs aumenta o número de novos neurónios no bolbo olfativo de murganhos saudáveis e com PD. As miR-124 NPs também aumentaram o número de novos neurónios no estriado de murganhos com PD, culminando na diminuição dos seus défices motores.

Curiosamente, as miR-124 NPs demonstraram ser capazes de reduzir a morte celular e aumentar a diferenciação neuronal de células SVZ privadas de oxigénio e glucose, sugerindo um possível envolvimento no AVC. Como tal, administrámos as miR-124 NPs intravenosamente em murganhos previamente sujeitos a fototrombose (modelo de AVC). Inesperadamente, as miR-124 NPs demonstraram ser incapazes de melhorar os défices neurológicos dos murganhos, aumentar a neurogénese na SVZ e, modular a resposta inflamatória.

Assim, o uso de miR-124 NPs permitiu diminuir os danos causados pela PD e, aumentar a sobrevivência e diferenciação neuronal de células SVZ num modelo *in vitro* de AVC. Contudo, *in vivo*, no modelo de AVC usado, estes efeitos benéficos não foram verificados. Concluindo, este trabalho evidencia o papel das miR-124 NPs no aumento da neurogénese da SVZ e a sua potencial utilização em estratégias de reparação cerebral.

Palavras chave: Células estaminais neurais; Nanopartículas carregadas com microRNA-124; Neurogénese; Doença de Parkinson; Acidente vascular cerebral; Reparação cerebral.

Table of contents

List of Figures

List of Tables

Abbreviations and Acronyms

6-OHDA	6-hydroxydopamine
AGO	Argonaute
AMPK	5' adenosine monophosphate-activated protein kinase
ATP	Adenosine triphosphate
Bax	Bcl-2-associated X protein
Bcl-2	B-cell lymphoma 2
BDNF	Brain-derived neurotrophic factor
Bim	Bcl-2-like protein 11
BLBP	Brain lipid-binding protein
BrdU	5-bromo-2'-deoxyuridine
BSA	Bovine serum albumin
cAMP	Cyclic adenosine monophosphate
CD	Cluster of differentiation
cdk5	Calpain/cyclin-dependent kinase 5
cDNA	Complementary deoxyribonucleic acid
CREB	cAMP response element binding protein
CSF	Cerebrospinal fluid
DA	Dopamine
DAB	3′-diaminobenzidine
DCX	Doublecortin
DGCR8	DiGeorge Syndrome Critical Region 8
Dlx2	Distal-less homeobox 2
DMEM	Dulbecco's modified Eagle medium
DNA	Deoxyribonucleic acid
EDTA	Ethylenediamine tetraacetic acid
EGF	Epidermal growth factor
EGFR	Epidermal growth factor receptor
EGTA	Ethylene glycol tetraacetic acid
Ezh2	Enhancer of zeste homolog 2
FDA	Food and Drug Administration
FGF-2	Fibroblast growth factor-2
FITC	Fluorescein isothiocyanate
FoxG1	Forkhead transcription factor G1
GAPDH	Glyceraldehyde 3-phosphate dehydrogenase
GCL	Granular cell layer
G-CSF	Granulocyte colony-stimulating factor
GDNF	Glial cell-derived neurotrophic factor
GFAP	Glial fibrillary acidic protein
GFP	Green fluorescent protein
GL	Glomerular layer
GLAST	Glutamate aspartate transporter
GTP	Guanosine-5'-triphosphate
HBSS	Hank's Balanced Salt Solution
Hes	Hairy and enhancer of split

HSC70	Heat shock cognate protein-70
HSP90	Heat shock protein-90
HUVEC	Human umbilical vein endothelial cells
i.p.	Intraperitoneal injections
iASPP	Inhibitory member of the apoptosis-stimulating proteins of p53 family
Iba1	Ionized calcium binding adaptor molecule 1
IFNγ	Interferon-gamma
IgG	Immunoglobulin G
IL-1β	Interleukin-1beta
IL-6	Interleukin-6
iPSC	Induced pluripotent stem cell
JNK	c-Jun N-terminal kinase
JSAP1	JNK pathway-specific scaffold protein 1
LNA	Locked nuclei acid
LPS	Lipopolysaccharide
Map-2	Microtubule-associated protein-2
MBD1	Methyl-CpG-binding domain protein 1
MCAO	Middle cerebral artery occlusion
MeCP2	Methyl CpG binding protein 2
MicroRNA	miRNA or miR
miRISC	miRNA-induced silencing complex
MPP	methyl phenyl pyridinium
MPTP	1-methyl-4-phenyl-1,2,3,6-tetrahydropyridine
MRI	Magnetic resonance imaging
mRNA	Messenger ribonucleic acid
mRS	post-stroke modified Rankin Score
mTOR	Mechanistic target of rapamycin
MWCO	Molecular weight cut-off
NeuN	Neuronal nuclei
NeuroD1	Neurogenic differentiation 1
NF-κB p65	Nuclear factor-κB p65
NMR	Nuclear magnetic resonance
NP	Nanoparticle
NSC	Neural stem cell
nt	Nucleotide
OB	Olfactory bulb
OGD	Oxygen and glucose deprivation
Olig2	Oligodendrocyte transcription factor 2
ON	Overnight
PACT	protein kinase R-activating protein
PAZ	Piwi-Argonaute-zwille
PBS	Phosphate-buffered saline
PBS-T	Phosphate-buffered saline with Triton X-100
PCNA	Proliferating cell nuclear antigen
PD	Parkinson's disease
PDL	Poly-D-lysine
PEG	Poly(ethylene glycol)
PEI	Poly(ethylenimine)

PFA	Paraformaldehyde
PFCE	Perfluoro-1,5-crown ether
pHH3	Phosphohistone H3
PI	Propidium iodide
PI3K	Phosphoinositide 3-kinase
PLA	Poly(lactic acid)
PLGA	Poly(lactic-co-glycolic acid)
PMSF	Phenylmethanesulfonyl fluoride
PS	Protamine sulfate
PSA-NCAM	Polysialylated neural cell adhesion molecule
PT	Photothrombotic stroke
PTBP	RNA binding polypyrimidine tract-binding protein
PVA	Poly(vinyl) alcohol
qPCR	Quantitative real-time polymerase chain reaction
RAN	Ras-related nuclear protein
REST	RE1 silencing transcription factor
RhoG	Ras homology growth-related
RMS	Rostral migratory stream
RNA	Ribonucleic acid
ROCK1	Rho-associated coiled-coil forming protein kinase 1
RT	Room temperature
SCP1	Small c-terminal domain phosphatase 1
SEM	Standard error of mean
SFM	Serum-free medium
SGZ	Subgranular zone
SN	S*ubstantia nigra*
Sox 2	Sex determining region Y-box 2
ssRNA	Single strand RNA
STAT3	Signal transducer and activator of transcription 3
SVZ	Subventricular zone
TACE	TNF-α converting enzyme
TBS	Tris buffer saline
TH	Tyrosine hydroxylase
TLR	Toll-like receptor
Tlx	Orphan nuclear receptor tailless
TNF-α	Tumor necrosis factor-alpha
tPA	Tissue plasminogen activator
TRAF6	TNF receptor associated factor 6
TRBP	Transactivation-response RNA-binding protein
TUNEL	Terminal deoxynucleotidyl transferase dUTP nick end labeling
USP	Ubiquitin-specific protease
VTA	Ventral tegmental area

Chapter 1

INTRODUCTION

1.1 Neural Stem Cells

Neurogenesis, the generation and development of nerve cells, was traditional viewed as a process exclusive of the embryonic and perinatal brain (Bizzozero 1894; Ramon y Cajal 1913). The acceptance of adult neurogenesis, a milestone in the field, was only made in the early 1990s (Nottebohm 2002). The first evidence of adult neurogenesis were presented by Joseph Altman and collaborators, in the 1960s (Altman 1962; Altman 1963). They showed that adult-born cells formed in the subventricular zone (SVZ) travel through the rostral migratory stream (RMS) to the olfactory bulb (OB) where they differentiate into mature neurons (Altman and Das 1965; Altman 1969). Still, the existence of post-natal new neurons in the OB and dentate gyrus of mammals was proven unequivocally only a few years later (Kaplan and Hinds 1977). Thereafter, several groups showed that adult neurogenesis was conserved from rodents (Kuhn et al. 1996; Kempermann et al. 1997) to humans (Eriksson et al. 1998; Kukekov et al. 1999), which rapidly led the scientific community to pursue the restauration of dysfunctional circuitries through the modulation of neurogenesis.

During the embryonic development, neuroepithelial cells and later radial glia cells originate neurons and glia cells based on spatial and temporal cues (Pearson and Doe 2004). Soon after birth, glial fibrillary acidic protein (GFAP)-expressing astrocyte-like cells assume the role of radial glia cells as neural stem cells (NSCs) (Doetsch et al. 1999; Garcia et al. 2004). NSCs can self-renew, proliferate and possess multipotent features, being able to differentiate into neurons, astrocytes and oligodendrocytes (Reynolds and Weiss 1992). These cells are found in discrete regions of the brain – neurogenic niches – that are mainly found in the SVZ lining the lateral ventricles and in the subgranular zone (SGZ) of the dentate gyrus of the hippocampus (Gage 2000; Ma et al. 2009). Neurogenesis in these germinal niches persist throughout life although it decreases with age (Kuhn et al. 1996). A rising number of evidence has also been pointing to the existence of other neurogenic regions in the brain, namely in the circumventricular organs located along the ventricular midline (Itokazu et al. 2006; Bennett et al. 2009), in the walls of the third and fourth ventricles (Lin et al. 2015), in the meninges of the spinal cord (Petricevic et al. 2011; Decimo et al. 2011), in the *substantia nigra* (SN) (Lie et al. 2002), in the amygdala (Bernier et al. 2002), in the cerebellum (Klein et al. 2005), among other regions, reviewed at (Lin 2015). All these regions share the ability to generate multipotent precursors that can be isolated and differentiated *in vitro*, however, they usually occur in low levels in physiological conditions being only perceptive after injury (Ming and Song 2005). These facts together with the lack of evidence for the presence of niche structures to house these cells make their role in brain homeostasis a matter of controversy.

Neurogenic niches are composed of NSCs and supporting cells – endothelial cells, astrocytes, ependymal cells, progenitors cells, neurons and microglia – that confer a specific microenvironment able to regulate in a fine-tuned way the self-renewal and differentiation of NSCs *in vivo* (Ming and Song 2011). A huge number of molecular players are involved in the modulation of the neurogenic process, including cell receptors, soluble factors released by neighbor cells, transcription factors, growth factors, cytokines, hormones, epigenetic regulators, non-coding RNAs, to name few, reviewed at (Ninkovic and Götz 2007; Ma et al. 2010; Mu et al. 2011). NSCs fate can be altered in response to pathological events or regulated by extrinsic signals (pharmacological stimuli). Indeed, it was shown that in the adult brain of Huntington patients NSCs increase their proliferative and migratory features, providing a clear

indication of their regenerative potential (Curtis et al. 2003). Other studies have confirmed that upon lesion SVZ cells had the capability to migrate towards the lesioned area. In some cases, they could even differentiate into the respective cell phenotype of the lesioned regions, leading ultimately to functional recovery (Arvidsson et al. 2002; Parent et al. 2002; Goings et al. 2004). As so, endogenous NSCs are a virtual unlimited source of new cells that upon an injury respond by proliferating, migrating towards the lesion and differentiating into neurons, raising high expectations for regenerative medicine. Therapeutic approaches based on augmentation of the brain natural endogenous response to injury overcome limitations related with cell transplantation, such as the low number of cells typically available for therapy, low cell survival after transplantation, immune rejection of grafted cells, teratoma formation, and ethical issues (Christie and Turnley 2012). This approach seems to be particularly feasible because numerous studies have demonstrated that growth factors (e.g. glial cell-derived neurotrophic factor (GDNF), brain-derived neurotrophic factor (BDNF), granulocyte colony-stimulating factor (G-CSF)), and other molecules (e.g. erythropoietin, pramipexole, ephrin-A1) are able to induce neurogenesis leading eventually to functional recovery (Dempsey et al. 2003; Kobayashi et al. 2006; Kadota et al. 2009; Winner et al. 2009; Jing et al. 2012). However, strategies based on enhancing endogenous NSCs activity are still limited to pre-clinical studies. Developing new platforms to efficiently deliver pro-neurogenic factors to NSCs is imperative to boost the endogenous reparative capacity of the adult brain.

1.1.1 Subventricular zone

In rodents, the SVZ stem cell niche, which includes the ventricular and subventricular zones, located between the lateral ventricles and the striatum, represents the largest germinal region in the adult brain. The SVZ comprises four major different types of cells: ependymal cells, NSCs (type B cells), transit amplifying cells (type C cells) and neuroblast (type A cells) (Figure 1.1 A, B). Ependymal cells form a monolayer that lines the ventricle walls creating a thigh barrier between the ventricle lumen and the brain parenchyma. These cells have cilia in direct contact with the ventricle lumen and they play a critical role in the regulation of the neurogenic process (Paez-Gonzalez et al. 2011). The NSCs or type B cells are slow dividing specialized astrocyte-like cells derived from radial glia with self-renewal and multipotent properties (Doetsch et al. 1997; Doetsch et al. 1999). These polarized cells project a cilium into the ventricle lumen, being in direct contact with the cerebrospinal fluid (CSF) in the apical region while the basal side have end-feet structures that contact with blood vessels. Therefore, NSCs can sense cues present both in the CSF and the blood. Type B cells share many features with brain astrocytes, including the expression of GFAP, brain lipid-binding protein (BLBP), and glutamate aspartate transporter (GLAST). Nevertheless, they also express markers of immaturity such as sex determining region Y-box 2 (sox 2) and nestin. Type B cells can be in a quiescent state or in an activated state (Codega et al. 2014). Activated B cells divide asymmetrically giving rise to type C cells, non-radial actively proliferating transit amplifying progenitors that express the transcription factors Ascl1 (also known as Mash1) and distal-less homeobox 2 (Dlx2) as well as the epidermal growth factor receptor (EGFR). After approximately three rounds of symmetrical divisions, type C cells generate immature neuroblast (type A cells) that will divide one to two times during their journey towards the OB (Ortega et al. 2013; Ponti et al. 2013). Type A cells express doublecortin (DXC) and polysialylated neural cell

adhesion molecule (PSA-NCAM), and have a high migratory capacity travelling long distances (up to millimeters) from the SVZ to the OB. Chains of neuroblasts coming from different paths converge in the anterior SVZ to form the RMS, a tube-like structure formed of specialized astrocytes and blood vessels that confer additional physical support to the migration (Lois and Alvarez-Buylla 1994; Lois et al. 1996; Doetsch and Alvarez-Buylla 1996; Lledo et al. 2006). Neuroblasts migrate rostrally until they reach the OB; once there, they detach from the RMS chains (tangentially oriented) and move radially towards different layers of the OB. These new neurons mature and integrate mainly as GABAergic granule interneurons in the granular cell layer (GCL) and in a lower extent as GABAergic or dopaminergic (smaller amount) periglomerular interneurons in the glomerular layer (GL). There is also a very small percentage of cells that differentiate into glutamatergic juxtaglomerular neurons (Brill et al. 2009; Ming and Song 2011).
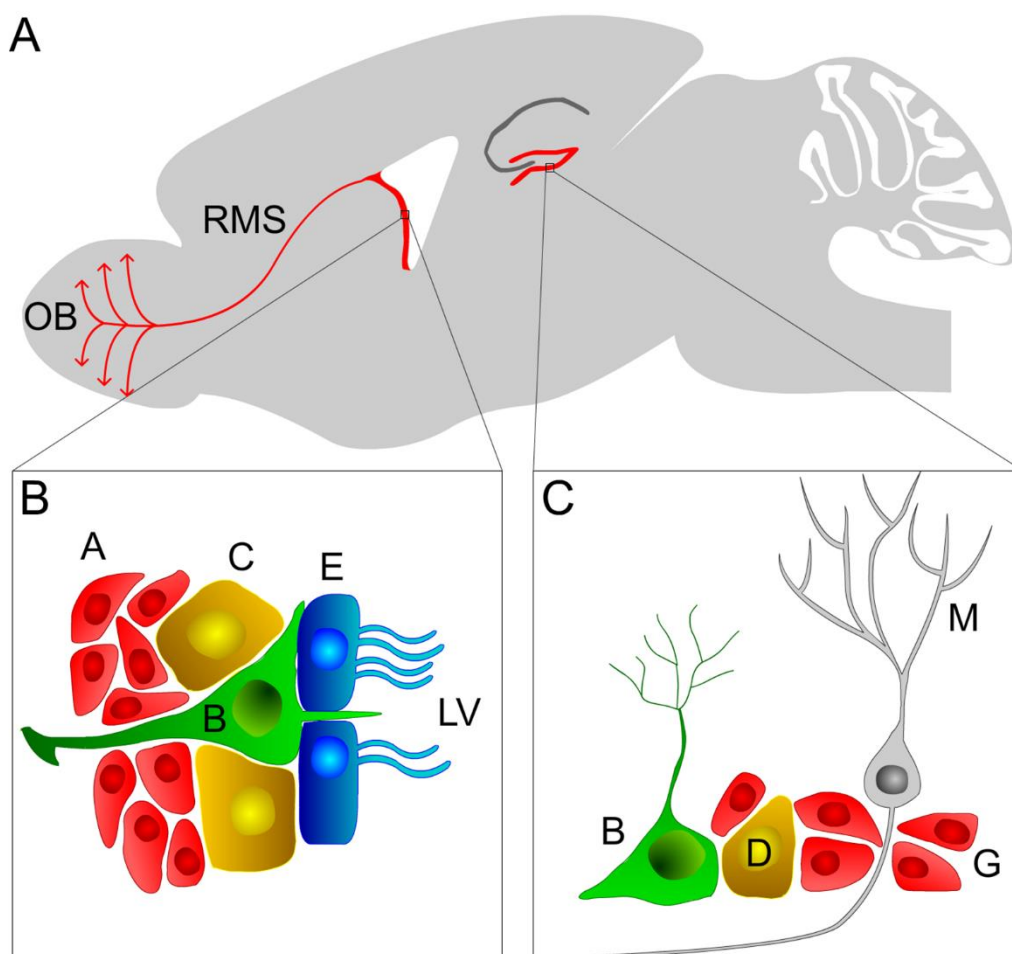
Figure 1.1 Localization and composition of neural stem cell (NSC) niches in the adult rodent brain.
(A) Sagittal rodent brain slice displaying the localization of the two main neurogenic niches: the subventricular (SVZ) and subgranular (SGZ) zones. (B) At the SVZ, type B NSCs cells contact with the lateral ventricles and give rise to C progenitor cells that differentiate into neuroblasts (type A cells). Physiologically, neuroblasts migrate through the rostral migratory stream (RMS) towards the olfactory bulb (OB) where they differentiate into mature neurons; E, ependymal cells. (C) Similarly, type I (or B) stem cells at the SGZ give rise to type II (or D) progenitor cells that in turn generate neuroblasts (type III or G cells), which ultimately differentiate into mature granule neurons (M).

The proliferation and migration rate of NSCs change in response to injury, which potentially makes them a good source of new cells for therapeutic purposes. Nevertheless, neural stem/progenitors cells

need to proliferate, migrate, mature and functionally integrate into existing circuitries to trigger an efficient regenerative response. There are also limitations regarding the suitability in the type of cells generated or their survival. Hence, it is essential to understand and/or identify molecular mediators able to enhance this neurogenic response and, therefore useful for the development of novel therapeutic strategies.

Isolation and culture of NSCs *in vitro* were pivotal to extend our knowledge regarding adult neurogenesis (Reynolds and Weiss 1992; Kilpatrick and Bartlett 1993). Free floating three-dimensional structures of thousands of cells – neurospheres – can be obtained from harvesting the SVZ cells and cultivate them into specific conditions: serum-free medium with mitogenic growth factors, namely epidermal growth factor (EGF) and fibroblast growth factor-2 (FGF-2), into a non-adherent substrate. These conditions select cells responsive to EGF that include type C cells (around 70%) and activated type B cells, both with self-renewal and proliferative abilities. Differentiation into neurons, oligodendrocytes and astrocytes can be achieved by cultivating neurospheres in the absence of mitogenic growth factors and into an adhesive substrate. Although the limitations associated with *in vitro* culture, such as the non-total representation of the NSCs *in vivo* population, the number of passages, the loss and/or change of biological properties to name a few, it is still a solid method to appraise neural stem/progenitors cells properties in different conditions, screening potential therapeutic molecules or expand cells for replacement therapies (Doetsch et al. 2002; Gil-Perotín et al. 2013).

Much is known about the germinal niches in rodents; notwithstanding translation of NSC-based brain repair strategies into humans requires sufficient knowledge of the human neurogenesis as well as differences and similarities regarding the SVZ stem cell niche among species. In humans, the SVZ also contains cells with NSC features that can be isolated and growth *in vitro* (Eriksson et al. 1998; Sanai et al. 2004). However, the human SVZ shows a distinct cytoarchitecture. A layer of multiciliated ependymal cells lines the ventricle wall followed by a gap layer, majorly devoid of cells, where a network of cytoplasmic projections derived from ependymal cells and astrocytes connect. SVZ astrocytes, with NSCs properties, accumulate after the gap layer organized in ribbon-like structures with some of the cells branching towards the ventricle lumen, similar to type B cells in rodents (Sanai et al. 2004; Quiñones-Hinojosa et al. 2006). Nonetheless, lower levels of proliferating cells as well as new neurons are found in the human SVZ when compared with rodents. Furthermore, there still is no consensus regarding the presence of a RMS structure in the human brain. A ventral extension of the lateral ventricle until the OB containing neuroblasts was reported in the human fetus during the late second trimester resembling the rodent RMS. Yet, no neuroblasts chain-like structures were found in the OB suggesting a putative migration of these newborn neurons towards other destinations (Guerrero-Cazares et al. 2011). Indeed, in the developing post-natal brain (up to 18 months) streams of DCX-positive cells were found in the gap layer migrating tangentially to the OB through an evident RMS as well as to the medial prefrontal cortex through a medial migratory stream. Nonetheless, SVZ-OB migratory activity seems to subside with age, being almost inexistent in adulthood (Sanai et al. 2011). Other studies showed a RMS structure similar to the one seen in rodents, but exhibiting a 75º rotation forward due to the massive development of the human frontal cortex (Curtis et al. 2007; Kam et al. 2009). The presence of stem/progenitors cells and neuroblasts along the human ventricle-olfactory axis suggests that these

cells may be responsive to cues induced by cell loss. Moreover, it was recently shown, in the human brain, that precursors cells derived from the SVZ are able to migrate and differentiate into interneurons in the striatum (Ernst et al. 2014). Likewise, some pathologies, such as stroke, stimulate neurogenesis and neuroblast migration to the injured striatum (Jin et al. 2006), demonstrating the potential of adult neurogenesis in humans. Hence, SVZ NSCs hold great potential in the search for novel brain repair therapies.

1.1.2 Subgranular zone

The SGZ contains an adult germinal niche composed of a smaller pool of NSCs when compared with the SVZ (Lois and Alvarez-Buylla 1993; Morshead et al. 1994). The SGZ of the dentate gyrus of the hippocampus is a narrow band of tissue located between the granule cell layer and the hilus. Astrocyte-like NSCs, also known as radial astrocytes, type I cells or type B cells, reside in this region and are able to generate proliferating intermediate progenitors named type II cells or type D cells. These cells give rise to type III cells or type G cells (immature neuroblasts; Figure 1.1 A, C). Type I cells express markers of immaturity, such as nestin and Sox2, beside the glial marker GFAP, and possess stemness properties (self-renewal and multipotency) (Palmer et al. 1997; Bonaguidi et al. 2011). Similar to SVZ NSCs counterparts, type I cells have also end-feet in direct contact with blood vessels and extend a long radial process that transverse the granular cell layer ramifying into the molecular layer of the hippocampus (Palmer et al. 2000; Filippov et al. 2003). Type I cells generate type II progenitors, intermediate progenitor cells with high proliferative capacity (immature state), which give rise to type III cells (mature state). Type III cells are DCX and PSA-NCAM expressing migratory neuroblasts. In contrary to SVZ neuroblasts, SGZ newborn neurons migrate short distances towards the granule cell layer where they differentiate into mature glutamatergic granule neurons (type M cells). These new neurons project their axons towards the CA3 region of the hippocampus and within a period of seven weeks became indistinguishable from the remaining neurons (Seri et al. 2001; Zhao et al. 2008; Bonaguidi et al. 2012; Berg et al. 2015; Sun et al. 2015a). SGZ-derived neurons are involved in learning and memory processes, especially during their maturation where they present increased plasticity (Shors et al. 2001; Schmidt-Hieber et al. 2004). Indeed, it is known that behavioral performance can be augmented by increasing SGZ neurogenesis, while neurogenesis downregulation culminates in behavioral impairments (Deng et al. 2010). The organization and structure of the human adult SGZ germinal niche is similar to the rodent, but it has a more limited proliferative capacity than the SVZ (Eriksson et al. 1998; Curtis et al. 2012). Actually, it is thought that human SGZ proliferating cells are present in a small number and are relatively unresponsive to pathological alterations (Boekhoorn et al. 2006; Lucassen et al. 2010; Low et al. 2011), while in rodents the presence of certain stimuli can increase SGZ NSCs responsiveness (Walker et al. 2008). External stimuli, including environment enrichment, learning, stress, physical activity to name a few, cause a plastic adaptation of both SVZ and SGZ neurogenic niches. For example, olfactory discrimination learning boosts the levels of new neurons in the OB through survival extension (Alonso et al. 2006), while hippocampus-dependent learning increases SGZ neuronal survival (Leuner et al. 2004). Also, enriched environment and physical exercise are inductors of hippocampal neurogenesis (Kempermann et al. 1997). Furthermore, SGZ neurogenesis

impairments in mice can be rescued by physical exercise (Lafenêtre et al. 2010). On the other hand, stress seems to negatively correlate with neurogenesis. An example is the reduction in the proliferation of type B and type D cells in the SGZ of mice exposed to stress cause by noise (Gonzalez-Perez et al. 2011). These examples show once more the ability of NSCs to adapt to different environments. Moreover, Spalding and colleagues showed that approximately 700 new neurons are generated every day in each hippocampus in humans during adulthood. Impressively, hippocampal neurogenesis declines in a modest way (around 4-fold) during the entire human lifespan (Spalding et al. 2013). These studies confirm a relevant role of adult SGZ neurogenesis in brain function. Therefore, defects in adult neurogenesis have been associated with neurological and psychiatric diseases. Concluding, even though SGZ presents a more limited proliferative and migratory activity than the SVZ, it still holds high potential for the development of future regenerative therapies for treating neurological disorders.

1.2 Neurogenesis in pathology

The discovery of NSCs in the adult mammalian brain and the increased knowledge about the composition and function of the neurogenic niches opened new avenues in understanding brain plasticity and function. Remarkably, neurogenesis is enhanced upon brain lesion injury possibly as an attempt for brain repair. Nevertheless, the role of neurogenesis in neurodegenerative disorders is still under debate. As so, the role of neurogenesis in Parkinson's disease (PD), which is a chronic pathology, and in stroke, an acute disorder, are discussed below.

Parkinson's disease

Parkinson's disease is a neurodegenerative disease that affects approximately 10 million people throughout the world (Hermanns 2011). PD is mainly characterized by the progressive degeneration of dopaminergic neurons in the SN leading to striatal dopamine (DA) depletion and the accumulation of alpha (α)-synuclein aggregates known as Lewy bodies (Spillantini et al. 1997; Damier 1999). The key symptoms that clinically define PD are rigidity, tremor, bradykinesia and postural instability. Currently, the standard treatment for PD is based on DA replacement (mainly using a precursor of DA, levodopa) with high efficacy in the early stages of the disorder. Nevertheless, during the time course of the disease these drugs lose effectiveness and cause side effects and severe psychiatric complications. Deep brain stimulation is also used in some patients, in more advanced stages of the disorder, with successful suppression of motor symptoms; however, it does not stop progression of the pathology. Several regenerative medicine approaches are under intense examination to address the impact of stem cells in PD. However, the low amount of data in post-mortem brain tissue from PD patients, together with contradictory experimental findings, make the role of adult neurogenesis in PD a high controversial subject within the scientific community. It was firstly shown that PD patients display impaired neurogenesis since they presented lower levels of cells expressing the marker for proliferation proliferating cell nuclear antigen (PCNA) in the SVZ, a decrease of nestin-positive cells (immature neural precursor cells) both in the OB and in the dentate gyrus of the hippocampus, as well as a reduction in beta (β)-III-tubulin-positive cells (neuronal marker) in the SGZ (Höglinger et al. 2004). DA seems to play a critical role in neurogenesis impairment. Indeed, PD progression negatively correlates to NSCs

numbers while the cumulative use of L-Dopa in PD patients seems to result in increased numbers of proliferating NSCs in the SVZ (O'Sullivan et al. 2011). The SN and the ventral tegmental area (VTA) project dopaminergic fibers that innervate the neurogenic niches in a specific pattern (Höglinger et al. 2014), and they are in close proximity to EGFR-positive cells that include all type C cells and a subset of type B cells (Doetsch et al. 2002; Höglinger et al. 2004). Advanced PD patients have not only significantly less amount of EGFR-positive cells in the SVZ, but also weaker expression of EGFR (O'Keeffe et al. 2009). In addition, EGF and EGFR levels were also found to be decreased in the striatum of PD patients (Iwakura et al. 2005). SVZ type C and A cells express both D1-like and D2-like DA receptors (Coronas et al. 1997; Höglinger et al. 2004). DA reduction in animal models leads to impairments in NSCs proliferation and EGFR expression that are D2-like receptor-mediated (Höglinger et al. 2004; Coronas et al. 2004; O'Keeffe et al. 2009; Lao et al. 2013). Alpha-synuclein also seems to be involved in neurogenesis impairments. Interaction between accumulated α-synuclein and p53 results in Notch1 signaling dysregulation in the SGZ of rats that potentially trigger some of the non-motor symptoms associated with the PD pathology (Crews et al. 2008; Desplats et al. 2012). Neural committed induced pluripotent stem cells (iPSCs) obtained from fibroblasts of patients with triplication of the α-synuclein gene (SNCA; associated with early onset of PD) were unable to develop neuronal complex networks when compared with control neural committed iPSC, also showing a correlation between α-synuclein expression and neurogenesis impairment (Oliveira et al. 2015). Hypermethylation of thousands of genes has been found in brain tissue of PD patients, specifically neurogenic-related genes such as Wnt, suggesting a critical role for Wnt-associated neurogenesis in PD (Zhang et al. 2016a). Inflammation is also a major player in neurodegenerative disorders and higher expression of inflammatory molecules in PD patients, such as tumor necrosis factor-alpha (TNF-α) or other cytokines (e.g. interleukin (IL)-6), correlates with non-motor symptoms, namely anxiety and depression, which precede the motor symptoms of the pathology (Reale et al. 2009; Lindqvist et al. 2012). Similar symptomatology is found in animal models of impaired neurogenesis (Revest et al. 2009) leading some groups to defend a robust developmental component in PD onset and progression.

On the other hand, the putative role of neurogenesis impairment on PD was challenged by Hol's group that analyzed brain tissue from healthy controls, PD patients and incidental PD (did not received L-Dopa treatment) in terms of SVZ proliferation. No significant differences neither in terms of proliferation in the SVZ between groups nor in GFAP-delta (δ)-positive cells (radial glia marker) were found in the study. Cultivation of neurospheres, obtained from the post-mortem tissue of the three analyzed groups, was achieve with similar efficiency and differentiation potential into neurons and glial cells. Moreover, treatment of human NSC lines with dopamine and dopamine agonists did not result in the stimulation of NSCs proliferation (van den Berge et al. 2011), indicating that DA depletion may not affect the neurogenic capacity of the PD brain. Isolation and culture of human derived NSC lines from the SVZ, cortex or SN of post-mortem PD patients was confirmed by Wang et al. (Wang et al. 2012b), although a high variability in the amount of SVZ proliferating cells isolated from different donors was found (van den Berge et al. 2010). Inconsistent data have been reported over the last years showing decrease, maintenance or even increase of neurogenesis in PD patients and animal models, reviewed at (van den Berge et al. 2013).

PD models are based on the administration of toxins such as 6-hydroxidopamine (6-OHDA), 1-methyl-4-phenyl-1,2,3,6-tetrahydropyridine (MPTP), rotenone, paraquat, to name a few, that cause selective death of dopaminergic neurons. Genetic models are used to model familial PD, but have also been instrumental to shed some light on PD mechanisms (Jagmag et al. 2015). The differential activation of dopamine receptors in NSCs (Höglinger et al. 2004; Coronas et al. 2004; Kippin et al. 2005) together with a high diversity of PD models (transgenic or toxin based models, acute or chronic administrations, different dosages and different spatial administration of toxins) (Dauer and Przedborski 2003) may explain the different results communicated. For example, in 6-OHDA-challenged rats it was reported either an increase (Liu et al. 2006; Arias-Carrión et al. 2006; Aponso et al. 2008) or decrease (Höglinger et al. 2004; Winner et al. 2006) of SVZ proliferation. In a 6-OHDA mouse model of PD a reduction in SVZ proliferation together with higher survival rate of newborn neurons was also reported in the OB (Baker et al. 2004; Sui et al. 2012). Recently, Fricke and colleagues reported that the 6-OHDA lesion does not affect neurogenesis (Fricke et al. 2016). These discrepancies have generated a high debate in the scientific community about the limitations of experimental models but also the design of studies including the question about the sample size, controls groups, the type of analysis performed to name a few.

Stroke

Stroke is the most costly and long term disabling condition in adulthood worldwide affecting approximately 800,000 people *per* year (Mozaffarian et al. 2015). During a stroke episode, the brain or specific areas of the brain are deprived of blood supply either by a ruptured artery (hemorrhagic stroke) or by occlusion of an artery due to a blood clot and/or atherosclerosis (ischemic stroke) (Kyle and Saha 2014). In both cases, there is deprivation of oxygen and nutrients, resulting in cell death and in many cases loss of neurological functions. Following an ischemic stroke, two distinct brain damage areas can be defined: ischemic core, which represents the irreversibly damage tissue supplied by the occluded artery; ischemic penumbra (and after the initial phase of approximately 24 hours: peri-infarcted area), which correspond to the tissue surrounding the ischemic core where neurons remain viable but stressed and vulnerable due to a reduction of the blood flow. Current treatments for ischemic stroke are essentially based in the systemic administration of tissue plasminogen activator (tPA) within the first 4.5 h after symptom onset, local administration of tPA and endovascular treatments or endarterectomy. The very narrow therapeutic window for a systemic lysis therapy is limiting the number of patients eligible for this treatment. Therefore, the development of novel therapeutic strategies also beyond this time is essential to counteract acute loss of brain tissue and to foster processes to enhance recovery of lost neurological function. In humans, evidence suggests that neurogenesis is enhanced in response to a stroke insult. Nevertheless, the molecular mechanisms behind post-ischemic neurogenesis are poorly understood. An increase in the levels of proliferating (Ki67-positive cells) and neural progenitors cells (PSA-NCAM-positive cells) were observed in the vicinity of the lateral ventricle wall in stroke patients compared with age-matched controls (Macas et al. 2006). Conversely, augmentation of SVZ neural progenitor cell proliferation was observed in the injured brain hemisphere of patients within 2 weeks from stroke onset (Marti-Fabregas et al. 2010). The presence of new neurons in non-germinal regions

has also been reported in the adult human brain after stroke. Indeed, DCX-positive neuroblasts were found in the ischemic penumbra of cortical infarcts close to the vasculature, suggesting an important role of angiogenesis in stroke-induced neurogenesis (Jin et al. 2006). Neural stem/progenitor cells expressing nestin and musashi-1 were also observed in the ischemic human cortex during the first month after injury (Nakayama et al. 2010). An increase in the number of NSCs were seen near the SVZ of a stroke patient. Moreover, enhancement of neurogenesis and formation of novel blood vessels were also found in the peri-infarct area of this patient, indicating once more the relevance of the vasculature for neurogenesis as well as the possible migration of newborn cells into injury sites (Minger et al. 2007). Indeed, stroke patients presenting a higher microvessel density in the peri-infarct area have longer survival rates (Krupinski et al. 1994). Altogether, these reports suggest that adult NSCs are responsive to stroke injury even in the aged brain, despite the limited number of studies in the human brain after stroke. Notwithstanding, these evidence support the hypothesis that enhancing the endogenous brain repair response is correlated with improved stroke recovery.

The use of animal models of stroke, namely rodents, has been of utmost importance to understand the neurogenic response to the injury as well as to shed light into the cellular and molecular mechanisms that occur after stroke (Kumar et al. 2016). The middle cerebral artery occlusion (MCAO) model, that can be transient or permanent, is one of the standard models of stroke. Nevertheless, other models such as the photothrombotic (PT) stroke model are starting to be more widely used due to its less invasiveness and high reproducibility. In accordance with the gathered data from humans, a bulk number of evidence also showed that neurogenesis and neuroblast migration from the SVZ to the injury site are augmented in stroke animal models (Lindvall and Kokaia 2015). The claims are supported by the presence of 5-bromo-2'-deoxyuridine (BrdU)- and DCX-double positive cells in the damaged striatum of rodents that gradually mature into neuronal nuclei (NeuN)-expressing cells (Arvidsson et al. 2002; Parent et al. 2002; Thored et al. 2006; Yamashita et al. 2006). Nevertheless, the number of SVZ migrating neuroblasts reaching the ischemic territory is insufficient to recover the cell loss observed, and their survival is minimal (Arvidsson et al. 2002). Although strong evidence of a stroke-induced SVZ-striatal neurogenesis are reported, studies showing cortical neurogenesis are limited (Jiang et al. 2001; Arvidsson et al. 2002; Parent et al. 2002). For example, the presence of BrdU-positive cells co-expressing a neuronal marker (microtubule-associated protein-2 (Map-2), β-III-tubulin, or NeuN) as well as SVZ-derived neuroblasts were found in the boundaries of the cortical ischemic area of rodent MCAO models of stroke (Jiang et al. 2001; Jin et al. 2003; Kreuzberg et al. 2010). In a PT mouse model of stroke, DCX-expressing cells (most likely migrating neuroblasts) seemed to migrate from the SVZ through the corpus callosum to the peri-infarcted cortex up to 1 year after the ischemic insult; however, they did not become mature neurons (Osman et al. 2011). The higher variability regarding stroke-induced neurogenesis in the cortex may be caused due to the animal model used, the location and size of the lesion as well as the surrounding environment that may provide differential cues. Indeed, both angiogenesis and inflammation are key regulators of adult neurogenesis. Inhibitors of angiogenesis have been shown to decrease both angiogenesis and neurogenesis (Plane et al. 2010), while infiltration of immune cells, due to blood brain barrier (BBB) breakdown, and increased reactivity of the resident microglia (brain immune cells) after MCAO resulted in the release of cytokines, chemokines and reactive

species that can control neurogenesis (del Zoppo et al. 2007). For example, the pro-inflammatory cytokine TNF-α either increases or decreases neurogenesis in a concentration-dependent manner (Bernardino et al. 2008). Altogether, these studies show that stroke induces neurogenesis in the human brain and in animal models of stroke. SVZ seems to be the major contributor for stroke-induced neurogenesis, despite the scarce evidence for cortical neurogenesis. Nevertheless, adult NSCs, namely the SVZ NSCs, showed to be a valuable source of new neurons with brain repair potential.

1.3 MicroRNAs

MicroRNAs (miRNA or miR) were firstly discovered in the 1990s but only in the 2000s these small molecules were identified as a novel class of biologic regulators, altering the view over the central dogma of molecular biology: DNA is transcribed into RNA being then translated into protein. miRNA are small non-coding RNAs with approximately 22 nucleotides (nt) in length that were firstly identified in *Caenorhabditis elegans*, but were rapidly found to be ubiquitous among plants and animals. The fundamental basis of miRNA pathways is conserved among these two kingdoms, yet miRNA mode of action is primarily different (mRNA cleavage *vs* mRNA translational repression and/or decay) (Bartel 2004). Transcription and function of miRNA are tightly regulated and complex processes that include several steps of regulation, reviewed at (Towler et al. 2015).

miRNA can be transcribed as independent transcription units or as miRNA genes located either in introns or exons of other genes (Rodriguez et al. 2004). In mammals, intronic miRNA originate the majority of the miRNA transcripts, being controlled independently of the host genome by different promotors (Monteys et al. 2010; Godnic et al. 2013; Ramalingam et al. 2014). miRNA genes are generally transcribed by RNA polymerase II generating an imperfect stem-loop structure flanked by single strand (ss)RNA, which is capped on the 5' end and polyadenylated in the 3' end and it is composed of hundreds to thousands of nt – pri-miRNA (Figure 1.2) (Lee et al. 2004; Cai et al. 2004). One arm of the pri-miRNA stem-loop comprises the sequence to generate either a single or a cluster of mature miRNA (Altuvia et al. 2005; Hertel et al. 2006). The microprocessor complex is composed of two RNA-binding proteins. DiGeorge Syndrome Critical Region 8 (DGCR8) interacts with pri-miRNA and recruits the RNase III enzyme DROSHA, which is responsible for cleaving the pri-miRNA in the stem-loop, forming the precursor-miRNA (Pre-miRNA). Pre-miRNA has a 5' phosphate group, a 2 nt overhang at 3' end and approximately 60 nt long (Figure 1.2) (Lee et al. 2003; Zeng and Cullen 2005). The heterodimer Exportin-5 and its co-factor GTPase RAN (ras-related nuclear protein; complex Exportin/RAN) mediate pre-miRNA translocation to the cytoplasm. Once the pre-miRNA is shuttled through the nuclear pore, hydrolysis of GTP leads to the complex disassembly and releases the pre-miRNA into the cytoplasm, where it will get mature (Yi et al. 2003; Lund 2004). Pre-miRNA is then recognized by the RNAse III Dicer that further cleaves the pre-miRNA into a 22 nt long miRNA duplex (MacRae et al. 2007). TRBP (transactivation-response RNA-binding protein) and PACT (protein kinase R-activating protein), although not essential for the process, increase Dicer accuracy facilitating the pre-miRNA processing (Chendrimada et al. 2005; Lee et al. 2006; Kim et al. 2014; Wilson et al. 2015). The miRNA duplex complex is loaded into the argonaute (AGO) protein in an ATP-dependent manner assisted by the heat shock cognate protein-70 and heat shock protein-90 (HSC70/HSP90) chaperone

machinery (Iwasaki et al. 2010). Altogether they form the miRNA-induced silencing complex (miRISC). The N-domain of AGO starts the unwind the miRNA duplex originating: a guide or mature strand, thermodynamically more stable and prevalent with higher biological activity that is retained in the miRISC complex; and a passenger strand (miR*), which is released to either be degraded or incorporated into another miRISC complex (Kwak and Tomari 2012; Noland and Doudna 2013; Meijer et al. 2014). The four AGO proteins expressed in humans (AGO-1, -2, -3 and -4) can perform non-cleavage inhibition of mRNA, but only AGO-2, the most abundantly expressed AGO protein, has nuclease activity, meaning that it is the only one able to cleave the target mRNA (Figure 1.2) (González-González et al. 2008; Valdmanis et al. 2012; Wang et al. 2012a). The majority of miRNA follows the canonical biogenesis pathway (described above); nevertheless, miRNA that are similar in structure and function but bypass some of the maturation steps of the canonical pathway have been described, the non-canonical miRNA. There are three major alternatives to synthesize these miRNA: i) Drosha/DGCR8-dependent and Dicer-independent pathway; ii) Drosha/DGCR8-independent and Dicer-dependent pathway; iii) Drosha/DGCR8-independent and Dicer-independent pathway, reviewed at (Abdelfattah et al. 2014; Daugaard and Hansen 2017).
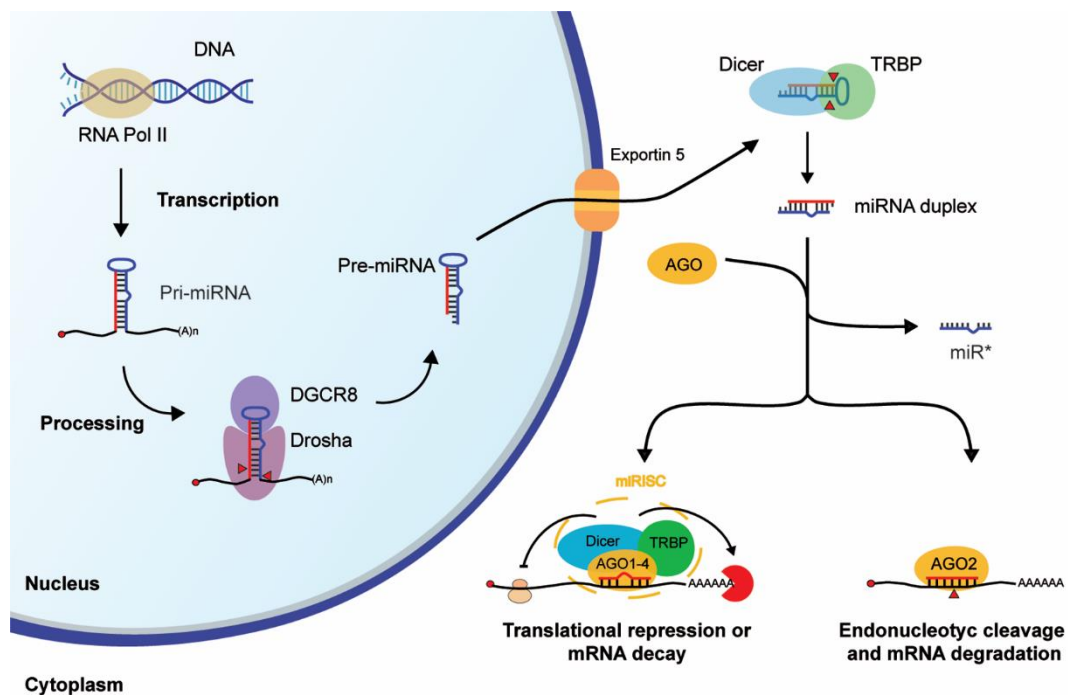
Figure 1.2 Schematic representation of the canonical pathway of microRNA (miRNA) biogenesis.
Briefly, miRNA are mostly transcribed by the RNA polymerase II into long transcripts called pri-miRNA that are processed into a miRNA precursor (pre-miRNA) of approximately 60 nucleotides (nt) long, by the microprocessor complex composed of DiGeorge Syndrome Critical Region 8 (DGCR8) and Drosha. The pre-miRNA is exported to the cytoplasm *via* Exportin 5 transporter, where it is further processed into a miRNA duplex (~22 nt) by Dicer and TRBP (transactivation-response RNA-binding protein) proteins. In the presence of proteins of the Argonaut family (AGO 1 to 4), the most thermodynamically stable strand of the miRNA duplex is selected as the guide/mature strand while the other, passenger strand (miR*), is released usually to be degraded. Following processing, miRNA are assembled into miRNA-induced silencing complexes (miRISC complex) composed of miRNA, AGO, Dicer and TBRP proteins. In some cases, mostly seen in plants, miRNA are able to bind mRNA with perfect of nearly perfect complementarity resulting in endonucleolytic cleavage and mRNA degradation. In other cases, mostly seen in animals, the miRNA binds to the target mRNA with incomplete pairing presenting mismatches and/or bulges, which results in mRNA translational repression and/or mRNA decay.

miRNA are able to regulate in a very precise way the expression of hundreds of different genes. The same miRNA can bind to numerous different mRNA and a single mRNA can present multiple miRNA binding sites, either for the same or for different miRNA (Friedman et al. 2009). The target recognition of the miRNA is mainly based on Watson-Crick pairing of a specific region from nt 2 to 8, seed sequence, and a match site in the 3'UTR (Bartel 2009; Wang 2014). miRNA can regulate translation of mRNA either by pairing with the target mRNA in a perfect or near perfect complementary way, mostly seen in plants, where AGO-2 cleaves the target mRNA (Figure 1.2) (Bartel 2004; Yekta et al. 2004; Karginov et al. 2010). In animals, the miRNA-mRNA interaction is mainly made through incomplete pairing with presence of mismatches and/or bulges. Herein, mRNA translational repression and mRNA destabilization/decay mechanisms prevail (Huntzinger and Izaurralde 2011; Eichhorn et al. 2014). There are still some controversies regarding the contribution of each mechanism for miRNA action. However, recent developments in the field indicate that miRNA action is time-dependent, promoting mRNA translational repression in an initial phase followed by a dominant effect of mRNA degradation in the steady-state (Djuranovic et al. 2012; Béthune et al. 2012; Meijer et al. 2013; Larsson and Nadon 2013; Eichhorn et al. 2014).

miRNA were found to be essential for several biological processes including self-renewal and cell differentiation, neuronal maturation, cell cycle and apoptosis, to name a few. Their presence in diverse biological fluids, such as blood, cerebrospinal fluid and urine, highlights its clinical relevance. Circulating miRNA are very stable and they seem to escape RNases by binding circulating proteins or exosomes (Sohel 2016). miRNA are involved in the control of central nervous system development and adult neurogenesis, which suggests a possible role of miRNA in brain pathologies. Indeed, in different CNS disorders a specific signature of miRNA in terms of expression not only in the affected tissue, but also in the circulant fluids has been reported. Deregulation of certain miRNA has been linked with pathological conditions including cancer, neurodegenerative disorders, inherited diseases, and many others (Jiang et al. 2009). As so, miRNA might be versatile molecules with a high clinical potential. Indeed, the same miRNA can bind to several different targets and control entire signaling pathways making them relevant therapeutic and/or target molecules for brain pathologies. Therefore, diverse novel technologies have been developed in order to improve exogenous miRNA function and stability. For example, miRNA mimics are non-natural double stranded RNA that once inside the target cell perform the same action as the endogenous miRNA, being used for gain of function studies (Wang 2009). Another example is anti-miRNA, antagomiR or blockmiR that are chemically engineered oligonucleotides, similar to miRNA mimics, used for loss of function/inhibition studies. These anti-miRNA are complementary to the mature sequence of a specific miRNA of interest and bind to it in an irreversible manner (Krutfeldt et al. 2005). Furthermore, there are still some gaps in our knowledge regarding the role of miRNA in the central nervous system as well as some contradictory information that need to be clarified for developing efficient miRNA-based therapies. For example, miRNA similar sequence and short length allied to limitations on the miRNA techniques can cause misinterpretations of the results, hampering the reproducibility needed for clinical translation (Witwer and Halushka 2016). Nevertheless, several miRNA technologies have already translated into clinical trials (Li and Rana 2014). A good example of miRNA-based therapeutics is the locked nuclei acid (LNA)-modified antisense

inhibitor of miR-122 (miravirsen), currently in phase II clinical trials, that showed to be highly effective in reducing the hepatitis C virus from chronic patients without causing serious side effects (Lindow and Kauppinen 2012). Our knowledge regarding miRNA increased during the past years leading to stability and nuclease resistance improvement of miRNA by chemical modifications as well as the development of some promising miRNA-based strategies currently in clinical trials. Still, the delivery of miRNA into tissues, namely into the brain, is a major limitation for the development of miRNA-based therapies. Thus, improvements on brain delivery strategies for miRNA are pivotal.

1.4 MicroRNA-124

The miR-124 was firstly identified in mice and it is transcribed from three different loci: miR-124-1 on chromosome 14, miR-124-2 on chromosome 3 and miR-124-3 on chromosome 2. The three copies have similar mature sequence and are highly conserved among species, including mice and humans. The expression levels of miR-124 increase in the prenatal period peaking at the end of the fetal development and remain elevated in the post-natal brain (Krichevsky et al. 2003). miR-124 accounts for 25% to 48% of the total miRNA in the adult brain, and it is highly expressed among all brain regions except the pituitary gland. Outside the CNS, miR-124 is 100-times less expressed than in the brain, being also considered a neuronal specific miRNA, since it is mostly expressed in neuronal cells (Lagos-Quintana et al. 2002; Mishima et al. 2007; Baroukh and Van Obberghen 2009). miR-124 is able to regulate hundreds of non-neural genes that are responsible for neural phenotype acquisition and maintenance being known as a master regulator of neurogenesis (Lim et al. 2005; Conaco et al. 2006). Expression of miR-124 is initiated during the transition of NSCs to progenitor cells and enhanced with neuronal maturation (Cheng et al. 2009; Akerblom et al. 2012). It has been shown that overexpression of miR-124 results in forced neuronal differentiation both in progenitor cells (Visvanathan et al. 2007; Yu et al. 2008) and in HeLa cells (Lim et al. 2005). Lentiviral overexpression of miR-124 precursor in combination with other factors, namely miR-9, also led to a forced differentiation of human neonatal foreskin fibroblasts into functional mature neurons (Yoo et al. 2011). *In vivo*, miR-124 overexpression in the SVZ increased the number of newborn neurons without affecting their migratory capability (Cheng et al. 2009; Akerblom et al. 2012), while its downregulation led to a 30% reduction of post-mitotic neurons (Cheng et al. 2009). Knockdown of miR-124-1 in mice resulted in a smaller brain size, neuronal dysfunction and axonal miss-sprouting in the dentate gyrus (Sanuki et al. 2011). miR-124 not only promotes neuronal commitment, but it also controls the choice among neuronal and astrocytic differentiation through fine-tuning the expression of a critical epigenetic regulator, Ezh2 (Neo et al. 2014), inhibition of the signal transducer and activator of transcription 3 (STAT3) signaling (Krichevsky et al. 2006), and reduction of Sox9 expression (Cheng et al. 2009) (Figure 1.3). miR-124 expression enhances axonogenesis by regulating the level of cytoskeletal proteins (Yu et al. 2008; Gu et al. 2014), and regulates dendritic differentiation by targeting the ras homology growth-related (RhoG) pathway (Figure 1.3) (Franke et al. 2012). Moreover, miR-124 is required for homeostatic plasticity, a compensatory adjustment in neuronal activity (Hou et al. 2015).

Several miR-124 predicted targets that contribute to its neurogenic potential have been confirmed experimentally (Figure 1.3). The REST pathway is one of them. REST regulates miR-124 transcription

in non-neuronal cells and it is responsible for inhibiting the expression of neural genes. In neuronal cells, miR-124 keeps REST silent promoting the expression of pro-neuronal genes (Conaco et al. 2006; Visvanathan et al. 2007). The small c-terminal domain phosphatase 1 (SCP1), a critical inducer of chick and mouse embryonic neurogenesis and part of the REST signaling pathway is downregulated by miR-124 (Visvanathan et al. 2007). Other components of the REST signaling pathway including the methyl CpG binding protein 2 (MeCP2) and coREST also present binding sites for miR-124 (Wu and Xie 2006). Moreover, miR-124 controls the transition of a chromatin-remodeling complex, changing the BAF complex subunits from neural-progenitor-specific to neuron-specific, an essential step for post-mitotic neural development and dendritic outgrowth during embryogenesis (Yoo et al. 2009). Another important target of the miR-124 is the RNA binding polypyrimidine tract-binding protein 1 (PTBP1). During neuronal differentiation, miR-124 decreases PTBP1 levels increasing the amount of PTBP2 in the cells and triggering neuron-specific alternative splicing patterns (Makeyev et al. 2007). Interestingly, it was shown that downregulation of PTBP by miR-124 is sufficient to generate functional neurons from fibroblasts (Xue et al. 2013). The Notch signaling pathway is of utmost importance for the maintenance of neural stem/progenitor cells. The Notch receptor is expressed by NSCs, which in the presence of its ligand Jagged1 contributes to self-renewal and maintenance of the undifferentiated state. In rodents SVZ, overexpression of miR-124 represses Jag1 translation leading to NSCs differentiation (Cheng et al. 2009; Liu et al. 2011). Additionally, miR-124 represses the expression of the transcription factor Sox9 in the SVZ, a regulator of gliogenesis (Cheng et al. 2009). Although many aspects of the miR-124 regulatory network need to be unveiled, these data clearly support the idea that miR-124 is able to modulate both embryonic and adult neurogenesis, namely in the SVZ.
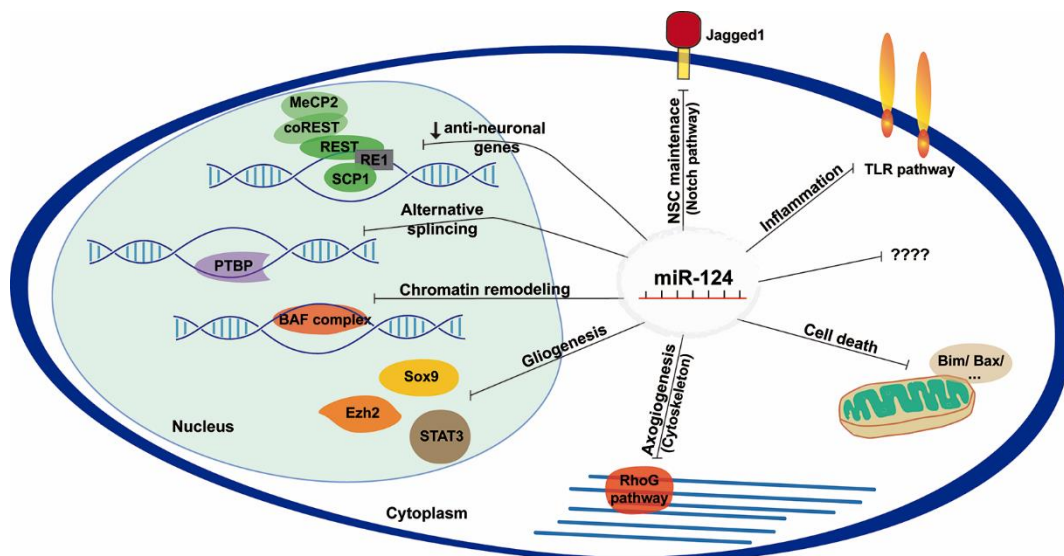
Figure 1.3 Schematic representation of miR-124 molecular targets and pathways experimentally identified. miR-124 induces neuronal differentiation by targeting mRNA of proteins inhibiting neuronal differentiation, such as the REST pathway and the Jagged1 protein, a Notch ligand. miR-124 also regulates alternative splicing through targeting the PTBP protein and chromatin remodeling through the BAF complex. The choice between neuronal and glial fate is also controlled by miR-124 once it downregulates Sox9, STAT3 and the epigenetic regulator Ezh2. miR-124 is not only an inducer of neurogenesis, but it also improves axonogenesis by regulating cytoskeleton proteins (RhoG), decreases inflammation (TLR pathway) and cell death. Bax, Bcl-2-associated X protein; Bim, Bcl-2-like protein 11; Ezh2, enhancer of zeste homolog 2; MeCP2, methyl CpG binding protein 2; PTBP, RNA binding polypyrimidine tract-binding protein; REST, RE1 silencing transcription factor; STAT3, signal transducer and activator of transcription 3; TLR, toll-like receptor.

miR-124 is a brain-specific miRNA, specially expressed in neurons; nevertheless, in the past decade new evidence have pointed to the importance of this miRNA in the regulation of cell death and inflammatory processes, resulting in neuroprotection in PD (Kanagaraj et al. 2014; Wang et al. 2015a; Gong et al. 2016), alleviation of cell death in Alzheimer's disease (Fang et al. 2012) or reduction of infarct volume in stroke (Doeppner et al. 2013; Sun et al. 2013a), among others, reviewed at (Sun et al. 2015b). Microglia cells are the first line of defense in the brain and in a physiological situation they show an active but ramified morphology (resting state). Upon injury, these cells become stimulated either in a classical way, M1 state, perpetuating inflammation, or in an alternative pattern, M2 state, with anti-inflammatory properties. Ponomarev and others showed that miR-124 was expressed in resting microglia, but it was undetectable in peripheral monocytes and macrophages. However, in a mouse model of autoimmune encephalomyelitis, characterized by activation of microglia and the infiltration of peripheral macrophages in the brain parenchyma, miR-124 expression was reduced approximately 70% in microglia and it was slightly expressed in the infiltrated macrophages during the disease onset and recovery, indicating a role of miR-124 in the maintenance of microglia quiescent state (Ponomarev et al. 2011). Moreover, administration of exogenous miR-124 into macrophages decreased pro-inflammatory markers and increased anti-inflammatory ones through downregulation of the C/EBP-α-PU.1 pathway. As so, miR-124 showed to be a key regulator of microglia quiescent state and a modulator of peripheral monocytes/macrophages (Ponomarev et al. 2011; Ponomarev et al. 2013; Veremeyko et al. 2013). In human intermediate monocytes, obtained from patients with allergies and bronchial asthma, miR-124 expression levels were also elevated and cells presented M2 characteristics (Veremeyko et al. 2013). In fact, reduction of miR-124 expression levels was shown to be needed to induce microglial reactivity (Freilich et al. 2013), while its overexpression results in lower levels of TNF-α in reactive macrophages (Sun et al. 2016). miR-124 mediates repression of ubiquitin-specific protease 2 (USP2) and USP14, and the modulation of toll-like receptor (TLR) signaling (Figure 1.3; e.g. STAT3, TNF-α converting enzyme (TACE), necrosis factor (NF)-κB p65 and TNF receptor-associated factor 6 (TRAF6)) that facilitates its anti-inflammatory properties (Sun et al. 2013b; Qiu et al. 2015).

The miR-124 is also involved in brain disorders such as PD and stroke. In fact, from all the miR-124 validated targets 25% are altered in PD (Sonntag 2010). Expression levels of miR-124 were decreased not only in cell lines of dopaminergic neurons (MN9D and SH-SY5Y) subjected to a methyl phenyl pyridinium (MPP) iodide or MPTP insult (*in vitro* models of PD), but also in the SN of a MPTP PD mouse model (Kanagaraj et al. 2014; Wang et al. 2015a; Gong et al. 2016). *In vitro*, miR-124 knockdown resulted in augmented oxidative stress, autophagy and apoptosis, while its overexpression had the opposite effect. These effects were associated with the modulation of calpain/cyclin-dependent kinase 5 (cdk5) pathway, 5' AMP-activated protein kinase and mechanistic target of rapamycin (AMPK/mTOR) signaling pathway and Bim (B-cell lymphoma (Bcl)-2-like protein 11; an apoptotic regulator) (Kanagaraj et al. 2014; Wang et al. 2015a; Gong et al. 2016). Wang and colleagues also reported that mice treated with miR-124 agomiR in the lateral ventricle, 2 days before the MPTP intoxication, had lower dopaminergic neurodegeneration in the SN and higher dopamine levels in the striatum when compared with non-treated MPTP-mice. The neuroprotective role of miR-124 was explained by the inhibition of the autophagic and apoptotic processes due to downregulation of the Bim

protein and a consequent reduction of translocation of Bcl-2-associated X protein (Bax) to the mitochondria (Figure 1.3) (Wang et al. 2015a).

In stroke, miR-124 was found to be decreased in the serum of patients within the first 24 h and correlated with a worse stroke prognosis (Liu et al. 2015). Nevertheless, Ji and others reported increased levels of miR-124 in exosomes obtained from serum of a stroke patient (Ji et al. 2016). In the ischemic brain of rodents, miR-124 is decreased in neural progenitors cells of the SVZ and in the ischemic core (Liu et al. 2011; Sun et al. 2013a). There is some controversy regarding miR-124 functions in stroke. Some studies reported that the downregulation of miR-124 resulted in a reduction of infarct volumes in rodent MCAO models of stroke (Liu et al. 2013; Zhu et al. 2014). Others observed that miR-124 overexpression previous to the MCAO insult in mice resulted in neuroprotection, reduced inflammation and increased neurogenesis leading ultimately to amelioration of stroke-induced neurological deficits (Doeppner et al. 2013; Sun et al. 2013a). More recently, Hamzei Taj and colleagues reported that mice subjected to MCAO benefited from an injection of a miR-124 mimic into the striatum two days after the lesion. The miR-124 treatment resulted in lower infarct volumes and behavior deficits together with the regulation of the inflammatory response by shifting the microglia from a more pro-inflammatory state (ionized calcium binding adaptor molecule 1 and cluster of differentiation 16/36 (Iba1/CD16/32)-positive cells) to an anti-inflammatory state (Iba1/CD206-positive cells) (Hamzei Taj et al. 2016b; Hamzei Taj et al. 2016a). It is of importance to notice that miR-124 functions may vary dependent of the context. For example, in a rat model of epilepsy miR-124 led to a robust increase of microglia (CD11b-positive cells), a slight increase of astrocytes (GFAP-positive cells), and higher levels of inflammatory cytokines including IL-1β, TNF-α, and IL-6 (Brennan et al. 2016).

Altogether, these studies point towards the use of miR-124 as a broad therapeutic molecule in neurodegenerative disorders and acute brain pathologies, where it may act as neuroprotectant, anti-inflammatory mediator and enhancer of endogenous brain repair mechanisms.

1.5 Nanoparticles for drug/genetic material delivery

The unique features of miRNA make them valuable and versatile tools for clinical applications as biomarkers for diagnosis and prognosis of pathologies and/or therapeutic molecules that can act on diverse key targets or even pathways that are disease-related. miRNA are hydrophilic, negatively charged molecules with high molecular weight. These features make them extremely unstable *in vivo* (low half-life time in plasma and high clearance rate) and hamper the uptake of miRNA into target cells. Another important aspect to consider in miRNA-based therapeutics is dosage. High dosages of miRNA can result in saturation of the miRNA machinery leading to cellular toxicity, off-target effects that can cause toxicity in non-target tissues, and immunological response that can be harmful for the recipient (Chen et al. 2015). As so, improvement of brain delivery vehicles is of major importance.

Several micro- and nanomaterials have been developed over the last decades to carry therapeutic molecules into the brain parenchyma. Lipid-based carriers, polymeric NPs, inorganic NPs, viral vectors, micelles, nanofibers, among others are examples of therapeutic carriers that have been intensively studied to improve drug delivery into the brain and reduce peripheral accumulation.

NPs are colloidal carriers that can have a natural (e.g. Albumin, chitosan) or synthetic origin. Synthetic NPs can be polymeric (e.g. poly(ethylenimine) (PEI), poly(lactic-co-glycolic acid) (PLGA), poly(lactic acid) (PLA)) or inorganic (e.g. gold, silica). NPs can vary in size from 1 to 1000 nm and in shape from spherical, cubic, rod-like, among other forms. Moreover, NPs transport their cargo entrapped, adsorbed or covalently bound to the surface and can be positively or negatively charged or zwitterionic (Figure 1.4). Cationic NPs (positively charged) are commonly used for genetic material delivery, since they can interact with DNA and/or RNA (negatively charged) and still present a positive net charge, which allow them to bind the negatively charged plasma membrane of the target cell in a higher extent than their negative or neutral counterparts (Lorenz et al. 2006). However, positively charged NPs seem to be more toxic than neutral and anionic ones (Goodman et al. 2004; Schaeublin et al. 2011). Interestingly, NPs with high positive charges seem to cause membrane damage and, eventually toxicity to the BBB (Lockman et al. 2004). Yet, some NP formulations with moderate positive charge (up to 15 mV) have been reported as efficient vehicles to cross the BBB (Jallouli et al. 2007; Gao et al. 2014). On the other hand, negative NPs tend to cause intracellular damage. Cellular uptake is usually more efficient for spherical small NPs (from 20 nm to 50 nm), although studies suggest that small NPs are more toxic than larger ones (Jiang et al. 2008). Also for systemic delivery, a clear inverse relationship between NP size and BBB penetration has been showed. For example, low size gold NPs (15 nm) accumulate 3- and 250-times more in the mouse brain than 100 nm and 200 nm gold NPs, respectively. However, low size NPs (< 15 nm) can be disadvantaged, since 4 nm NPs are rapidly taken up by the reticuloendothelial system or transported across the endothelium of major arteries before reaching the brain (Sonavane et al. 2008).

The attachment of functional groups and coatings into NPs can be advantageous to improve cellular uptake, to prevent endolysosomal degradation or to enhance specificity of the NPs to the target cell, decreasing off-target effects (Figure 1.4). The use of diverse surfactants and/or ligands/receptors is also essential for systemic applications, since they can be recognized and interact directly or indirectly with brain endothelial cells or increase blood time circulation improving the passage of NPs through the BBB. For example, the use of peptides, proteins, antibodies against specific receptors or transporters of the brain endothelium (e.g. transferrin receptor, lactoferrin receptor) improve brain penetration by direct contact with the BBB (Wiley et al. 2013; Gromnicova et al. 2013; Shilo et al. 2014). In addition, the use of specific ligands in NPs can improve specificity of the NPs to the cell population of interest. For example, delivery of monoclonal anti-CD15 antibody conjugated superparamagnetic iron oxide NPs is able to specifically bind to NSCs and can be used as a probe to monitor endogenous NSCs in the rat brain (Jiang et al. 2008). Anti-fouling molecules such as poly(ethylene glycol) (PEG) are also important coating molecules for NPs. PEGylated NPs present minimal surface charge leading to lower NP opsonization and lower reticuloendothelial system uptake (Li and Huang 2009). Grafting NPs with PEG decreases protein adsorption and slows down their clearance (Lee et al. 2009; Walkey et al. 2012). Moreover, due to its improved blood circulation time, PEGylated NPs accumulate more efficiently in the brain (Martinez-Veracoechea and Frenkel 2011; Nance et al. 2012). In addition, the use of amphiphilic ligands/peptides increases hydrophobicity of NPs and therefore, is also used to improve NPs ability to cross lipid membranes or the BBB (Guerrero et al. 2010). Taken together, the advantages of NPs are a

high load of cargo, the ability to protect the cargo, a high stability both *in vivo* and storage, and easiness to be modulated in terms of size, shape, surface and chemistry. Thus, NPs are attractive vehicles to transport molecules into the CNS.
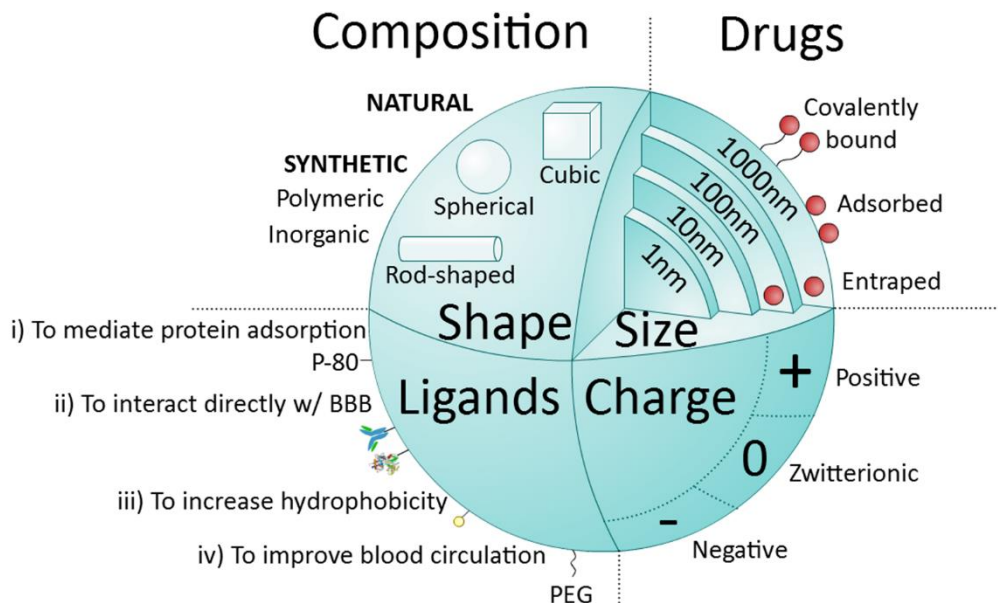
Figure 1.4   Main nanoparticle (NP) features.
NPs can be classified into natural, when molecules such as proteins (albumin), polysaccharides, chitosan, among others are used, or synthetic. Synthetic NPs can be made of very common polymers such as poly(lactic-co-glycolic acid) (PLGA), poly(ethylenimine) (PEI), polyesters (poly(lactic acid) (PLA), or from inorganic agents like gold, silica or alumina. NPs can vary in size (1-1000 nm) and are able to deliver drugs into cells by entrapping, adsorbing or covalently binding them. NPs can assume different shapes (spherical, cubic, rod-like) and charges (negative, zwitterionic, positive). Another important feature of NPs is the possibility of functionalization with different types of ligands. Ligands are distributed into four major categories: i) capable of mediating protein adsorption (e.g. poly(sorbate) 80 (P-80)); ii) able to interact directly with the BBB (e.g. transferrin proteins, antibody or peptides); iii) capable of increasing hydrophobicity (e.g. amphiphilic peptides); and iv) able to improve blood circulation (e.g. poly(ethylene glycol) (PEG)).

NPs can be used not only as vehicles to deliver therapeutic agents but also as imaging agents or both. The so called theranostic agents confer diagnosis and therapy at once and normally take advantage of nanosystems that are by themselves imaging agents, such as gold, silica, iron oxide NPs, quantum dots and carbon nanotubes (Xie et al. 2010). For example, liposomes encapsulating citicoline (an inherent chemical exchange saturation transfer (CEST) magnetic resonance imaging (MRI) signal) can be detected in the brain following transient MCAO in rats in a label-free fashion, namely in the areas where BBB was disrupted (Liu et al. 2016). In fact, we have developed a NP formulation composed of material approved for other applications by the Food and Drug Administration (FDA): a polymeric agent, PLGA; a cationic peptide, protamine sulfate, which allows an efficient complexation of negatively charged molecules, namely miRNA; and perfluoro-1,5-crown ether (PFCE), a compound detectable by ^{19}F MRI. This formulation showed to be very effective in promoting intracellular delivery of miR-132 into endothelial cells, which subsequently exerted a pro-survival and pro-angiogenic effect in these cells when exposed to hypoxic conditions both *in vitro* and *in vivo*. Moreover, transplanted cells previously transfected with this NP formulation were tracked by ^{19}F MRI *in vivo* in an ischemic limb mouse model (Gomes et al. 2013). ^{19}F MRI is the ideal tool for non-invasive repeated imaging in a living organism, providing high resolution and contrast and quantitative analysis of target cells.

1.5.1 Brain delivery routes

Brain delivery of NPs can be achieved by different types of administration being the most commonly used in research the intracerebral, intranasal and/or systemic administrations (Figure 1.5). Even though, intracerebral administration is a highly invasive procedure, it guarantees delivery of high dosages of therapeutic molecules in a precise way for a long period of time. Moreover, intracerebral injections bypass issues such as immunogenicity, biodistribution, pharmacodynamics, and failure in crossing the BBB. As so, this route of administration is of major importance in pre-clinical studies specially for proof-of-principle studies. Intranasal administration has been highly studied since it is a method that circumvents the BBB. Intranasal delivery is also rapidly absorbed, non-invasive and non-destructive method of drug administration. Nevertheless, dosage, physicochemical properties of the therapeutic formulation and surface area of the nasal cavity (50% in rodents and 5% in humans) hamper the delivery of effective dosages of pharmaceuticals in most brain regions (Zhang et al. 2016c). Moreover, in pathologies such as PD, patients may present several alterations in nasal cycle, nasal mucosa pH and mucociliary clearance time (Kotan et al. 2013) that may account for reduced biodistribution and bioavailability of NPs. Systemic administration, namely intravenous injection, is much less invasive compared to intracerebral administration. Systemic delivery also allows the delivery of higher dosages of drug than the intranasal strategy, since it is a compartment with higher extent. Nevertheless, the BBB, which is a very selective barrier involved in the complex mechanisms of brain homeostasis and protection, represents the major obstacle for the passage of novel drugs targeting the brain parenchyma (Almutairi et al. 2016). Although some molecules with appropriate lipophilicity, size and charge can diffuse from blood into the brain, most molecules, both large (e.g. polypeptides, antibodies, interference RNA, miRNA) and small, are unable to overcame the BBB. As abovementioned, the use of NPs, especially when functionalized with diverse ligands can improve brain delivery through the BBB.

Beside all the efforts made in the development of NPs for brain delivery, further research is needed to clarify the differences in the transport of NPs in healthy and disease animal models, always bearing in mind the limitations of an experimental model which cannot fully mimic a given human disease. Indeed, no systematic studies have been performed to elucidate how the physicochemical properties of NPs may affect its transport across the BBB and brain localization in PD and stroke models. However, recent successes using antibodies to cross the BBB (Zhou et al. 2011; Yu et al. 2011; Niewoehner et al. 2014) might inspire NP bioengineers to design new formulations with enhanced properties. Addressing safety issues is also very important to translate this research area into potential clinical therapies. For example, systemic delivery of NP formulations targeting the brain still accumulate significantly in other regions of the body, such as liver, spleen, kidney among other organs/tissues, before being eliminated. Thus, it is important to design nanoformulations that only after reaching the brain are remotely triggered to release the drug instead of doing so in other places of the body (Li et al. 2015). It is expected that future developments in triggerable nanoformulations will facilitate the clinical translation of NPs. Another important issue that deserves further investigation is the development of NPs that can target specific brain cells. For instance, in neurodegenerative disorders targeting specific brain cells, such as dopaminergic neurons (main target in PD), microglia (neuroinflammation), or neural

stem cells (neuronal repair), might enhance its potential therapeutic value. In conclusion, the development of new platforms that are able to exploit brain alterations occurring in these disorders in combination with promising therapeutic and/or imaging agents is essential to develop more efficient non-invasive and brain-directed therapies able to reach the clinic.
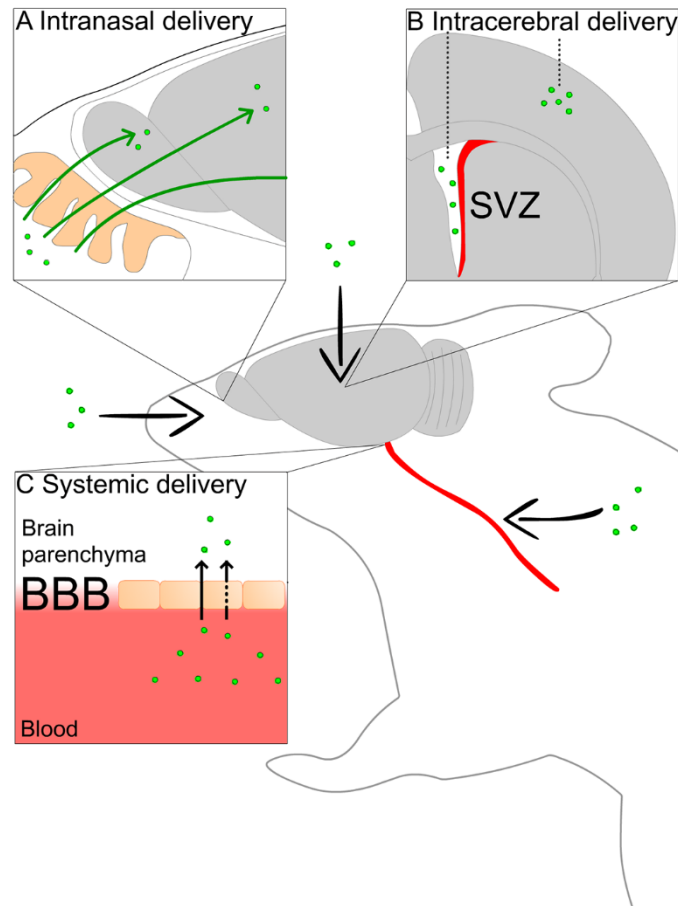
Figure 1.5 Administration of nanostructured materials to target the brain.
A) intranasal, (B) intracerebral and (C) intravenous or intraperitoneal delivery pathways. Nanomaterials delivered by the intranasal route (A) target several brain regions, including neurogenic and non-neurogenic regions. Intracerebral injections (B) maximize the amount of materials and their cargo that interact locally with cellular components of the neurogenic niche, such as the subventricular zone (SVZ) or other relevant areas. The intravenous or intraperitoneal administration (C) may require additional coatings of the surface of nanoparticles to allow an efficient passage through the blood brain barrier (BBB). Nanomaterials are shown in green; figure represents a rodent model.

1.6 Objectives

To date, no causative therapies are available in common acute and neurodegenerative CNS disorders that can restore lost neurological function. Several regenerative medicine approaches address this issue i.e. by the use of stem cells therapies (Schapira 2009). Indeed, NSCs can be an inexhaustible source of neurons that can be recruited and/or transplanted to promote brain repair (Pluchino et al. 2003; Lindvall and Kokaia 2010). miR-124 has been described as a key neuronal fate determinant and, more recently, it has been identified as anti-apoptotic and anti-inflammatory molecule. Intracellular delivery of miRNA may be accomplished by chemical modification, liposome/microvesicle encapsulation, viral infection and electroporation. However, these strategies raise safety issues, limitations in stability and versatility, and do not allow an accurate non-invasive imaging of the reprogramming factors' spatial release within cells. The use of NPs constitutes a powerful platform to overcome these limitations by allowing protection, stability and spatio-temporal control of pro-neurogenic factors. To overcome these limitations, we proposed to use novel biodegradable NPs, developed by the Lino Ferreira lab that have already given proofs of an efficiently intracellular release of miRNA and can be monitored by MRI (Gomes et al. 2013).

The main goal of this project was to study the inductive effect of NPs loaded with miR-124 (miR-124 NPs) in terms of differentiation of SVZ stem/progenitor cells *in vitro* and to evaluate their therapeutic potential *in vivo*, namely in mouse models of PD and stroke. To achieve the main goal of the project we performed studies to:

1) Evaluate the effects of miR-124 NPs on SVZ NSCs *in vitro*, namely on cell survival, differentiation, proliferation, axonogenesis, as well as the identification of putative miR-124 molecular targets;

2) Disclose the neurogenic and functional effects of miR-124 NPs in a pre-clinical mouse model of PD;

3) Unravel the effects of miR-124 NPs on cell viability, proliferation and neurogenic potential of SVZ cultures exposed to glucose and oxygen deprivation (*in vitro* model of stroke);

4) Assess the role of miR-124 NPs in the modulation of stroke outcome *in vivo*.

Chapter 2

MATERIALS AND METHODS

2.1 Synthesis of PLGA nanoparticles

Poly(lactic-co-glycolic acid) (PLGA) NPs were prepared as described by Gomes and colleagues (Gomes et al. 2013). Briefly, PLGA (Resomers 502 H; 50:50 lactic acid/glycolic acid; Boehringer Ingelheim Lda, Ingelheim, Germany) was covalently conjugated to fluoresceinamine (Sigma-Aldrich, Taufkirchen, Germany). NPs were prepared by dissolving PLGA (100 mg) in a solution of dichloromethane/trifluoro-ethanol (1:8) containing PFCE (100 mg, Fluorochem, Derbyshire, UK). This solution was then added dropwise to a poly(vinyl) alcohol (PVA) solution (5% w/v in water), stirred and sonicated using ultrasonicated probe. Immediately after the solution was added dropwise in 40 mL Milli-Q water under stirring condition and left to stir for 3 h. NP suspension was dialyzed using dialysis membrane (MWCO of 50 kDa) for 3 days against Milli-Q water. NPs were coated with protamine sulfate (PS) in 1:1 (w/w) ratio by agitation at room temperature (RT) for 1 h. After this incubation period, NPs were dialyzed (MWCO of 12 kDa) against Milli-Q water for 3 days, followed by freezing and lyophilization to obtain a dry powder that was stored in a desiccator at RT.

2.2 Complexation of nanoparticles and microRNAs

NPs were weighed and sterilized under ultraviolet light before being resuspended in SVZ cell culture medium devoid of growth factors (*in vitro* experiments) and sonicated (Transsonic T460/HH, Elma Schmidbauer GmbH, Singen, Germany). To this suspension (1 to 20 µg/mL final concentration, specified in the text) a total of 200 nM of microRNA (miRNA or miR; 50 pmol of miR-124 or scramble-miR, both from GE Healthcare Dharmacon Inc., Chicago, USA) were added and allowed to complex for 45 min at 37 ºC with intermittent agitation. Void NPs were prepared using the same procedure but without adding miRNA. For *in vivo* experiments complexation of NPs was done in a similar manner, but using saline solution instead of SVZ cell culture medium to suspend the NPs. All miRNA were purchased from GE Healthcare Dharmacon Inc. and were provided annealed, desalted and in the 2'-hydroxyl form and were resuspended in sterile RNA free water. miR-124 mature sequence is 5'UAAGGCACGCGGUGAAUGCC3'.

2.3 Characterization of nanoparticles

Particle size and zeta potential of NP suspensions were determined using light scattering *via* a Zeta PALS zeta potential analyzer and ZetaPlus Particle Sizing Software (Brookhaven Instruments Corporation, NY, USA). Size measurements were performed at 25 ºC, and data were recorded at a 90º angle, with an equilibration time of 2.5 min and individual run times of 60 s. The diameters described are number-weighted average diameters. The zeta potential of NPs was determined in aqueous solutions at 25 ºC.

2.4 Subventricular zone cell culture

One to three day-old C57BL/6 mice were used to obtain subventricular zone (SVZ) cell cultures as described previously (Agasse et al. 2008b). SVZ fragments were dissected from 450 µm-thick coronal brain sections and placed into Hank's Balanced Salt Solution (HBSS) solution supplemented with 100

U/mL penicillin and 100 μg/mL streptomycin (all from Life Technologies, Carlsbad, CA, USA) and digested in 0.025% trypsin, 0.265 mM EDTA (all from Life Technologies), followed by mechanical dissociation. The single cell suspension was diluted in serum-free medium (SFM) composed of Dulbecco's modified Eagle medium [(DMEM)/F12 + GlutaMAX™-I)] supplemented with 100 U/mL penicillin, 100 μg/mL streptomycin, 1% B27 supplement, 10 ng/mL epidermal growth factor (EGF), and 5 ng/mL basic fibroblast growth factor-2 (FGF)-2 (all from Life Technologies) and plated onto uncoated petri dishes (Corning Life Science, NY, USA). Cells were allowed to develop in an incubator with 5% CO_2 and 95% atmospheric air at 37 ºC for five to six days. In these conditions, SVZ cells grow in suspension and generate neurospheres that are rich in neural and progenitor stem cells at distinct stages of differentiation and with proliferative and self-renewing abilities (Agasse et al. 2008b; Bernardino et al. 2008; Maia et al. 2011; Santos et al. 2012a). Neurospheres were then seeded onto 0.1 mg/mL poly-D-lysine- (PDL, Sigma-Aldrich) coated plates in SFM devoid of growth factors to induce cell differentiation.

2.5 Cell transfection

Five to six-day-old neurospheres were seeded onto 0.1 mg/mL PDL coated 6-well plates for quantitative (q)PCR analysis or in PDL-coated glass coverslips in 24-well plates for all the remaining experiments, in SFM medium devoid of growth factors. SVZ cells were allowed to form a cell monolayer for two days before testing the experimental conditions used. SVZ cell monolayer was then incubated with 1 to 20 μg/mL of void NPs or NPs complexed with 200 nM of miR-124 (miR-124 NPs) or scramble-miR (scramble-miR NPs) for 4 h in SFM devoid of growth factors at 37 ºC in an incubator with 5% CO_2 and 95% atmospheric air. Then, non-internalized NPs were washed out and SVZ cells were allowed to grow as a monolayer for different timepoints according to the parameter evaluated – Chapter 3.

2.6 Oxygen and glucose deprivation and experimental treatments

In Chapter 4, 2-days-old cell monolayer cultures were exposed to oxygen and glucose deprivation (OGD) for 1 h by replacing the SFM devoid of growth factors by 0.15 M phosphate-buffered saline (PBS) and incubating the cells in a MIC-101 modular incubator chamber (Billups-Rothenberg Inc., Del Mar, CA, USA) at 37 °C in a 5% CO_2 and 95% N_2 gas environment (0.1% O_2). SVZ cell cultures were then incubated in fresh medium (OGD non-treated cells) or transfected with 1 μg/mL of NPs alone or complexed with 200 nM of miR-124 or scramble-miR (under reoxygenation) in SFM devoid of growth factors for 24 h. A non-OGD control was used to compare the response of SVZ cells in normoxic *versus* OGD conditions. SVZ cells were then allowed to grow as monolayer for two or seven days to analyze cell death and proliferation or neuronal differentiation, respectively.

2.7 Internalization studies of miRNA NPs

SVZ cells were transfected with 10 μg/mL of fluorescein isothiocyanate-labeled NPs (FITC-NPs) complexed with 400 nM of miR-Dy547 (GE Healthcare Dharmacon Inc.) for 4 h at 37 ºC, rinsed and maintained in SFM medium devoid of growth factors for 24 h. Thereafter, cells were fixed with 4%

paraformaldehyde (PFA), permeabilized and blocked with 6% bovine serum albumin (BSA; Amresco LLC, Solon, USA) and 0.5% Triton X-100 (Fisher Scientific, Pittsburgh, PA, USA) in 0.1 M of PBS for 1 h at RT. SVZ cells were then incubated at 4ºC overnight (ON) with primary antibodies all prepared in 0.3% BSA and 0.1% Triton X-100 solution: anti-FITC, anti-nestin, anti-glial fibrillary acidic protein (anti-GFAP) and anti-doublecortin (DCX) (Table 2.1). After rinsing with PBS the respective Alexa Fluor-conjugated secondary antibodies were used (Table 2.2). Whenever appropriated, nuclei were stained with Hoechst-33342 (4 µg/mL in PBS, Life Technologies) for 5 min at RT. Thereafter, cells were mounted in Fluoroshield Mounting Medium (Abcam Plc.) and photomicrographs were taken using a confocal microscope (AxioObserver LSM 710, Carl Zeiss, Jena, Germany).

2.8 Immunocytochemistry

SVZ cultures were fixed with 4% PFA at different timepoints: 48 h for cell commitment or 7 days for SVZ differentiation and miR-124 targets expression (sox9 and jagged1). Cells were then permeabilized and blocked against non-specific binding sites for 1 h with 0.25% Triton X-100 and 3% BSA (cytoplasmic staining) or 6% BSA (nuclear staining). Cells were subsequently incubated ON at 4 ºC with a primary antibody (Table 2.1). Cells were then incubated for 1 h with the corresponding secondary antibody (Table 2.2) followed by Hoechst-33342 nuclear staining and mounted in Fluoroshield Mounting Medium (Abcam Plc.). Photomicrographs were taken using an AxioImager microscope or AxioObserver LSM 710 confocal microscope (both from Carl Zeiss).

Table 2.1 Primary antibodies used for immunostaining.

REACTIVITY	HOST	SUPLIER	DILUTION
Nestin	Mouse monoclonal	Abcam Plc	1:100
GFAP	Rabbit polyclonal	Abcam Plc	1:200
FITC	Goat polyclonal	Abcam Plc	1:200
FITC	Mouse monoclonal	Sigma-Aldrich	1:100
DCX	Goat polyclonal	Santa Cruz Biotechnology	1:200
Ki67	Rabbit polyclonal	Abcam Plc	1:50
GFAP	Mouse monoclonal	Abcam Plc	1:200
NeuN	Mouse monoclonal	Merck Millipore	1:100
Olig2	Rabbit polyclonal	Merck Millipore	1:200
Phospho-JNK	Rabbit polyclonal	Cell Signaling	1:100
Tau	Mouse polyclonal	Cell Signaling	1:200
Sox9	Rabbit polyclonal	Merck Millipore	1:200
Jagged1	Goat polyclonal	Santa Cruz Biotechnology	1:100

GFAP, glial fibrillary acidic protein; FITC, fluorescein isothiocyanate; DCX, doublecortin; NeuN, neuronal nuclei; Olig2, oligodendrocyte transcription factor 2; JNK, c-Jun N-terminal kinase.

Table 2.2 Secondary antibodies (Alexa-Fluor conjugated) used for immunostaining.

REACTIVITY	HOST - ALEXA	SUPLIER	DILUTION
Anti-goat	Donkey – Alexa 488	Life Technologies	1:200
Anti-goat	Donkey – Alexa 647	Life Technologies	1:200
Anti-goat	Donkey – Alexa 546	Life Technologies	1:200
Anti-mouse	Donkey – Alexa 647	Life Technologies	1:200
Anti-mouse	Donkey – Alexa 488	Life Technologies	1:200
Anti-mouse	Donkey – Alexa 546	Life Technologies	1:200
Anti-rabbit	Goat – Alexa 350	Life Technologies	1:200
Anti-rabbit	Donkey – Alexa 488	Life Technologies	1:200
Anti-rabbit	Donkey – Alexa 546	Life Technologies	1:200

2.9 Cell Survival studies
2.9.1 Propidium iodide incorporation

SVZ cells were treated with NPs and maintained in culture for 48 h after transfection. Propidium iodide (PI; 5 µg/mL; Sigma-Aldrich) was added in the last 10 min of the experimental protocol. Subsequently, cells were fixed with 4% PFA for 10 min, stained with Hoechst-33342 (4 µg/mL, Life Technologies) for 5 min at RT and mounted in Fluoroshield Mounting Medium (Abcam Plc.). Photomicrographs of PI incorporation were taken using an AxioImager microscope (Carl Zeiss, Göttingen, Germany).

2.9.2 TUNEL assay

SVZ cells were fixed with 4% PFA and permeabilized in 0.25% Triton X-100 for 30 min at RT. After permeabilization cells were incubated for 10 min with 3% H_2O_2. Cells were then allowed to react for terminal transferase (0.25 U/L) biotinylated dUTP (6 M) nick-end labeling of fragmented DNA in TdT buffer (pH 7.5) (all from Roche, Basel, Switzerland) for 1 h at 37 ºC in a humidified chamber. The enzymatic reaction was stopped by rinsing with PBS. Cells were then incubated for 1 h with rhodamine (1:200, Vector Laboratories, Burlingame, CA, USA), rinsed and stained with Hoechst-33342 (4 µg/mL in PBS; Life Technologies) as described previously. Then, cells were mounted in Fluoroshield Mounting Medium (Abcam Plc.). Photomicrographs were obtained using an AxioImager microscope (Carl Zeiss).

2.10 BrdU incorporation

5-bromo-2'-deoxyuridine (BrdU; 10µM, Sigma-Aldrich) was added to cultures 4 h before the end of the experiment. Thereafter, cells were fixed in 4% PFA and BrdU was exposed following permeabilization with 1% Triton X-100 for 30 min at RT and an incubation with 1 M HCL for 40 min at 37 ºC. Nonspecific binding sites were blocked with 6% BSA and 0.3% Triton X-100 for 1 h, followed by incubation with anti-BrdU Alexa-Fluor 594 conjugated antibody (Life Technologies) in 0.3% BSA and 0.3% Triton X-100 for 2 h at RT. Cells where then stained with Hoechst-33342 and mounted in Fluoroshield Mounting Medium (Abcam Plc.). Photomicrographs of BrdU incorporation were taken using a confocal microscope (AxioObserver LSM 710, Carl Zeiss).

2.11 Quantitative PCR analysis

Total RNA was isolated from SVZ cell cultures according to the illustra RNAspin mini RNA isolation kit manufacturer's instructions (GE Healthcare Life Sciences, Cleveland, OH, USA). cDNA was prepared from 1 µg total RNA using the iScript cDNA synthesis kit (Bio-Rad Laboratories, Inc., Hercules, CA, USA). Briefly, 1 µg of RNA was mixed with 4 µL of 5x reaction mix and 1 µL of reverse transcriptase followed by the reaction in a T100 thermal cycler (Bio-Rad Laboratories, Inc.): 5 min at 25 ºC, 30 min at 42 ºC and 5 min at 85 ºC. qPCR was performed by adding 0.5 µL of sample cDNA to 5 µL SYBR Green PCR master mix (Bio-Rad Laboratories, Inc.) and 1 µL of GAPDH, Sox9 or Jag1 primers (all Qiagen, Austin, TX, USA) in a total volume of 10 µL. The thermocycling reaction was performed in a CFX Connect real-time system (Bio-Rad Laboratories, Inc.): 3 min at 94 ºC followed by 40 cycles of 15 s at 94 ºC denaturation step, 30 s at 60 ºC annealing and elongation step. Quantification of target genes was performed relative to the reference gene GAPDH using the comparative Ct method, as previously reported by us (Santos et al. 2012a; Bernardino et al. 2012).

2.12 *In vivo* studies

All animal experimental procedures were performed in accordance with institutional approved guidelines for the care and use of laboratory animals: Malmö/Lund Ethical Committee for Animal Research and European Community guidelines (86/609/EEC; 2010/63/EU). Adult male C57BL/6 mice with 10-12-week-old (Harlan Laboratories Models, SL, Castellar, Spain) were used for the experiments performed in Chapter 3 while 9-week-old C57BL/6 J male mice (Charles River, Sulzfeld, Germany) were used in Chapter 4. For each experimental setting mice were housed in the same room and in similar cages under controlled conditions: 12 h light/dark cycle in RT (22 ºC) and *ad libitum* access to food and water. All animals were assigned to experimental groups before entering study.

2.13 Animal models of disease and treatments

2.13.1 6-OHDA model of Parkinson's disease and miRNA-loaded NPs treatments (intraventricular administration) – Chapter 3

Mice were anesthetized with an intraperitoneal (i.p.) injection of ketamine (90 mg/kg of mouse weight; Imalgene 1000, Merial, Lyon, France) and xylazine (10 mg/kg of mouse weight; Rompun 2%, Bayer, Leverkusen, Germany) before placing them in the digital stereotaxic frame (51900 Stoelting, Dublin, Ireland). An incision was performed with a scalpel to expose the mouse skull and scales were defined after setting the zero at the bregma point. In order to mimic Parkinson's disease (PD) phenotype a total of 10 µg of 6-hydroxydomine (6-OHDA; Sigma-Aldrich) dissolved in 0.02% of ascorbic acid (Fagron, Inc., St. Paul, MN, USA) was injected *per* animal in the right striatum (Anterior-posterior: −0.6 mm, Medial-lateral: −2.0 mm, Dorsoventral: −3.0 mm) (Virgone-Carlotta et al. 2013) with a Hamilton syringe at a speed of 0.2 µL/min. After injections, mice were kept warm (37 ºC) until they recovered from surgery. In sham-operated animals (healthy animals) the same procedure was performed but a saline solution (2 µL at 0.2 µL/min of 0.9% NaCl) was used instead of 6-OHDA.

To unveil the effect of our NP formulation in a mouse model for PD, mice were subjected to a double stereotaxic injection to deliver the 6-OHDA toxin into the right striatum, as described previously, and the NP formulations into the right lateral ventricle. As so, an intraventricular injection of 2.5 µL of miR-124 NPs (1 µg/mL of NPs loaded with 0.5 pmol miR-124) or saline solution (0.9% NaCl) was performed in the right hemisphere (Anterior-posterior: −0.5 mm, Medial-lateral: −0.7 mm, Dorsoventral: −2.9 mm) (Eiriz et al. 2014) using a Hamilton syringe at a speed of 0.5 µL/min. Four experimental groups were tested: 1) mice injected with saline both in the striatum and in the lateral ventricle – "Healthy Saline" (n=5, 0.9% NaCl); 2) mice injected with saline in the striatum and miR-124 NPs in the lateral ventricle- "Healthy miR-124 NP" (n=5, 2.5 ng NPs and 0.5 pmol miR-124); 3) mice injected with 6-OHDA in the striatum and saline in the lateral ventricle- "6-OHDA Saline" (n=4, 0.9% NaCl); 4) mice injected with 6-OHDA in the striatum and miR-124 NPs in the lateral ventricle- "6-OHDA miR-124 NP" (n=4, 2.5 ng NPs and 0.5 pmol miR-124). Mice were maintained in controlled conditions during the four weeks of experimental procedure before being euthanized. For internalization studies 3 µL of 10 µg/mL of FITC-NPs complexed with 1 pmol of miR-Dy547 (dissolved in saline solution) were injected into the lateral ventricle of 2 mice as described above. Twenty-four hours after injection mice were euthanized by perfusion and penetration of NPs evaluated in coronal sections by fluorescence microscopy.

2.13.2 Photothrombotic model of stroke and miRNA-loaded NPs treatments (intravenous administration) – Chapter 4

Unilateral photothrombotic (PT) cortical ischemia in the right primary motor cortex (Tennant et al. 2011) was performed as described previously (Walter et al. 2015). Briefly, animals were anesthetized with isoflurane (1.5 to 2% during surgery; Isobeta vet 100%, MSD, AN Boxmeer, The Netherlands) and placed into a stereotaxic frame. The local analgesic Marcain (AstraZeneca, Södertälje, Sweden) was injected followed by a scalp incision exposing the mouse skull. The subcutaneous connective tissue was remo ved and the skull bone was dried. An optic fiber with an aperture of 2 mm per 4 mm was placed in the right hemisphere (center +1.5 mm lateral and +0.5 mm anterior related to Bregma) and it was illuminated with a cold light source (Schott KL 1500 LCD, intensity: 3200 K/5D) for 20 min. A photosensitizing dye, Rose Bengal (0.1 mL at 10 mg/mL; Sigma-Aldrich), was injected intraperitoneally 5 min before the illumination. After illumination, the scalp incision was sutured and the mice were allowed to recover in their home cages. In sham-operated mice, the same procedure was performed but mice were injected with saline solution (0.1 mL of 0.9% NaCl) instead of the photosensitizer. Body temperature was monitored during the surgery and kept between 36 ºC and 37.5 ºC using a self-regulating heating pad. After surgery, mice temperature and body weight were monitored daily during the experiments and were not altered outside physiological ranges (data not shown).

After surgery, mice were allowed to wake up from anesthesia. Immediately after, mice were placed in a restrainer and injected in the tail vein with a total volume of 150 µL of either saline solution, void NPs, scramble-miR NPs or miR-124 NPs, respectively. Mice were divided into 8 different experimental groups: i) Sham-operated saline mice (n = 6, 0.9% NaCl); ii) Sham-operated void NPs mice (n = 5, 1 mg NPs); iii) Sham-operated scramble-miR NPs mice (n = 6, 1 mg NPs and 4 nmol scramble-miR); iv) Sham-operated miR-124 NPs mice (n = 5, 1 mg NPs and 4 nmol miR-124); v) PT-operated saline mice

(n = 16, 0.9% NaCl); vi) PT-operated void NPs mice (n = 11, 1 mg NPs); vii) PT-operated scramble-miR NPs mice (n = 12, 1 mg NPs and 4 nmol scramble-miR); viii) PT-operated miR-124 NPs mice (n = 12, 1 mg NPs and 4 nmol miR-124). Mice were maintained in controlled conditions during the 48 h or 14 days of experimental procedure before being euthanized. To reveal whether the NPs used in the study reached the brain parenchyma, pilot experiments were carried out. After PT, 3 mice were injected either with 1 mg, 5 mg or twice in intervals of 6 h with a dosage of 5 mg of FITC-NPs as described above. After 4 or 24 h, mice were perfused with 4% PFA and penetration of NPs was evaluated in coronal sections by fluorescence microscopy.

2.13.3 Proliferating cell labelling – BrdU incorporation

To label dividing cells, BrdU dissolved in a sterile solution of 0.9% NaCl was administered intraperitoneal (i.p.), at 50 mg *per* kg of animal body weight, in the three days (every 12 h) following the stereotaxic procedure (Chapter 3) or the intravenous injections (14 days protocol, Chapter 4).

2.14 Behavior analysis

2.14.1 Apomorphine-induced rotation test

At week 2 post-stereotaxic injections, mice (from section 2.13.1) received in the neck a subcutaneous injection of 0.5 mg/kg of apomorphine hydrochloride (Sigma-Aldrich) dissolved in 1% ascorbic acid and 0.9% NaCl. Mice were placed in round testing bowls for 45 min and their rotation behavior was recorded using a digital camera. Number of net contralateral turns = contralateral turns − ipsilateral turns; data are presented as percentage of 6-OHDA saline mice.

2.14.2 Rotating pole test

Rotating pole test was performed as described previously (Ruscher et al. 2009). Mice (from section 2.13.2) were trained for 2 days to traverse an elevated wooden pole (750 mm above ground, diameter 15 mm, length 1,500 mm) that was rotating at 0, 3 or 10 rotations *per* min (rpm) to the right or left. Mice were evaluated on the day before surgery (day -1) and on days 2, 7 and 14 after surgery. Mice were attributed a score from 0 to 6: 0, the mouse falls off the pole immediately upon placement of the pole; 1, the mouse is unable to traverse the pole remaining sitting or trying to go backwards; 2, the mouse falls off the pole while crossing or the hind limbs do not contribute to forward movement; 3, the mouse manages to reach the platform but it is constantly slipping with the fore- and/or hind limbs; 4, the mouse traverses the pole with more than four slips; 5, the mouse crosses the pole with one to three slips; 6, the mouse traverses the pole with no foot slips.

2.14.3 Grid test

Mice (from section 2.11.2) were trained to cross a grid (600 mm length) before surgery. Each mouse was evaluated before surgery (day 0) and at days 2, 7 and 14 after surgery. Each misstep of the paretic paws was counted as one fault and the number of faults was scored from 0 to 6: 0 – 6 and more faults; 1 – 5 faults; 2 – 4 faults; 3 – 3 faults; 4 – 2 faults; 5 – 1 fault; 6 – no fault.

2.15 Tissue collection

Mice were euthanized at different timepoints: 4 weeks after 6-OHDA lesion for immunohistochemistry analysis (dopaminergic lesion evaluation and neurogenesis, total of 18 mice) – Chapter 3; 2 days after PT for protein extraction and serum collection (analysis of pro-inflammatory cytokines, total of 27 mice) and 14 days after stroke for immunohistochemistry (infarct volume and neurogenesis, total of 46 mice) – Chapter 4. At 2 days after surgery, animals were deeply anesthetized with isoflurane and subjected to a thoracotomy to expose the heart to collect a blood sample from the left ventricle. Samples were centrifuged at 10,600 g for 5 min and serum was stored at -80 ºC until further use. After blood collection, mice were decapitated and the brain was dissected and immediately frozen in isopentane (Sigma-Aldrich) on dry ice. The ischemic territory (infarct core and proximal peri-infarct tissue) was then dissected from the mice brains in a glove box at -20 ºC to avoid protein degradation. Thereafter, brain tissue was stored at -80 ºC until further processing. At 4 weeks and 14 days after surgery mice were deeply anesthetized with either a mixture of ketamine and xylazine or pentobarbital, respectively, and perfused intracardially with saline solution followed by ice cold 4% PFA (pH 7.4, Sigma-Aldrich). Brains were removed and post-fixed with 4% PFA for 24 h, followed by immersion in a 30% or 25% sucrose solution (Sigma-Aldrich). Thereafter, brains collected from 4-week-old mice were cryopreserved and 40 µm-thick coronal sections from the olfactory bulb (OB) or SVZ/striatum and *substantia nigra* (SN) regions were collected in series of six slices (spaced 240 µm from each other), using a cryostat (CM 3050S, Leica Microsystems, Wetzlar, Germany). On the other hand, brains collected from 14-day-old mice were sectioned on a microtome (SM 2000R, Leica Microsystems, Wetzlar, Germany) at 30 µm-thick coronal sections. For infarct volume measurement sections spaced 460 µm to each other were collected from the start until the end of the lesion. Sections were stored at -20 °C in an antifreeze solution made in PBS containing 30% glycerol and 30% ethylene glycol. To analyze the penetration of NPs into the brain parenchyma mice were euthanized 4 or 24 h after injection of FITC-NPs and fixed in 4% PFA as described above.

2.16 Lesion evaluation
2.16.1 Dopaminergic neurons evaluation

For each animal subjected to stereotaxic injection (Chapter 3), eight consecutives 40 µm-thick coronal sections containing the SN, distanced 260 µm from each, were stained against tyrosine hydroxylase (TH), a marker of dopaminergic neurons. Photomicrographs of the whole SN regions were obtained in a AxioImager microscope (Carl Zeiss) under a 4x and 10x objective, respectively. ImageJ software (National Institute of Health, USA) was used to calculate the number of TH-positive (TH+) cells in the SN. Data are presented as a percentage of the contralateral (non-lesioned) hemisphere.

2.16.2 Infarct volume measurements

For each PT operated animal, the 30 µm-thick coronal sections, distanced 460 µm from each other were stained against the neuronal marker NeuN (neuronal nuclei). Stained sections were digitalized at 9600 dpi (CanoScan 8800F, Canon, Tokyo, Japan) and processed with the ImageJ software (National

Institute of Health, USA). For each animal, the infarct volume (mm^3) was calculated by subtracting the area of the non-lesioned ipsilateral hemisphere from the area of the intact contralateral hemisphere followed by their volumetric integration. Mice whose infarct volume was lower than 0.2 mm^3 or higher than 6.0 mm^3 were excluded from the study.

2.17 Immunohistochemistry

Free-floating brain sections were rinsed three times in PBS followed by the quenching of the endogenous peroxidases activity with 3% H_2O_2 (Sigma-Aldrich) for 20 min at RT. Slices were then rinsed three times for 10 min each with PBS followed by permeabilization and blocking using 5% normal donkey serum (Jackson ImmunoResearch Laboratories Inc., Suffolk, UK) dissolved in PBS-T (PBS with 0.25% of Triton X-100) for 1h at RT. Sections were incubated ON at 4 ºC with either an anti-TH or an anti-NeuN antibody (Table 2.3) in PBS-T with 3% normal donkey serum. Thereafter, sections were rinsed in PBS-T three times and incubated with the respective biotinylated secondary antibody (Table 2.4) in PBS-T with 2% normal donkey serum for 90 min at RT. Visualization was achieved *via* the Vectorstain ABC kit (Vector) using either 3, 3′-diaminobenzidine (DAB) (Sigma-Aldrich) in Tris buffer saline (TBS: 20 mM Tris and 137 mM NaCl solution, pH 7.6) containing 0.08% H_2O_2 or 3,3-diaminobenzidine-tetrahydrochloride (DabSafe, Saveen Werner, Sweden), 8% $NiCl_2$ and 3% H_2O_2. Sections were dehydrated in consecutive higher concentrations of ethanol, 2 min in 70% ethanol, two times 2 min in 95% ethanol, 2 times 2 min in absolute ethanol, followed by two times 2 min in xylol and mounted using Pertex (Histolab AB, Gothenburg, Sweden).

For fluorescence stainings, an adapted experimental protocol described elsewhere was used (Wojtowicz and Kee 2006). Briefly, free-floating sections were rinsed three times in PBS and incubated with 2 M HCl for 25 min at 37 ºC to induce DNA denaturation and exposure of BrdU. Sections were then incubated in blocking solution – 2% of normal donkey serum and 0.3% Triton X-100 in PBS – for 2 h at RT, followed by a 48 h incubation ON at 4 ºC using the primary antibodies described in Table 2.3. Thereafter, sections from 6-OHDA mice were incubated for 2 h at RT with Hoechst (1:10,000) and the respective secondary antibodies (Table 2.4). On the other hand, sections from PT mice were incubated with biotin-streptavidin secondary antibody and DAPI (4',6-diamidino-2-phenylindole; 1:10,000) for 1 h at RT followed by incubation with streptavidin Alexa Fluor 488 and Cy3 anti-goat for 2 h.

Then, a simplified version of this protocol was used to study penetration of NPs into brain parenchyma. Briefly, brain coronal sections were incubated in blocking solution for 1 h at RT and then incubated with the anti-FITC in combination with anti-CD31 or anti-NeuN or anti-GFAP (Table 2.3) for 48 h at 4 ºC. Thereafter, sections were incubated with Hoechst-33342 (1:10,000) and the respective secondary antibodies (Table 2.4) for 2 h at RT. Finally, sections were mounted in Fluoroshield Mounting Medium (Abcam Plc.). Photomicrographs were obtained using an LSM 510 or AxioObserver LSM 710 confocal microscope (Carl Zeiss).

Table 2.3 Primary antibodies used for immunohistochemistry of coronal brain sections.

REACTIVITY	HOST	SUPLIER	DILUTION
TH	Mouse monoclonal	Transduction Laboratories	1:1000
NeuN	Rabbit polyclonal	Merck Millipore	1:5000
NeuN	Mouse monoclonal	Merck Millipore	1:1000
DCX	Goat polyclonal	Santa Cruz Biotechnology	1:1000
BrdU	Rat monoclonal	AbD Serotec	1:500
FITC	Goat polyclonal	Abcam Plc	1:500
CD31	Mouse monoclonal	Abcam Plc	1:1000
NeuN	Rabbit monoclonal	Cell Signaling Technology	1:1000
GFAP	Rabbit polyclonal	Dako	1:20000

BrdU, 5-bromo-2'-deoxyuridine; DCX, doublecortin; CD31, cluster of differentiation 31; FITC, fluorescein isothiocyanate; GFAP, glial fibrillary acidic protein; NeuN, neuronal nuclei; TH, tyrosine hydroxylase.

Table 2.4 Secondary antibodies (biotinylated or fluorescent) used for immunohistochemistry in coronal brain slices.

REACTIVITY	HOST	SUPLIER	DILUTION
Anti-mouse	Goat biotinylated	Vector Laboratories	1:200
Anti-rabbit	Donkey biotinylated	Jackson ImmunoResearch Laboratories	1:400
Anti-mouse	Donkey – Alexa 546	Life Technologies	1:1000
Anti-goat	Donkey – Alexa 546	Life Technologies	1:1000
Anti-rat	Donkey – Alexa 546	Life Technologies	1:1000
Anti-rat	Biotin- streptavidin	Jackson ImmunoResearch Laboratories	1:200
Anti- streptavidin	Donkey – Alexa 488	Jackson ImmunoResearch Laboratories	1:200
Anti-goat	Donkey – Cy3	Jackson ImmunoResearch Laboratories	1:200
Anti-goat	Donkey – Alexa 488	Life Technologies	1:1000

2.18 Preparation of protein extracts

Whole protein extracts were obtained from the ischemic territory and corresponding regions in sham animals. Tissue homogenization was done by sonication (Cole Parmer Instruments Co., Chicago, U.S.A.) in lysis buffer containing 20 mM Tris (pH 7.5), 150 mM NaCl, 1 mM EDTA, 1 mM ethylene glycol tetraacetic acid (EGTA), 1 mM phenylmethanesulfonyl fluoride (PMSF), 2.5 mM sodium pyrophosphate, 1 mM β-glycerolphosphate, 1 mM sodium orthovanadate supplemented with protease inhibitor cocktail. Thereafter, tissue was incubated on ice for 10 min followed by a centrifugation (20,000 g at 4 ºC for 20 min) and the supernatant was collected for further analysis. Concentration of the whole protein collected was done by the Bradford assay using BSA (Sigma-Aldrich) dissolved in lysis buffer as standard.

2.19 Cytokine analysis from brain extracts and serum samples

The levels of different cytokines – namely interferon-gamma (IFNγ), interleukin-1beta (IL-1β), IL-6 and tumor necrosis factor-alpha (TNF-α) – were evaluated using a multiplex immunoassay kit according to the manufacturer's protocol (MesoScale Diagnostics, Gaithersburg, MD, USA) in the eight experimental groups tested. For this evaluation 50 µg of total protein from the protein extracts and 50

µL of serum collected from the same mice were used. Briefly, samples and calibrators were added to the 10-spot MULTI-SPOT® 96-well plate (a pre-coated plate with capture antibodies on independent and well-defined spots) and incubated at RT with shaking for 2 h. Thereafter, wells were rinsed with PBS with 0.05% of Tween-20 followed for 2 h incubation with shaking with the detection antibody solution. Then, after rinsed, 2x read buffer T was added to the wells and the plate analyzed on the MSD instrument.

2.20 Statistical analysis

Analysis of immunocytochemistry experiments were performed at the border of seeded neurospheres, where cells formed a pseudo-monolayer. The experiments were performed in three independent cultures, unless stated otherwise, and for each experimental condition at least 2 coverslips were assayed *per* culture. Percentage of fragmented nuclei, TUNEL+, PI+, BrdU+, Ki67+, Ki67/DCX--double positive (Ki67+/DCX+), Ki67+/GFAP+, NeuN+, GFAP+, oligodendrocyte transcription factor 2 (Olig2)+, Sox9+ and Jagged1+ was calculated from cell counts in five independent microscopic fields (approximately 150 cells *per* field) from each coverslip with a 40x magnification. Quantification of neurite ramification number and total neurite length positive for phospho-c-Jun N-terminal kinase (P-JNK) was performed in 4 independent cultures, with at least 2 coverslips *per* condition, in approximately 20 non-overlapping fields *per* coverslip (40x magnification).

In chapter 3 the quantification of DCX+, DCX+/BrdU+ and NeuN+/BrdU+ cell number was performed in the SVZ, OB (granule (GCL) and glomerular (GL) layers) and striatum of at least 3 animals, as described previously by us (Eiriz et al. 2014). For the SVZ, 5 slices spaced by 240 µm each were used. Cells were counted along the ventricle lateral wall from three different Z-axis-positions *per* field in a 40x magnification (totaling approximately 35 fields *per* mouse hemisphere). To obtain an unbiased density estimate, fields with the same mean total volume and total number of SVZ cells were selected. In the OB, two fields of GCL and six fields of GL from three different Z-axis-positions *per* field from 4 slices spaced by 240 µm each were counted *per* animal. In the striatum, two different Z-axis-positions from nine fields from 5 slices spaced by 240 µm each were counted *per* animal. A simplified version of the above-mentioned protocol was used to evaluate neurogenesis in the PT mouse model, Chapter 4. Briefly, quantification of DCX+, BrdU+ and DCX+/BrdU+ cell number was performed in the SVZ and in the peri-infarct cortex of at least 2 animals, in 30 µm coronal sections located +1 mm to bregma. Cells were counted along the slice thickness obtained by Z-stacks (40x magnification). To obtain an unbiased density estimate, fields with the same mean total volume and similar total number of SVZ cells were selected.

The software used for cell countings was ImageJ (NIH Image, Bethesda, MD, USA). Data are expressed as mean ± standard error of mean (SEM) or as medians with the 1st and 3rd quartile and whiskers. Statistical analyses have been performed with GraphPad Prism 6 software (GraphPad, San Diego, CA, USA) by using: unpaired two tailed Student's t test or ANOVA followed by Dunnett's or Bonferroni's or Tukey multiple comparison test (parametric values); or by Kruskal Wallis analysis followed by Dunn´s post hoc evaluation (non-parametric values), with $P < 0.05$ considered to represent statistical significance.

Chapter 3

MicroRNA-124 LOADED NANOPARTICLES ENHANCE BRAIN REPAIR IN PARKINSON'S DISEASE

3.1 Introduction

Neurogenesis occurs constitutively in the subventricular zone (SVZ) of the adult mammalian brain, including in humans (Gage 2000). Within this region, neural stem cells (NSCs) can self-renew, proliferate and give rise to new neurons, astrocytes and oligodendrocytes. In rodents, newborn neurons generated in the SVZ migrate through the rostral migratory stream (RMS) towards the olfactory bulb (OB) where they fully differentiate as mature interneurons (Ming and Song 2011). Adult neurogenesis homeostasis is altered in several brain disorders including Parkinson's disease (PD) (Sun et al. 2015b). PD is characterized by the loss of dopaminergic neurons present in the *substantia nigra* (SN) and degeneration of dopaminergic terminals in the striatum, leading to movement coordination impairments and cognitive deficits. Several factors have already been reported to improve functional recovery in PD animals models by increasing endogenous neurogenesis and migration of newly born neurons into the lesioned striatum (Kadota et al. 2009; Jing et al. 2012). However, an efficient therapy aiming at full regeneration has not yet been found. Therefore, it is imperative to develop new strategies to efficiently deliver pro-neurogenic factors to NSCs and to boost the endogenous regenerative capacity of adult brain.

A tightly controlled network of intrinsic and extrinsic signals, including small non-coding RNAs (e.g. microRNAs) (Santos et al. 2012a; Faigle and Song 2013; Eiriz et al. 2014; Zeng et al. 2014) regulate the neurogenic niche. MicroRNAs (miRNA or miR) have the ability to regulate hundreds of genes (Lim et al. 2005) due to inhibition of mRNA translation or induction of mRNA degradation (Bartel 2004). miR-124 is one of the most abundant miRNA in the adult brain (Lagos-Quintana et al. 2002). The expression of miR-124 is initiated during the transition from NSC to progenitor cell and it is enhanced with neuronal maturation (Cheng et al. 2009; Akerblom et al. 2012). Several studies have shown that the overexpression of miR-124 induces neuronal differentiation of both progenitor cells (Visvanathan et al. 2007; Yu et al. 2008) and HeLa cells (Lim et al. 2005). More recently, lentiviral overexpression of the miR-124 precursor (among other factors) was capable of inducing the differentiation of human neonatal foreskin fibroblasts into functional mature neurons (Yoo et al. 2011; Xue et al. 2013). *In vivo*, miR-124 overexpression in the SVZ niche increased the number of newborn neurons without affecting their migratory capability (Cheng et al. 2009; Akerblom et al. 2012). Additionally, miR-124 is intimately associated with brain pathologies and neurodegenerative disorders, such as PD. Indeed, within the miR-124 validated targets, one-fourth are de-regulated in PD (49 genes out of 202, MIRECORDS database) (Sonntag 2010). Significant decrease of miR-124 was described in the SN of 1-methyl-4-phenyl-1,2,3,6-tetrahydropyridine (MPTP)-intoxicated mice (PD mouse model) as well as in SH-SY5Y and MN9D dopaminergic neurons treated with methyl phenyl pyridinium (MPP) iodide, while its overexpression improved cell survival (Kanagaraj et al. 2014; Wang et al. 2015a; Gong et al. 2016). Therefore, increasing miR-124 intracellular levels likely stands for a novel therapeutic strategy to improve functional outcome in PD, reviewed at (Sun et al. 2015b).

Due to the short half-life and poor stability of miRNA, their efficient delivery into cells in a safe and controlled way remains a challenge (Chen et al. 2015). Viral vectors have a high capacity to deliver miRNA, however safety issues such as immunogenicity and the risk of triggering oncogenic transformation limits its translation potential (Guzman-Villanueva et al. 2012). Non-viral vectors such as

polymeric nanoparticles (NPs), which avoid these safety issues, have been used by us and others to efficiently deliver proneurogenic molecules, including miRNA, into cells (Maia et al. 2011; Santos et al. 2012a; Bernardino et al. 2012; Guzman-Villanueva et al. 2012). As so, we hypothesized that the use of polymeric NPs to deliver miR-124 could promote neurogenesis of SVZ NSCs both *in vitro* and *in vivo* and ultimately promote brain repair. To confirm this hypothesis we used a NP formulation formed by poly(lactic acid-*co*-glycolic acid) (PLGA) and perfluoro-1,5-crown ether (PFCE), a fluorine compound that can be tracked non-invasively by fluorine magnetic resonance imaging (^{19}F-MRI), and coated with protamine sulfate to complex miR-124 (Gomes et al. 2013). The neurogenic potential of this NP formulation was assessed both in physiologic conditions and in a 6-hydroxydopamine (6-OHDA) mouse model for PD.

3.2 Results

3.2.1 miRNA-loaded NPs are efficiently internalized by SVZ cells

Novel polymeric PLGA-based NPs developed by us were used to deliver miR-124 into SVZ cells (Figure 3.1 A). These NPs have an average size of ~210 nm and are coated with protamine sulfate, a cationic peptide that confers a positive surface charge (+5.7 ± 1.2 mV, n=3) to the NPs, allowing their complexation with miRNA (negatively charged molecule) (+1.7 ±0.7 mV, n=3). Moreover, NPs have in their core PFCE, a nontoxic fluorine compound commonly used in nuclear magnetic resonance (NMR) imaging applications, allowing *in vivo* non-invasive tracking of NPs (Figure 3.1 A) (Ruiz-Cabello et al. 2011; Gomes et al. 2013). First, the ability of distinct SVZ cell phenotypes to internalize NPs was evaluated by confocal analysis. SVZ cells were treated with 10 µg/mL of fluorescein isothiocyanate (FITC)-labeled NPs complexed with Dy547-labeled miRNA mimic (a fluorescent scramble-miR) for 4 h, washed out to remove non-internalized NPs, and maintained in culture for additional 24 h. A fluorescence scramble-miR was used since it does not alter significantly the formulation characteristics, such as size, zeta potential, complexation, and it is easier to track. The intracellular uptake of miRNA NPs by neural stem/progenitor cells and neuroblasts was evaluated by co-staining doublecortin (DCX), glial fibrillary acidic protein (GFAP) or nestin (Figure 3.1 B, C, D). At this timepoint, primary SVZ cultures contain approximately 10-20% neurons, 15-20% astrocytes and 70-80% immature cells (nestin- positive and GFAP-negative, nestin$^+$/GFAP$^-$, data not shown). We have found that miR-Dy547 NPs were efficiently internalized by neuroblasts (DCX$^+$; Figure 3.1 B), type B cells (GFAP$^+$/nestin$^+$; Figure 3.1 C, D), immature progenitor cells (nestin$^+$ cells; Figure 3.1 C arrow), and by astrocytes (GFAP$^+$; Figure 3.1 D arrowhead).

miR-Dy547 and FITC-NPs labeling was located preferentially in aggregates during the initial hours but at 24 h post-transfection it was found spread all over the cell cytoplasm including in the cellular processes of type B cells, immature progenitor cells and new neurons (Figure 3.1 B-D). The huge heterogeneity in cell phenotypes and density found in SVZ cultures hamper an extensive tracking of miR-Dy547 FITC-NPs inside SVZ cells. Nevertheless, miR-Dy547 FITC-NPs were found internalized in all SVZ cell types analyzed suggesting that this formulation represents an efficient miRNA delivery vector. Importantly, our formulation was efficiently internalized and able to deliver miR-124 into stem/progenitor and immature cells, the cell population that in response to increased levels of miR-124

may differentiate into mature neurons. In accordance, internalization in mature neurons was not analyzed due to its already high basal expression of miR-124 (Cheng et al. 2009).
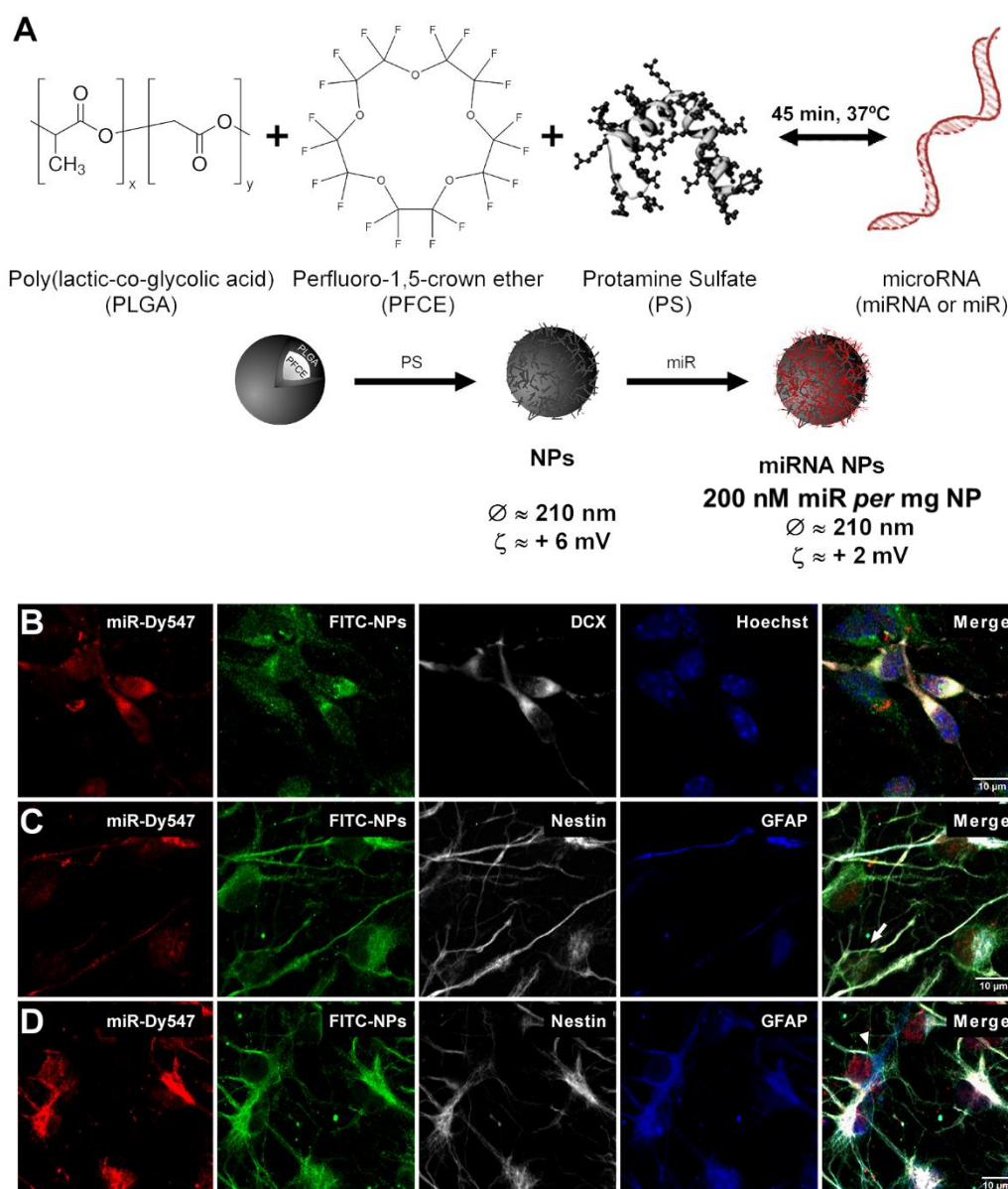
Figure 3.1   miRNA loaded NPs are internalized by SVZ stem/progenitor cells.
(A) Composition and physical properties of miRNA NPs. (B, C, D) Photomicrographs of SVZ stem/progenitor cells after transfection with 10 µg/mL of FITC-NPs (green) complexed with miR-Dy547 (red) and stained against immature neuronal marker DCX (white), and nuclear marker Hoechst (blue) (B) or the immature progenitor marker nestin (white) and the glial marker GFAP (blue) (C, D). FITC-NPs and miR-Dy547 were found internalized in all cell types analyzed. White arrow shows a cell that is only positive for nestin (immature cell) and arrowhead shows a cell exclusively positive for GFAP (astrocyte). Cells positive for both nestin and GFAP markers (type B cells) are also observed (C, D). Scale bar: 10 µm. Abbreviations: FITC, fluorescein isothiocyanate; DCX, doublecortin; GFAP, glial fibrillary acidic protein; NPs, nanoparticles; SVZ, subventricular zone.

3.2.2 Cellular toxicity of NPs

Next, the toxic effect of NPs on SVZ cells was assessed by nuclear condensation/fragmentation (Figure 3.2 A), terminal deoxynucleotidyl transferase-mediated dUTP nick end labeling (TUNEL; Figure 3.2 B, D) and propidium iodide (PI) incorporation (Figure 3.2 C, E) analysis, using different

concentrations of NPs 1, 10 and 20 µg/mL either complexed with 200nM of miR-124 or not (void NPs). A first screening in terms of cell toxicity was performed by quantifying the number of fragmented/condensed nuclei (labeled with Hoechst). Concentrations up to 1 µg/mL of void NPs (12.4 ± 1.3) and up to 10 µg/mL of miR-124 NPs (10.8 ± 0.2) did not induce significant nuclear condensation/fragmentation as compared with non-treated cells (Figure 3.2 A, 9.1 ± 0.9, **P < 0.01, ***P < 0.001). Scramble-miR NPs at 10 µg/mL were nontoxic as well (10.6 ± 1.4, n=3).
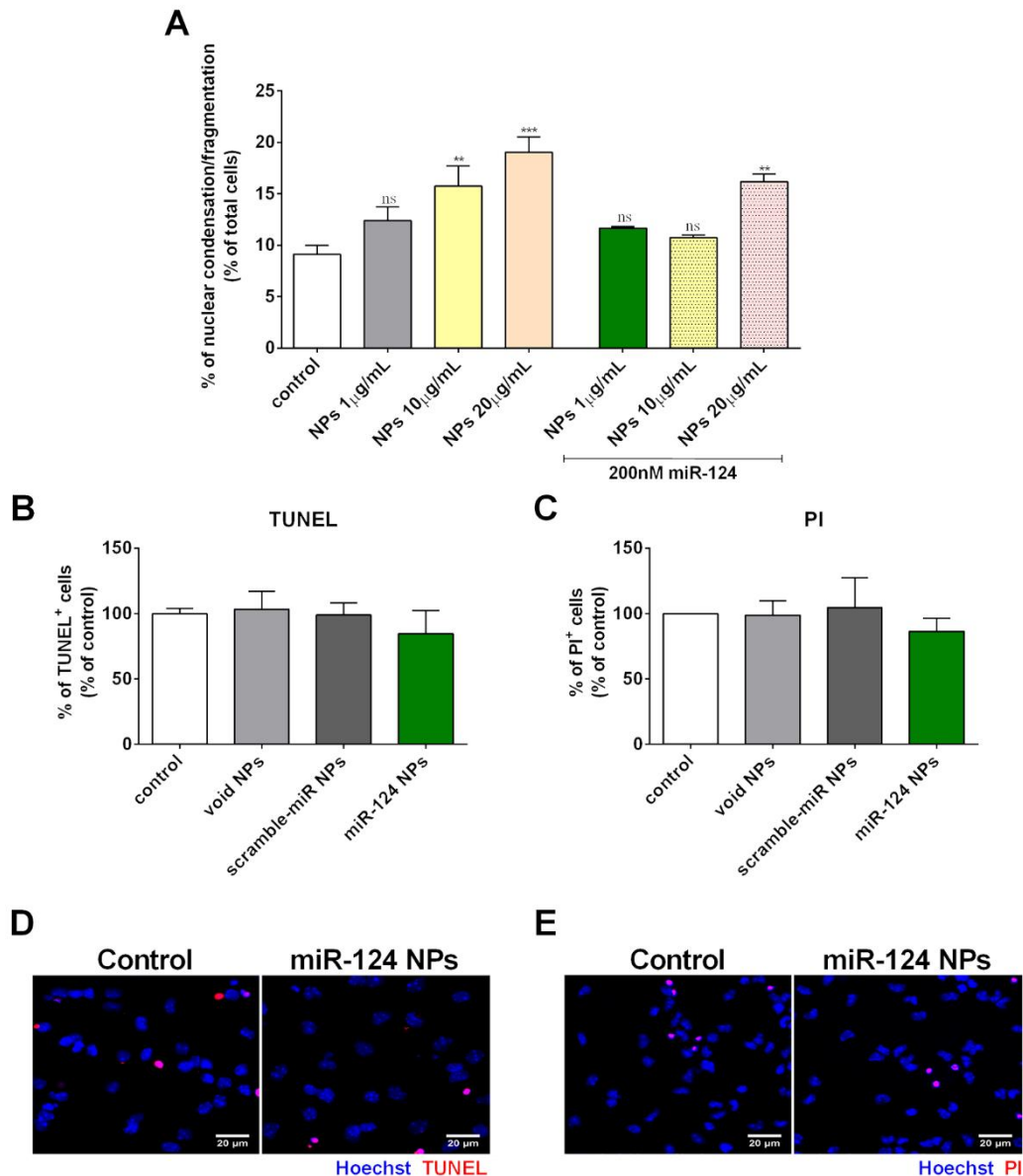
Figure 3.2 Viability studies in SVZ cells treated with NPs.
SVZ stem/progenitor cells were treated for 4 h with NPs and then maintained in culture for 2 days. Percentage of (A) cells with nuclear condensation/fragmentation, (B) TUNEL^{+} apoptotic cells and (C) propidium iodide (PI)[+] necrotic cells. Representative confocal digital images of (D) TUNEL, (E) PI, and Hoechst (blue) stainings in control cultures and in miR-124 NPs-treated cultures. Both TUNEL and PI stainings are shown in red. Scale bar: 20 µm. Data are expressed as mean ± SEM (n=3-13). **P < 0.01, ***P < 0.001 using Dunnett's multiple comparison test and compared with control. (B, C) Data are presented as percentage of control (set to 100%). ns, non-significant. Abbreviations: NPs, nanoparticles; TUNEL, Terminal deoxynucleotidyl transferase dUTP nick end labeling; SVZ, subventricular zone.

Parameters such as composition, size, and superficial charge among other factors influence NP toxicity. NPs with higher surface charge generally present higher toxicity (Fröhlich 2012), which may

explain the highest cytotoxicity of void (+5.7 ± 1.2 mV) *versus* miRNA NPs (+1.7 ±0.7 mV). Importantly, 1 µg/mL NPs either complexed or not with miRNA revealed no cytotoxicity. This concentration was then used to evaluate apoptosis and necrosis in SVZ cells treated with void NPs or miRNA NPs (scramble-miR or miR-124) by TUNEL and PI staining, respectively. We have found that 1 µg/mL NPs (void, scramble-miR or miR-124) did not induce apoptosis (Figure 3.2 B, D) or necrosis/late-apoptosis (Figure 3.2 C, E). Based on these results, 1 µg/mL NPs complexed with miR-124 was selected to perform the subsequent experiments.

3.2.3 miR-124 NPs prompt neuroblasts proliferation

Next, we examined the effect of miR-124 NPs in cell proliferation by analyzing 5-bromo-2'-deoxyuridine (BrdU) and Ki67 staining 48 h after cell treatments. BrdU is a marker for cells undergoing S phase of the cell cycle, while all cycling cells (G1, S, G2 and M phases) express the Ki67 marker. Overall, total cell proliferation was not affected as compared with control cultures (Figure 3.3 A, B). However, cells treated with miR-124 NPs showed a higher number of proliferating neuroblasts (Ki67$^+$/DCX$^+$; Figure 3.3 C, E; control 100.0 ± 9.8, miR-124 NPs 196.0 ± 32.0, *P < 0.05, **P < 0.01) and a lower number of proliferating astrocyte-like cells (Ki67$^+$/GFAP$^+$; Figure 3.3 D, F; scramble-miR NPs 125.4 ± 10.5, miR-124 NPs 52.9 ± 13.2, *P < 0.05) when compared with the respective controls. Thus, our results indicate that miR-124 NPs favor neuroblast proliferation while decreasing the proliferation of astrocytic-like cells.
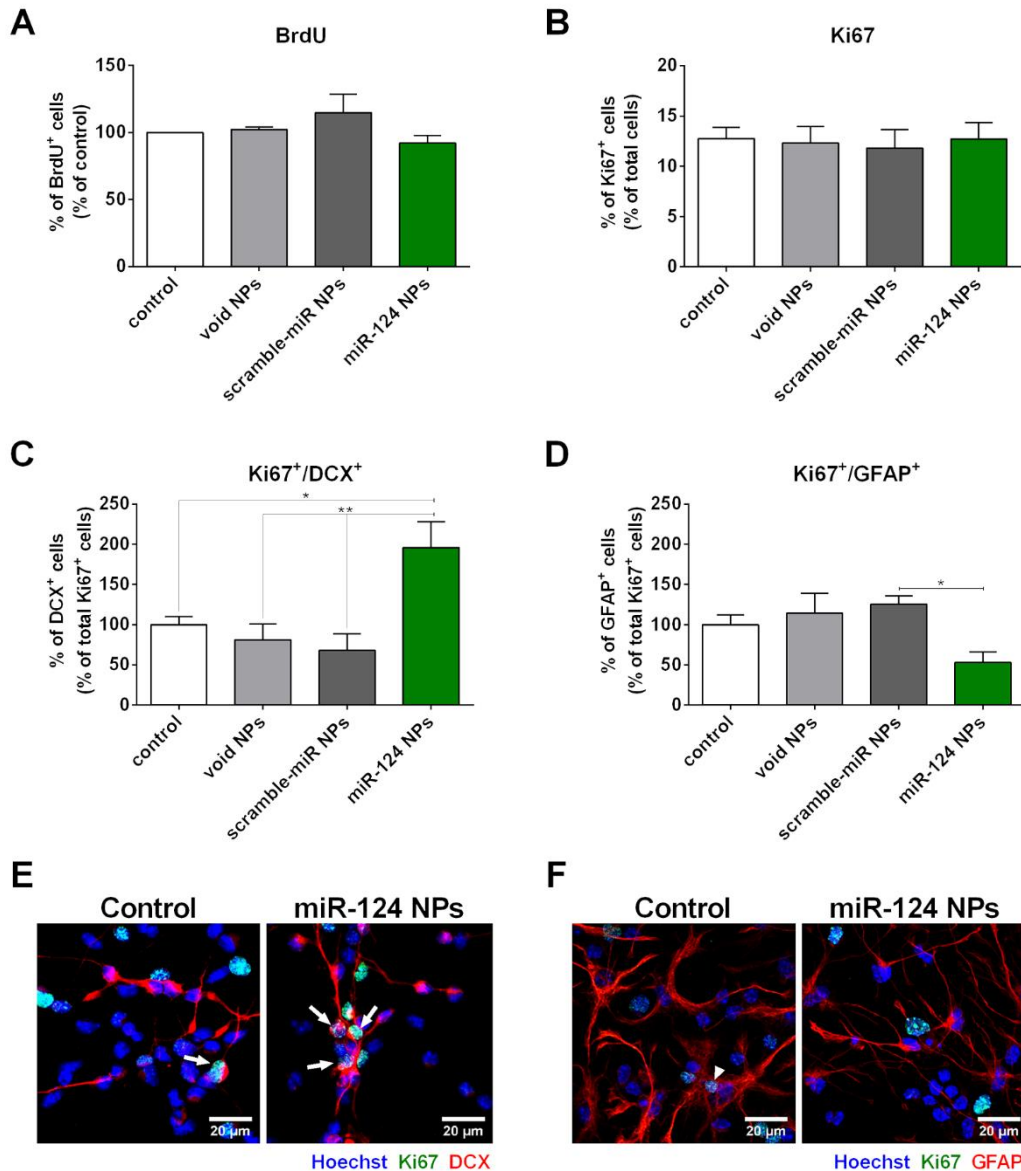
Figure 3.3 miR-124 NPs favor neuroblast proliferation.
SVZ stem/progenitor cells were treated for 4 h with NPs and then maintained in culture for 48 h. (A, B) Bar graphs depict the percentage of BrdU+ and Ki67+ cells, respectively. Percentage of (C) DCX+ or (D) GFAP+ cells co-labeled with Ki67 staining. Representative fluorescence photomicrographs of (E) DCX/Ki67 and (F) GFAP/Ki67 immunostainings in control cultures and in miR-124 NPs-treated cultures. Nuclei are shown in blue, Ki67 in green and, DCX and GFAP in red. Scale bar: 20 μm. White arrows depict double-positive cells. Data are expressed as mean ± SEM (n=2-3). *P < 0.05, **P < 0.01 using Bonferroni's multiple comparison test. (A, C, D) Data are presented as percentage of control (set to 100%). Abbreviations: BrdU, 5-bromo-2'-deoxyuridine; DCX, doublecortin; GFAP, glial fibrillary acidic protein; NPs, nanoparticles; SVZ, subventricular zone.

3.2.4 miR-124 NPs induce neuronal differentiation by repressing key non-neuronal genes

The ability of miR-124 NPs to induce neuronal differentiation was then assessed. As shown in Figure 3.4, miR-124 NPs led to a 2.5-fold increase in the number of mature neurons (NeuN; Figure 3.4 A, B; scramble-miR NPs 135.0 ± 11.8, miR-124 NPs 243.6 ± 20.2, ***P < 0.001) while reducing to approximately 25% the number of astrocytes (GFAP; Figure 3.4 C, E; scramble-miR NPs 45.8 ± 1.1, miR-124 NPs 34.2 ± 2.2, *P < 0.05) as compared with scramble-miR NPs-treated cells. No effects were

found in terms of oligodendrocyte differentiation (oligodendrocytes transcription factor 2, Olig2; Figure 3.4 D, F). Although the oligodendrocytic lineage is dependent on Olig2 expression, a subpopulation of stem/progenitor cells also express Olig2 (Menn et al. 2006). These data are in accordance with the results shown in Figure 3.3.
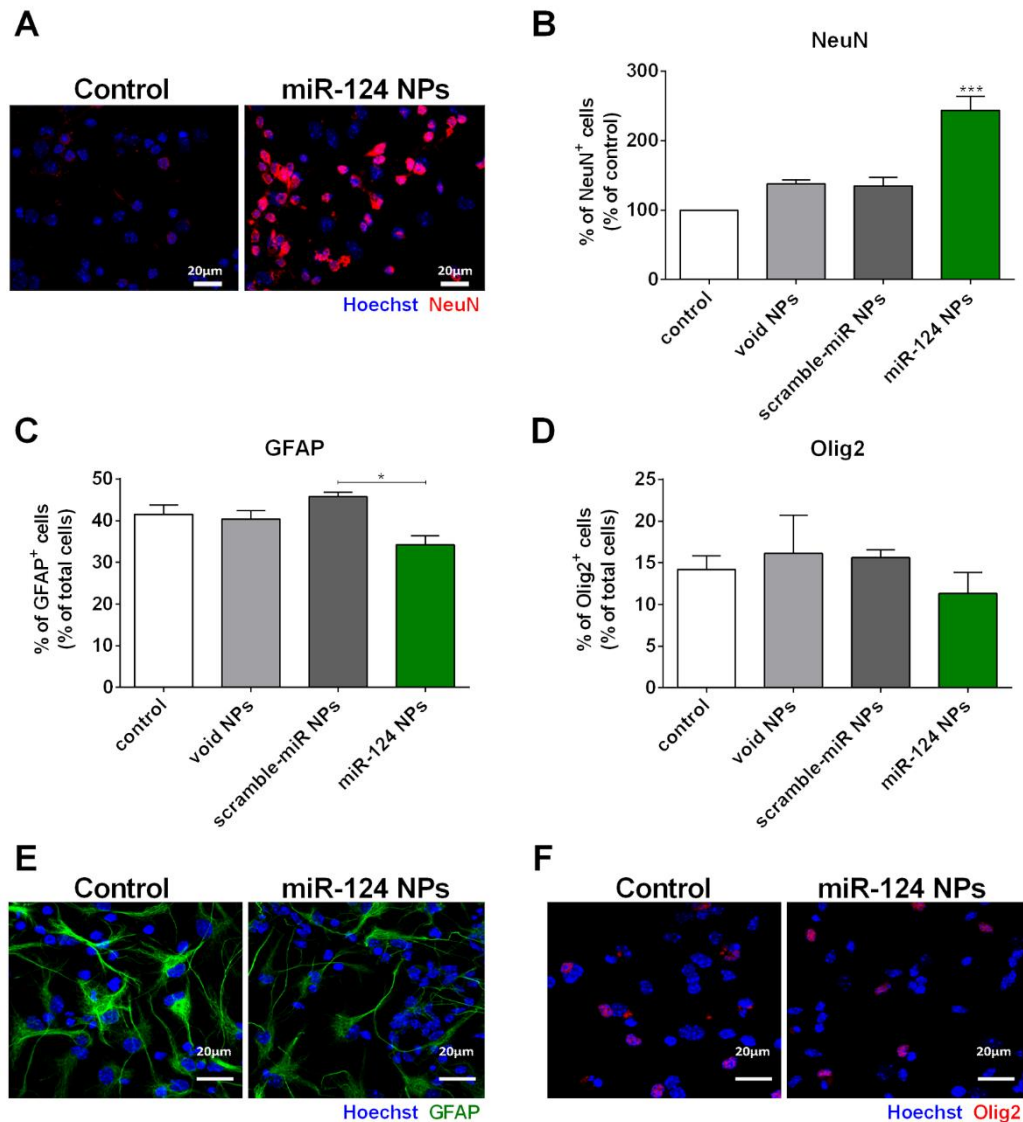
Figure 3.4   miR-124 NPs promotes neuronal differentiation over glial differentiation.
SVZ stem/progenitor cells were treated for 4 h with NPs and then maintained in culture for 7 days. (A) Representative fluorescence photomicrographs of NeuN immunostaining (red) in control cultures and cultures transfected with 1 µg/mL of miR-124 NPs. Hoechst was used for nuclear staining (blue); scale bar: 20 µm. (B) Percentage of NeuN-immunostained neurons, (C) GFAP-immunostained astrocytes and (D) Olig2-immunostained oligodendrocytes in SVZ cultures. Representative fluorescence photomicrographs of (E) GFAP (green) and (F) Olig2 (red) immunostainings in control cultures and in miR-124 NPs-treated cultures. Nuclei are shown in blue. Scale bar: 20 µm. Data are expressed as mean ± SEM (n=3-6). *P < 0.05, ***P < 0.001 using Bonferroni's multiple comparison test. In (B) data are presented as relative to control (set to 100%) and the statistics compares miR-124 NPs against all other experimental conditions (control, void and scramble-miR NPs). Abbreviations: GFAP, glial fibrillary acidic protein; NeuN, neuronal nuclei; NPs, nanoparticles; Olig2, oligodendrocyte transcription factor 2; SVZ, subventricular zone.

Sox9 and jagged1 are validated miR-124 targets and seem to play a role in neurogenesis regulation. Therefore, the mRNA and protein levels of Sox9 and Jagged1 (Jag1) were evaluated by

qPCR and immunocytochemistry, respectively. As expected, miR-124 NPs induced a reduction of approximately 30% in mRNA (Figure 3.5 A; SOX9: control 1.0 ± 0.0, miR-124 NPs 0.7 ± 0.1; JAG1: control 1.0 ± 0.0, miR-124 NPs 0.6 ± 0.1, **P < 0.01, ***P < 0.001) and a reduction of almost 50% in protein levels (Figure 3.5 B-E; Sox9: control 100.0 ± 0.1, miR-124 NPs 55.4 ± 7.0; Jagged1: control 100.0 ± 0.1, miR-124 NPs 51.8 ± 15.4) of both Sox9 and Jagged1. Altogether, our results indicate that miR-124 NPs modulate SVZ cells fate and downregulate Sox9 and Jagged1, leading to a robust enhancement of neurogenesis and a slight reduction in the number of astrocytes.
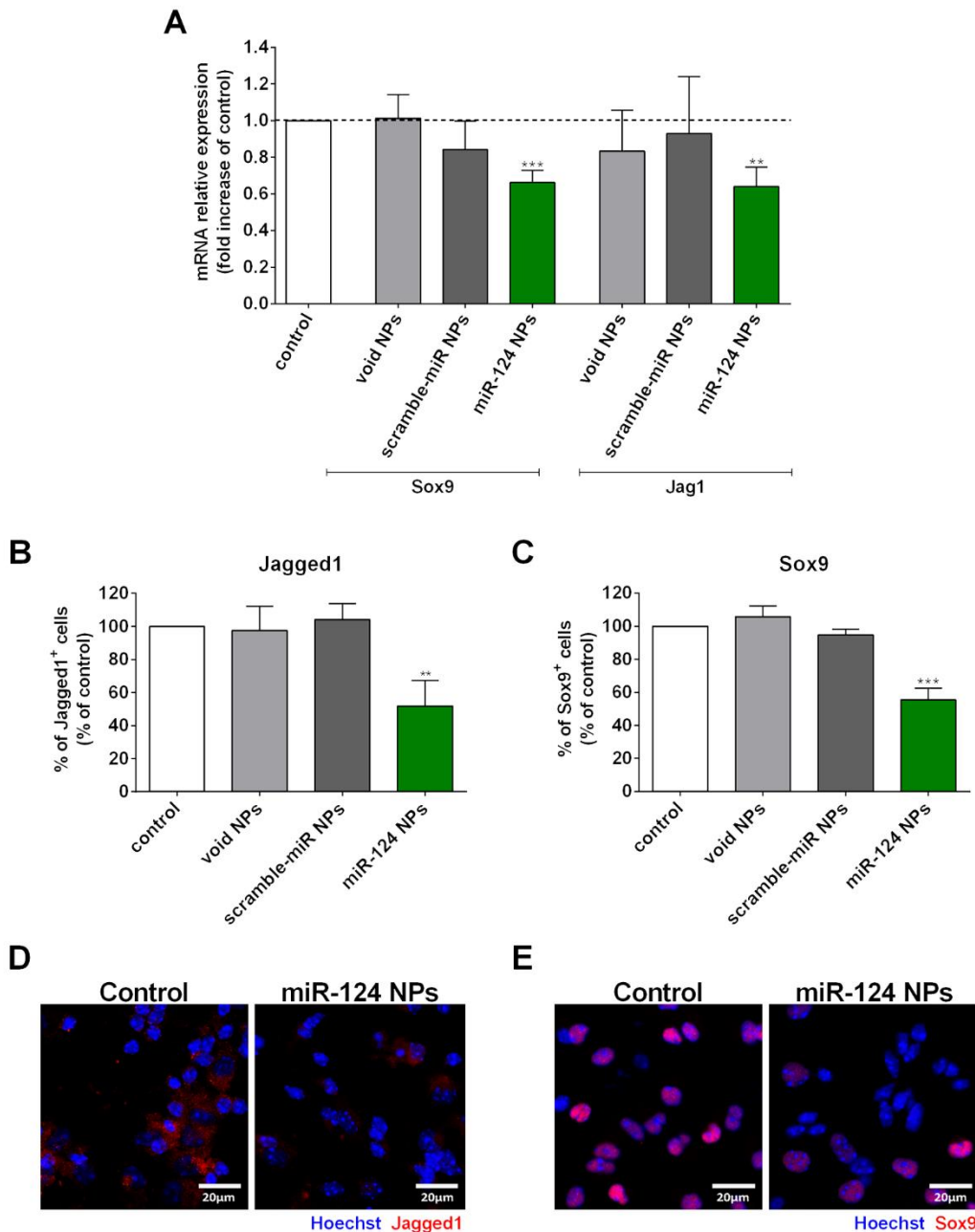
Figure 3.5   miR-124 NPs target Sox9 and Jagged1 mRNA and protein levels.
SVZ cells were treated for 4 h with NPs and maintained in culture for 5 or 7 days. (A) Sox9 and Jag1 mRNA expression 5 days after NPs treatment. Gene expression was normalized to GAPDH. Data are expressed as mean ± SEM (n=3-6). All data are presented as fold increase of control (set to 1). Percentage of (B) Jagged1+ and (C) Sox9+ cells in SVZ cultures 7 days after treatment with 1µg/mL miR-124 NPs. Representative fluorescence photomicrographs of (D) Jagged1 and (E) Sox9 immunostainings in control cultures and in miR-124 NPs-treated cultures. Nuclei are shown in blue. Scale bar: 20 µm. Data are expressed as mean ± SEM (n=3-6). **P < 0.01, ***P < 0.001 using Bonferroni's multiple comparison test and compared with control. (B, C) Data are presented as percentage of control (set to 100%). Abbreviations: NPs, nanoparticles; SVZ, subventricular zone.

3.2.5 miR-124 NPs promote axonogenesis

To evaluate the effect of miR-124 NPs on neuronal maturation and axonogenesis, SVZ cells were transfected with miR-124 NPs for 4 h and the activation of stress-activated protein kinases (SAPK)/Jun amino-terminal kinases (JNK) pathway was analyzed 24 h post-transfection by immunocytochemistry against phospho (P)-JNK, the JNK active form. miR-124 NPs induced a 1.6 and 2-fold increase in the number (Figure 3.6 A; control 1.5 ± 0.1, miR-124 NPs 2.4 ± 0.4, *P < 0.05, **P < 0.01) and length (Figure 3.6 B; control 78.2 ± 9.6, miR-124 NPs 153.8 ± 31.5) of P-JNK$^+$ axons emerging out of the neurospheres, respectively. Accordingly, in miR-124 NPs-treated cultures P-JNK immunoreactivity was robust while control cultures showed a more diffuse and weak staining. Also, as reported previously by us, the P-JNK staining co-localized with Tau, a microtubule-associated protein able to modulate the stability of axonal microtubules in mature and immature neurons (Agasse et al. 2008a; Bernardino et al. 2008) (Figure 3.6 C).
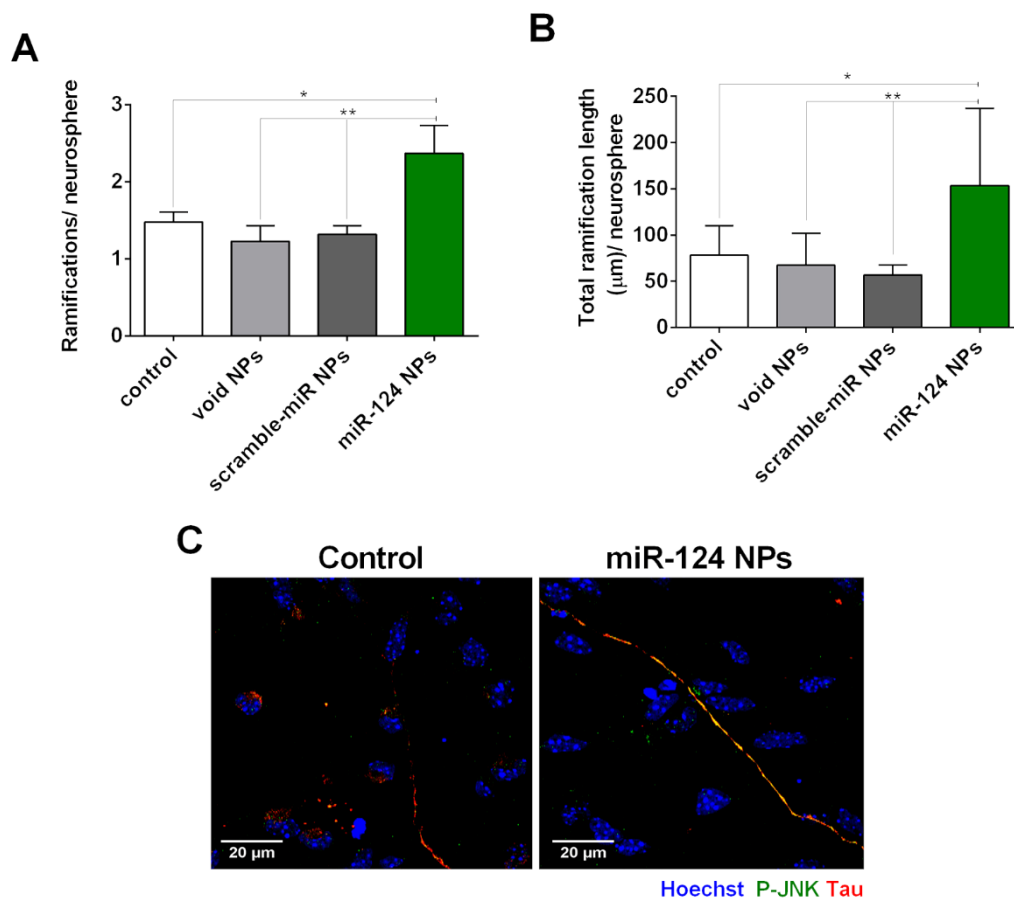
Figure 3.6   miR-124 NPs activate the SAPK/JNK pathway in Tau$^+$ axons.
SVZ stem/progenitor cells were treated for 4 h with NPs and then maintained in culture for 24 h. Bar graphs display (A) number of ramifications and (B) the total ramification length (μm) of P-JNK$^+$ fibers *per* neurosphere. (C) Representative fluorescence photomicrographs of P-SAPK/JNK (green), Tau (red), and Hoechst (blue) staining in control cultures and in miR-124 NPs-treated cultures; scale bar: 20 μm. Data are expressed as mean ± SEM (n=3-5). *P < 0.05, ** P < 0.01 using Bonferroni's multiple comparison test. Abbreviations: NPs, nanoparticles; P-SAPK/JNK, phospho- stress-activated protein kinase/Jun amino-terminal kinase; SVZ, subventricular zone.

3.2.6 miR-124 NPs increase the number of migrating neuroblasts that reach the OB and the lesioned striatum leading to motor amelioration of the PD symptoms

Next, we evaluated the effect of miR-124 NPs in SVZ neurogenesis in physiological conditions (healthy mice) and in a mouse model for PD obtained by unilateral injection into the striatum of the toxin 6-OHDA (6-OHDA-challenged mice). For that purpose, miR-124 NPs were unilaterally injected into the lateral ventricle, followed by 3 days of intraperitoneal injections with BrdU (every 12h) (Figure 3.7 A). miR-124 NPs were injected into the right lateral ventricle to facilitate the interaction with type B cells, which project one cilium each into the ventricle lumen (Santos et al. 2012b); alternatively, miR-124 NPs may interact with ependymal cells to induce a paracrine effect over SVZ stem/progenitor cells. Indeed, miR-Dy547 loaded FITC-NPs delivered into the ventricular lumen were easily detected, lining the lateral ventricle of the SVZ, at 24 h after administration (Figure 3.7 B). Then, to unveil the effect of our NP formulation in a pre-clinical mouse model for PD, mice were subjected to a double stereotaxic injection to deliver 6-OHDA into the right striatum and the NPs into the right lateral ventricle (Figure 3.7 A). Unilateral injections of 6-OHDA in mice and/or rats is known to be advantageous when compared with other PD mice models, due to the presence of side-biased motor impairments (Ungerstedt and Arbuthnott 1970; Iancu et al. 2005). Moreover, this mouse model for PD (10 µg 6-OHDA in the striatum) was chosen based in the following parameters: reduced SVZ neurogenesis (about 40% reduction in DCX$^+$/BrdU$^+$ cells in the SVZ, Figure 3.7 D); dopaminergic degeneration (about 50% dopaminergic death in the SN: 48.1 ± 6.1, n=10 mice); functional motor deficits (Figure 3.11 D); and low mortality rates (in opposite to models such as involving injections in the *SN* or in the medial forebrain bundle).

Mice were euthanized 4 weeks after stereotaxic surgeries and the number of neuroblasts (DCX$^+$), and proliferating neuroblasts (DCX$^+$/BrdU$^+$) were quantified in the SVZ (Figure 3.7) and in the Granular cell layer (GCL) and glomerular layer (GL) of the OB (Figure 3.8). First, we found that miR-124 NPs were not able to alter the total number of DCX$^+$ (Figure 3.7 C) and DCX$^+$/BrdU$^+$ cells (Figure 3.7 D, E-H) in the SVZ of both healthy and 6-OHDA-challenged mice as compared with the respective saline group. Nevertheless, the levels of proliferating neuroblasts (DCX$^+$/BrdU$^+$ cells) in 6-OHDA-challenged mice were approximately 50% lower than in healthy mice, suggesting a negative influence of striatal dopamine depletion over neuroblast proliferation and/or migration into lesioned regions (striatum) or into the OB. However, the total number of neuroblasts (DCX$^+$; Figure 3.7 C) was not affected by dopamine depletion.
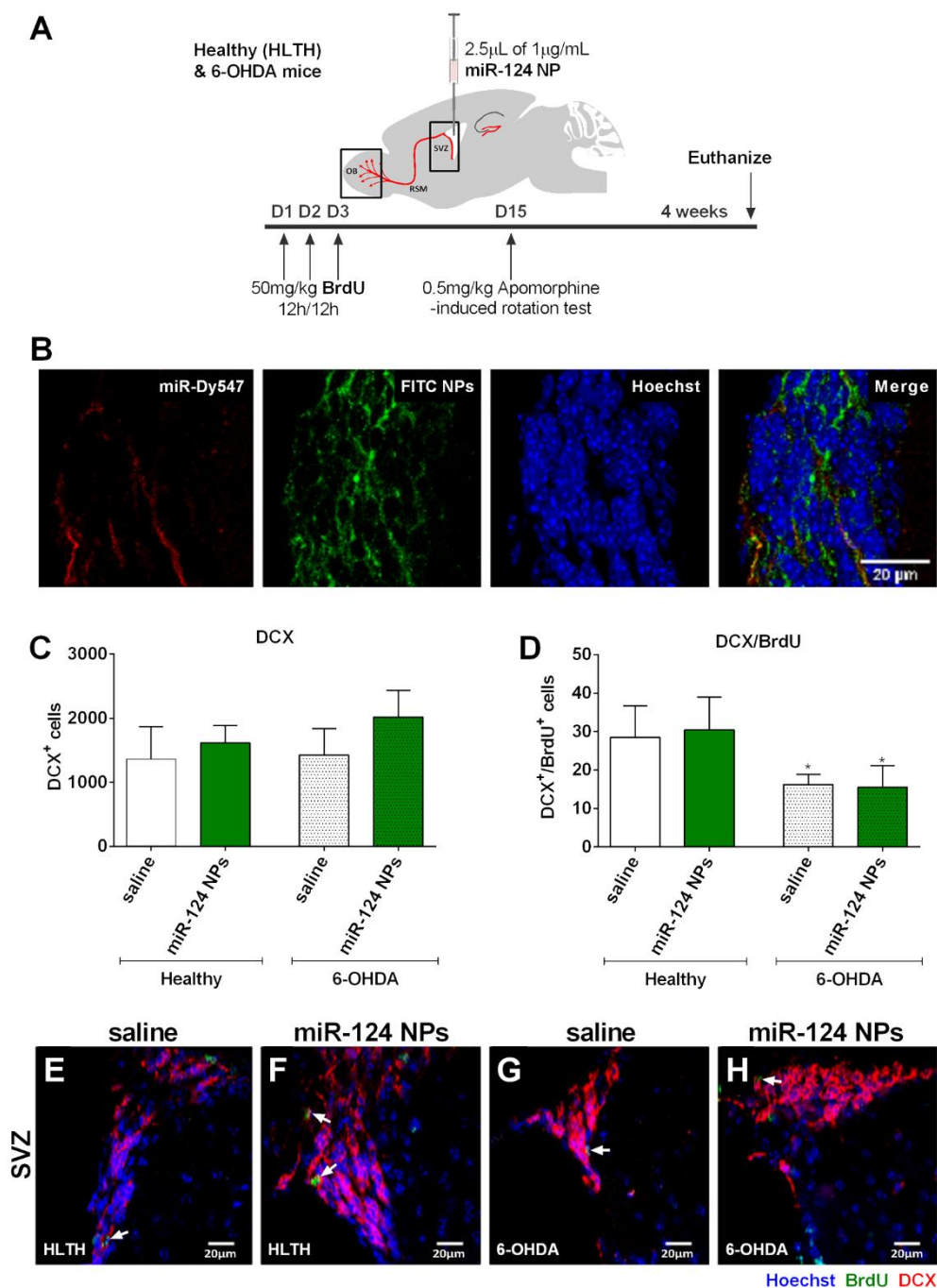
Figure 3.7   miR-124 NPs do not affect the number of proliferating SVZ neuroblasts both in the healthy and in a 6-OHDA-challenged mouse model of PD.
(A) Experimental design for the *in vivo* experiments consisting in an intracerebroventricular injection with miR-124 NPs or saline solution followed by the injection of 6-OHDA into the right striatum. Then, mice received BrdU injections (every 12 h) during the following 3-day upon surgery. After 4 weeks mice brains were collected for processing. (B) Representative photomicrographs of SVZ 24 h after injection, into the lumen of the lateral ventricle of mice, of 10 µg/mL of FITC-NPs (green) complexed with miR-Dy547 (red) and stained against the nuclear marker Hoechst (blue). (C, D) Bar graphs depict total (C) DCX$^+$ and (D) DCX$^+$/BrdU$^+$ cells counted in the SVZ. Data are expressed as mean ± SEM (n=3–5 mice) *P < 0.05 using Student's unpaired t-test as compared with saline healthy mice. (E-H) Representative confocal digital images of BrdU (green), DCX (red) and Hoechst (blue) staining observed in the SVZ of healthy (saline (D) or miR-124 NPs (E)) and 6-OHDA-injected mice (saline (F) or miR-124 NPs (G), respectively). Scale bar: 20 µm; white arrows indicate DCX$^+$/BrdU$^+$ cells. Abbreviations: 6-OHDA, 6-hydroxidopamine; BrdU, 5-bromo-2'-deoxyuridine; DCX, doublecortin; FITC, fluorescein isothiocyanate; NPs, nanoparticles; PD, Parkinson's disease; SVZ, subventricular zone.
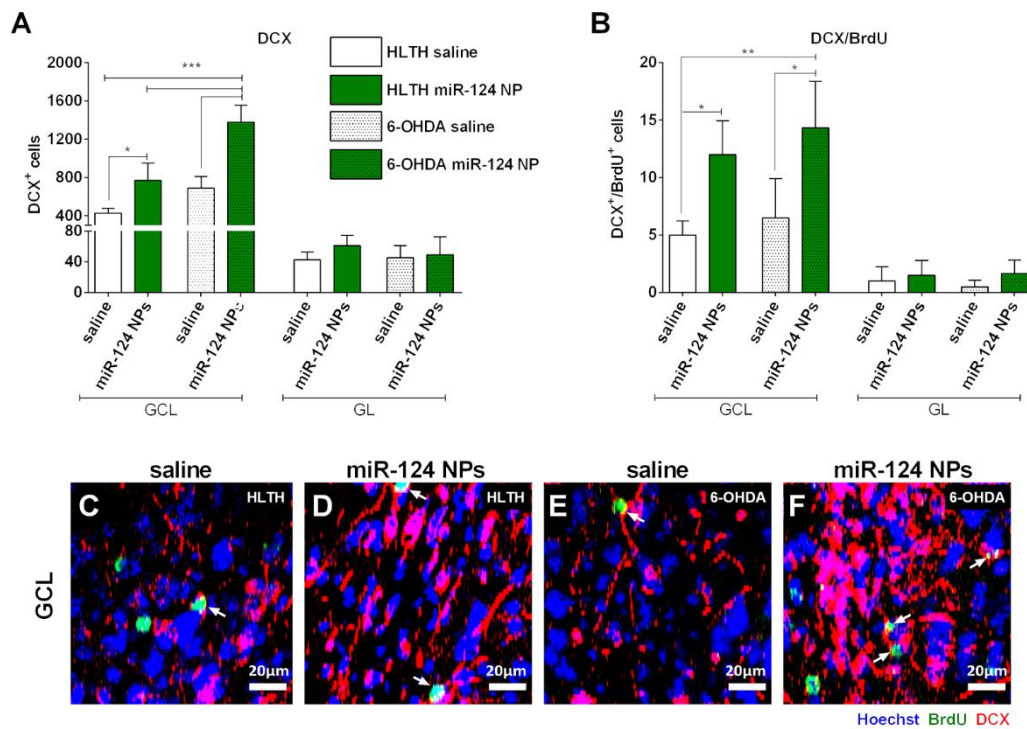
Figure 3.8 miR-124 NPs induce migration of SVZ-derived neuroblasts towards the granule cell layer (GCL). (A, B) Bar graphs depict the effect of miR-124 NPs in the total number of (A) DCX$^+$ and (B) DCX$^+$/BrdU$^+$ cells in the granule cell layer (GCL) and glomerular layer (GL) of healthy or 6-OHDA-challenged mice. Data are expressed as mean ± SEM (n=3–5 mice) *P <0.05, **P < 0.01, ***P < 0.001 using Bonferroni's multiple comparison test. (C-F) Representative confocal digital images of BrdU (green), Hoechst (blue) and DCX (red) staining observed in the GCL of healthy mice (saline (C) or miR-124 NPs (D)) or 6-OHDA-challenged mice (saline (E) or miR-124 NPs (F)), respectively. Scale bar: 20µm; white arrows indicate DCX$^+$/BrdU$^+$ cells. Abbreviations: 6-OHDA, 6-hydroxidopamine; BrdU, 5-bromo-2'-deoxyuridine; DCX, doublecortin; NPs, nanoparticles; SVZ, subventricular zone.
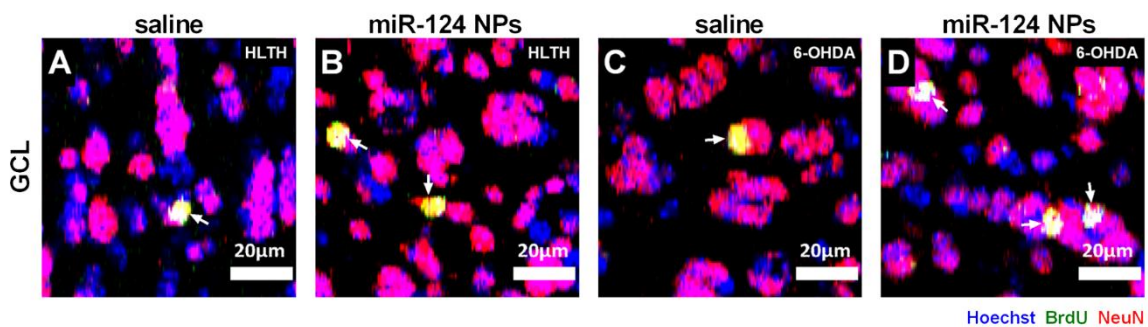
Figure 3.9 miR-124 NPs induce integration of mature neurons in the granule cell layer (GCL) of the olfactory bulb (OB). Representative confocal digital images of BrdU (green), Hoechst (blue) and NeuN (red) staining observed in the GCL of healthy mice (saline (A) or miR-124 NPs (B)) or 6-OHDA-injected mice (saline (C) or miR-124 NPs (D)), respectively. Scale bar: 20µm; white arrows indicate NeuN$^+$/BrdU$^+$ cells. Abbreviations: 6-OHDA, 6-hydroxidopamine; BrdU, 5-bromo-2'-deoxyuridine; NeuN, neuronal nuclei; NPs, nanoparticles.

Granular cell layer and glomerular layer of the OB are the endpoint of SVZ-derived cells. In healthy animals, a significant increase in the number of DCX$^+$ (Figure 3.8 A; GCL healthy mice: saline 426.4 ± 22.6, miR-124 NPs 769.5 ± 91.22, *p<0.05, ***p<0.001) and DCX$^+$/BrdU$^+$ (Figure 3.8 B-D; saline 5.0 ± 0.5, miR-124 NPs 12.0 ± 1.5, *p<0.05, **p<0.01) cells was found in the GCL of mice treated with miR-124 NPs as compared with saline animals. Then, we found that the number of DCX$^+$ and DCX$^+$/BrdU$^+$

cells was not significantly different between healthy saline and 6-OHDA saline mice (without miR-124 NPs treatment). Interestingly, miR-124 NPs increased the number of DCX$^+$ (Figure 3.8 A, C, D; GCL 6-OHDA mice: saline 687.3 ± 61.2, miR-124 NPs 1379.0 ± 101.7) and DCX$^+$/BrdU$^+$ (Figure 3.8 B, E, F; GCL 6-OHDA mice: saline 6.5 ± 1.7, miR-124 NPs 14.3 ± 2.3) cells found in the GCL of 6-OHDA-challenged animals as compared with miR-124 NPs-treated healthy mice. We also observed migrating neuroblasts that fully differentiated into mature neurons (NeuN$^+$/BrdU$^+$; Figure 3.9).

In physiological conditions SVZ neuroblasts migrate through the rostral migratory stream towards the OB; however, upon injury these neuroblats can migrate through the lesion to minimize the damage (Santos et al. 2012b). Accordingly, some proliferating neuroblasts (DCX$^+$/BrdU$^+$) as well as mature neurons (NeuN$^+$/BrdU$^+$; Figure 3.10 A-C) were found in the striatum of 6-OHDA-challenged mice, demonstrating that dopaminergic depletion *per se* activated endogenous brain repair mechanisms. Importantly, miR-124 NPs further increased the number of mature neurons found in the lesioned striatum of 6-OHDA-challenged mice (Figure 3.10 A-C). As expected, the levels of NeuN$^+$/BrdU$^+$ cells in the striatum were almost inexistent in healthy mice.

To unveil if our treatment has any impact into the amelioration of PD symptoms in the 6-OHDA-challenged mice we performed a behavioral analysis based on the apomorphine-rotation test (Figure 3.9 D), a classical test used to characterize PD lesion extent and therapeutic effects. Two weeks after the stereotaxic injections, apomorphine was administrated subcutaneously and rotation to the contralateral or ipsilateral side registered for 45 min. As expected, healthy mice, both saline and miR-124 NPs-treated mice, exhibited a net rotation near zero, while 6-OHDA-challenged saline mice presented a significant increase in the net contralateral rotations that was reversed at some extent in miR-124 NPs-treated mice (Figure 3.10 D; 6-OHDA mice: 100.0 ± 4.9, miR-124 NPs 33.6 ± 22.4, *P < 0.05, #P < 0.05). Although any significant differences were found in the levels of dopaminergic neurons in the SN (saline 33.3 ± 1.5, miR-124 NPs 28.9 ± 3.4) and in the amount of dopaminergic fibers in the striatum of 6-OHDA-challenged mice (percentage of area occupied by tyrosine hydroxylase fibers: saline 12.2 ± 1.2; miR-124 NPs 16.2 ± 7.1), the boost of neurogenesis caused by our formulation seems to partly rescue the motor impairments of 6-OHDA-challenged mice.
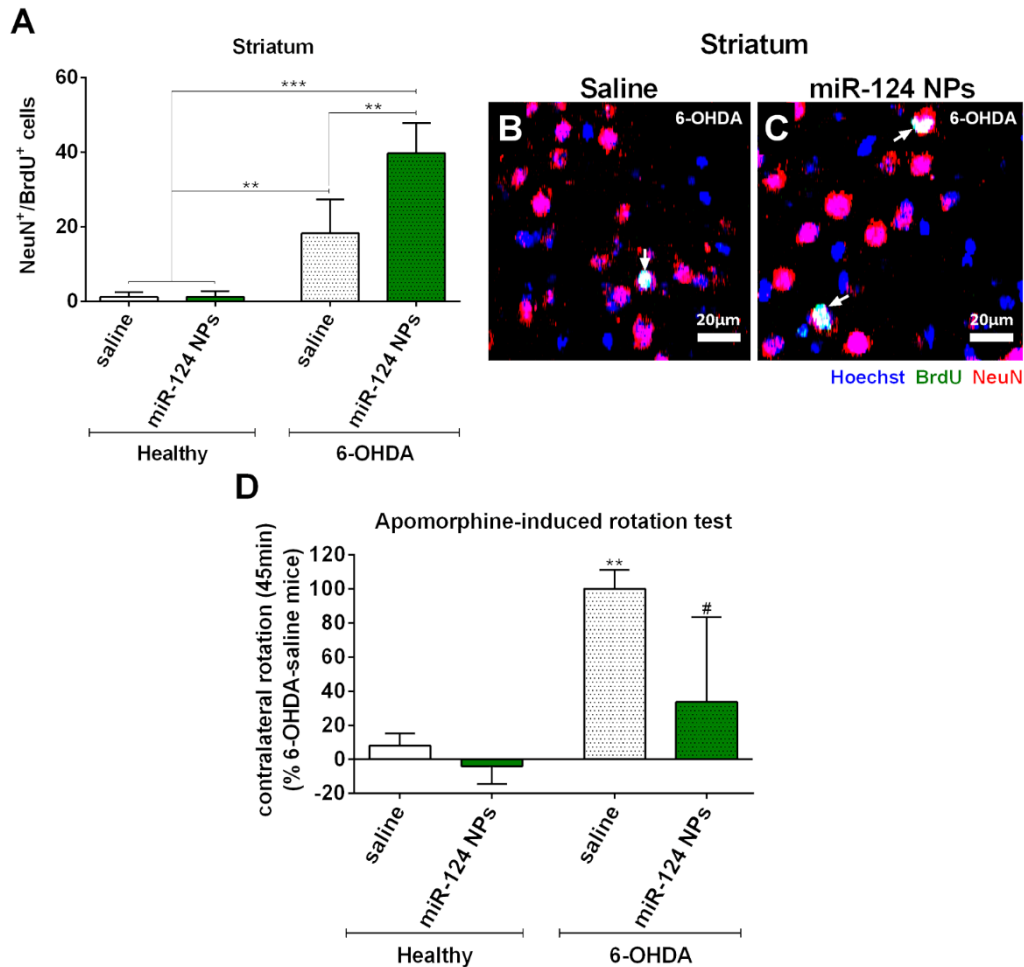
Figure 3.10   miR-124 NPs induce integration of mature neurons into the lesioned striatum of 6-OHDA-challenged mice and ameliorate the PD phenotype.
(A) Bar graph depict the effect of miR-124 NPs on the total number of NeuN+/BrdU+ cells found in healthy or 6-OHDA-challenged mice. (B, C) Representative confocal digital images of BrdU (green), Hoechst (blue) and NeuN (red) staining observed in the striatum of 6-OHDA-challenged mice (saline (B) or miR-124 NPs (C). Scale bar: 20 µm; white arrows highlight NeuN+/BrdU+ cells. (D) Bar graph illustrates the net rotation to the contralateral side of healthy or 6-OHDA-challenged mice. Data are expressed as mean ± SEM (n=4-6 mice) #P<0.05, **P < 0.01, ***P < 0.001 using Bonferroni's multiple comparison test. (D) Results are set to 100%; # displays the difference between 6-OHDA-lesioned saline and miR-124 NPs mice. Abbreviations: 6-OHDA, 6-hydroxidopamine; BrdU, 5-bromo-2'-deoxyuridine; NeuN, neuronal nuclei; NPs, nanoparticles; PD, Parkinson's disease.

3.3 Discussion

In this study, we unveil the effect of miR-124 NPs as a possible therapeutic strategy to improve PD outcome in 6-OHDA mice. *In vitro*, we observed that miR-124 NPs were efficiently internalized by neural stem/progenitors cells and neuroblasts and promoted their neuronal commitment and maturation. Expression of Sox9 and Jagged1, two miR-124 targets and stemness-related genes, were also decreased upon miR-124 NPs treatment. *In vivo*, and to the best of our knowledge, we were the first showing not only the ability of a NP formulation to modulate the endogenous neurogenic niche in PD but also its ability to ameliorate PD motor symptoms. Notably, we were able to demonstrate the pro-neurogenic potential of miR-124 NPs both in physiologic conditions and in a pre-clinical mouse model for PD.

miRNA-based therapies have been emerging in the last few years. Indeed, some clinical trials using miRNA-based therapies are being performed (e.g. MRX34 from Mirna Therapeutics) (Wahid et al. 2014). Nevertheless, one of the major concerns in the translation of miRNA-based therapies to the clinic is the efficient delivery of these molecules into cells. The physicochemical properties of miRNA (hydrophilic nature and negative charge) as well as their easy cleavage by nucleases make the transfection efficiency a challenge by itself (Guzman-Villanueva et al. 2012; Chen et al. 2015). Primary SVZ cell cultures contain a mixture of stem (type B cells) and progenitor cells (type C cells) able to proliferate and generate neurons and glial cells (Santos et al. 2012b). In this study, we showed that our NP formulation is able to efficiently protect and deliver miRNA into SVZ cells, specifically into stem/progenitor and immature cells, the cell population that can differentiate into mature neurons in response to increased levels of miR-124. In fact, we showed recently that the same NP formulation was able to rapidly release miRNA in human umbilical vein endothelial cells (HUVEC), with only 50% of miR-Dy547 co-localizing with FITC-NPs at 24 h post-transfection (Gomes et al. 2013). Moreover, the retention of about 30% of NPs or miR-Dy547 within the endolysossomal compartments was associated with the ability of the NP formulation to present miRNA to the RNA-induced silencing complex (miRISC) machinery. This characteristic culminated in a higher biologic effect than the commercial transfection system SIPORT, either in normoxia or hypoxia conditions (Gomes et al. 2013). miR-124 NPs did not cause any toxic effect in the SVZ cells at the concentration used – 1 µg/mL – neither in terms of apoptosis nor in terms of necrosis/late apoptosis. Besides, our polymeric NP formulation can be traced by ^{19}F MRI technique due to the presence of a nontoxic fluorine compound – PFCE (Gomes et al. 2013). The theranostic feature of our NPs makes it an attractive model to future clinical studies and an alternative to the NPs being currently used for MRI clinical application, such as superparamagnetic iron oxide NPs. Other important feature is the use of Food and Drug Administration (FDA)-approved materials in its composition (Gomes et al. 2013), which can be engineered in terms of surface ligands making its delivery more specific and facilitating the translation to the clinic. Altogether, the NP formulation developed by us can overcome issues related with safety and traceability that other miRNA-delivery agents such as viral vectors and liposomes cannot (Guzman-Villanueva et al. 2012; Chen et al. 2015).

Herein, we also showed that miR-124 NPs favor neuroblast proliferation while decreasing the proliferation of astrocytic-like cells. In accordance, others have showed that viral overexpression of miR-124 is able to promote the commitment of type C progenitor cells towards a neuronal fate while reducing the stem/progenitor cell pool (Cheng et al. 2009; Akerblom et al. 2012). In physiological conditions, the expression of miR-124 is also increased during the transition from progenitors towards mature neuronal cells (Cheng et al. 2009; Akerblom et al. 2012). As hypothesized by us, our formulation was able to efficiently increase neuronal differentiation as compared with control cultures while it slight reduce the astrocytic population and maintain the oligodendrocyte population. In accordance, Akerblom and colleagues reported an increased number of astrocytes after miR-124 inhibition (Akerblom et al. 2012) and Neo and colleagues showed that miR-124 was able to control the choice between neuronal or astrocytic differentiation (Neo et al. 2014).

miR-124 targets include several non-neuronal-related genes including Sox9 (Notch downstream effector involved in glial fate specification and in the maintenance of stem cells in an undifferentiated state) (Stolt et al. 2003; Cheng et al. 2009; Åkerblom and Jakobsson 2014) and jagged1 (Notch1 ligand involved in stem cell self-renewal) (Nyfeler et al. 2005; Cheng et al. 2009; Åkerblom and Jakobsson 2014), among others. We observed that miR-124 NPs were able to reduce both mRNA and protein levels of Sox9 and Jag1, indicating a role of these miR-124 targets in the robust enhancement of neurogenesis.

Axon formation and neurite outgrowth are essential processes for the maturation and integration of newborn neurons; these processes are dependent on JNK pathway activation (Oliva et al. 2006). We demonstrated that miR-124 NPs are able to promote axonogenesis by increasing both the number of ramifications and length of P-JNK positive neuritis. JNK can phosphorylate and activate several transcription factors in the nucleus, including c-Jun, which may transduce cell death signals (Weston 2002; Varfolomeev and Ashkenazi 2004; Bode and Dong 2007). However, P-JNK immunoreactivity was localized in Tau[+] axons, but not in the nucleus, suggesting that miR-124 NPs promote axonogenesis instead of inducing apoptosis. Additionally, neither apoptosis nor late-apoptosis/necrosis was induced by 1 µg/mL miR-124 NPs. Indeed, growing literature supports a role of JNK in cell proliferation, survival, and differentiation. For instance, it was shown that JNK1 and the JNK pathway-specific scaffold protein, JSAP1, promote neural differentiation of embryonic stem cells (Xu et al. 2003; Amura et al. 2005). Activated JNK may also foster axonogenesis and neuronal polarization by targeting cytoskeletal proteins, such as the Tau protein (Yoshida et al. 2004; Oliva et al. 2006). Our results are also in accordance with a previous report showing that miR-124 is able to control neurite outgrowth during neuronal differentiation presumably by regulating cytoskeleton proteins (Yu et al. 2008). Additionally, it has been shown by others that miR-124 promotes neurite elongation in human neuroblastoma and mouse P19 cell lines by repressing Rho-associated coiled-coil forming protein kinase 1 (ROCK1), an upstream repressor of the phosphoinositide 3-kinase (PI3K)/Akt pathway (Gu et al. 2014). In sum, the activation of the SAPK/JNK pathway found in Tau-expressing axons suggests that miR-124 NPs enhance axonogenesis and neuronal maturation in SVZ cells.

In vivo we proved that miR-Dy547 FITC-NPs injected into the lateral ventricle could reach and be internalized by SVZ cells. This interaction could occur through direct interaction with type B cells that project a cilium into the ventricle (Santos et al. 2012b) or by paracrine effect *via* ependymal cells. After, the effects of miR-124 NPs in a 6-OHDA-based pre-clinical mouse model for PD was assessed by double stereotaxic injections to deliver 6-OHDA into the right striatum and NPs into the right lateral ventricle.

Under physiologic conditions SVZ-derived neuroblasts migrate towards the GCL and GL of the OB, where they integrate as mature interneurons (Ming and Song 2011). However, neurogenesis rate may fluctuate in response to brain injury or degeneration. Previous reports showed that miR-124 overexpression promotes neurogenesis and decreases SVZ proliferation in physiological conditions. Moreover, it does not interfere with migration nor OB integration (Cheng et al. 2009; Akerblom et al. 2012), but it endorses a preferential integration of new neurons into the GCL rather than the GL (Akerblom et al. 2012). Accordingly, we showed that a single intracerebroventricular administration of

miR-124 NPs is able to modulate SVZ neurogenesis, culminating in the enrichment of new neurons in the GCL of the OB. Importantly, migrating neuroblasts that reach the GCL fully differentiated into mature neurons. Although we do not know the neuronal phenotype generated by DCX$^+$ neuroblasts found in the GCL, we do know that the GCL contains mostly SVZ-derived GABAergic interneurons (Bédard and Parent 2004; De Marchis et al. 2004).

Then, we hypothesized that miR-124 NPs are also able to boost neurogenesis in a mouse model of PD. Inconsistent data have been reported over the last years showing decrease, maintenance or even increase of neurogenesis in PD models and PD patients, reviewed at (van den Berge et al. 2013). The differential activation of dopaminergic receptors in NSCs (Höglinger et al. 2004; Coronas et al. 2004; Kippin et al. 2005) together with a high diversity of PD models (transgenic or toxin based models, acute or chronic administrations, different dosages and different spatial administration of toxins (Dauer and Przedborski 2003) may explain distinct outcomes. Having in mind these limitations, herein we showed that the 6-OHDA mouse model for PD developed by us is in accordance with the reports showing impaired SVZ neurogenesis. Some reports showed that injection of 6-OHDA in mice led to a reduction in SVZ proliferation (Baker et al. 2004; Sui et al. 2012), yet the levels of neuroblasts in SVZ and RMS were not affected and a higher survival of neurons in the OB was detected (Sui et al. 2012; Fricke et al. 2016). We also observed a reduction in SVZ proliferation caused by 6-OHDA that did not interfere with the number of DCX$^+$ cells at the SVZ, nor with the migration or OB integration. Nevertheless, more studies are needed to hamper our knowledge regarding the neurogenesis process in PD to improve future therapeutic regenerative strategies.

Even in pathological conditions, a single dose of miR-124 NPs was able to efficiently increase the number of migrating neuroblasts reaching the GCL to levels higher than the ones obtained when miR-124 NPs were administered in healthy animals. Importantly, miR-124 NPs potentiated the migration of SVZ-derived neurons towards the striatal damaged area. The above-mentioned alterations culminated with the amelioration of the behavior of PD mice treated with miR-124 NPs, seen by the apomorphine-induced rotation test. For this behavior analysis we took advantage of the side-biased motor impairments obtain from unilateral injection of 6-OHDA to induce a PD mouse models (Ungerstedt and Arbuthnott 1970; Iancu et al. 2005). Apomorphine is a dopamine receptor agonist that at low doses causes contralateral turning by stimulating both supersensitive D1 and D2 receptors preferentially on the denervated side of mice, allowing not only to characterize lesion extension but also to detect therapeutic effects (Millan et al. 2002). As so, we did observe a significant decrease of the net contralateral rotation induced by the apomorphine of 6-OHDA-challenged mice treated with miR-124 NPs when compared with saline, despite the levels of dopaminergic neurons in the SN of 6-OHDA-challenged mice were similar between the two groups. We anticipate that the higher levels of new neurons found in the striatum of 6-OHDA-challenged miR-124 NPs-treated mice may contribute to the recovery outcome.

3.4 Conclusions

In sum, we proved that the uptake of miR-124 NPs by SVZ stem/progenitor cells resulted in the repression of Sox9 and Jagged1 proteins and the activation of SAPK/JNK pathway, promoting an

increase in neurogenesis and axonogenesis. *In vivo*, a single administration of a small amount of miR-124 (0.5 pmol) delivered by our NP formulation increased the number of migrating SVZ-derived neuroblasts that reached the GCL of the OB, both in healthy and a PD mouse model. Importantly, miR-124 NPs also potentiated the migration of SVZ-derived neurons into the 6-OHDA lesioned striatum. The formulation promoted not only neurogenesis at the SVZ-OB axis but also the migration and maturation of new neurons into the lesioned striatum, indicating its value as a strategy to improve brain repair for PD. Moreover, our formulation also leads to motor amelioration of the PD symptoms found in 6-OHDA-challenged mice (see Figure 3.11 for a summary of the results obtained). As so, evidence of behavior improvement in pre-clinical models of PD can open new avenues in the development of novel therapeutic approaches. The systemic delivery of miR-124 NPs by intravenous or intraperitoneal injections should be considered in future studies to circumvent the need of an invasive stereotaxic surgery.
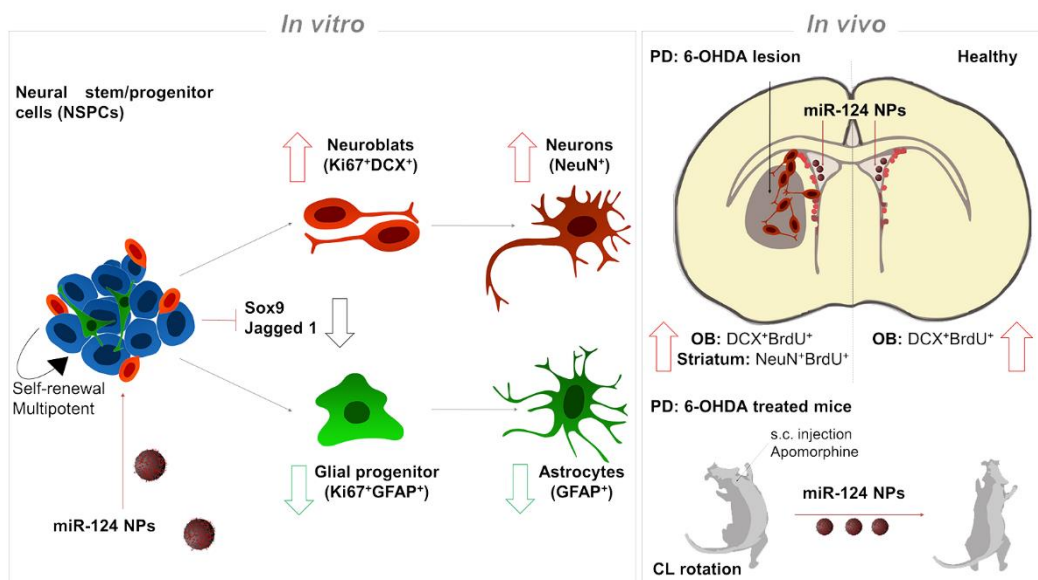
Figure 3.11 miR-124 loaded nanoparticles (miR-124 NPs) boost neuronal differentiation of neural stem/progenitors cells (NSPCs) from the subventricular zone (SVZ) *in vitro* and *in vivo*, ultimately leading to motor symptoms amelioration in a Parkinson's disease (PD) mice model.
Left panel (*In vitro*): SVZ NSPCs cultures treated with miR-124 NPs showed a shift from glial (Ki67+/GFAP+) to a neuronal fate (Ki67+/DCX+) culminating in a robust enhancement in the number of mature neurons (NeuN+) and a slight decrease of astrocytes (GFAP+). This neurogenic shift seems to be related with the downregulation of two miR-124 targets Sox9 and Jagged1. Right panel (*In vivo*): miR-124 NPs were injected in the lateral ventricles of healthy and 6-OHDA-challenged mice followed by intraperitoneal administration of BrdU. The number of proliferating neuroblasts (DCX+/BrdU+) in the olfactory bulb, the end-point of the SVZ-derived neuroblasts, was increased both in healthy and in 6-OHDA-challenged mice when compared with the saline counterparts. Moreover, levels of new neurons (NeuN+/BrdU+) found in the 6-OHDA-lesioned striatum were significantly increased by miR-124 NPs. Importantly, this enhancement of neurogenesis is accompanied by an amelioration of PD motor symptoms. In particular, 6-OHDA-challenged mice treated with miR-124 NPs showed a reduction in the net contralateral rotations upon subcutaneous administration of apomorphine. Abbreviations: 6-OHDA, 6-hydroxidopamine; BrdU, 5-bromo-2'-deoxyuridine; CL, contralateral side; DCX, doublecortin; GFAP, glial fibrillary acidic protein; NeuN, neuronal nuclei; OB, olfactory bulb; NPs, nanoparticles; PD, Parkinson's disease; s.c., subcutaneous.

Chapter 4

MicroRNA-124-LOADED NANOPARTICLES INCREASE SURVIVAL AND NEURONAL DIFFERENTIATION OF NSCs *IN VITRO* BUT DO NOT CONTRIBUTE TO STROKE OUTCOME *IN VIVO*

4.1 Introduction

After stroke, the adult brain attempts to compensate lost function by reorganizing itself, an action that involves multiple interconnected mechanisms such as cell genesis, astrogliosis, inflammation and neuronal plasticity. The proliferation and differentiation of cells derived from neural stem cells (NSCs) may replace lost neurons and thereby contribute to improve functional deficits (Lagace 2012; Lindvall and Kokaia 2015; Marlier et al. 2015). In addition, inflammatory cascades, either detrimental or beneficial, significantly contribute to acute tissue demise. However, an increased activation of immune cells as well as inflammatory molecules can be observed weeks after the insult and may contribute to restoration of brain function (Kuric and Ruscher 2014). Interestingly, therapeutic experimental approaches targeting detrimental inflammatory cascades have been translated into clinical trials aiming at improving neurological outcome of stroke patients, reviewed at (Lakhan et al. 2009; Simats et al. 2016).

MicroRNAs (miRNA or miR) are small endogenous, non-coding RNAs able to regulate hundreds of genes at the post-transcriptional level by inhibiting mRNA translation or inducing mRNA degradation (Bartel 2004). Previous reports showed that miR-124 levels were decreased in neural progenitor cells of the subventricular zone (SVZ) and in the ischemic core (Liu et al. 2011; Sun et al. 2013a), but seemed to be elevated in the plasma of rodents subjected to permanent occlusion of the middle cerebral artery (MCAO) (Laterza et al. 2009; Weng et al. 2011). In stroke patients, downregulation of plasma levels of miR-124 within the first 24 h was negatively associated with infarct size (Liu et al. 2015). In contrast, another study showed increased plasma levels of miR-124 and those were correlated with higher mortality during the first 3 months after stroke and a worse outcome based on post-stroke modified Rankin Score (mRS) (Rainer et al. 2016). In stroke models, overexpression of miR-124 prior to stroke decreased infarct volume, reduced microglial activation and improved neurogenesis *via* ubiquitin-specific protease (Usp)14-dependent REST degradation (Zhao et al. 2010; Doeppner et al. 2013). In addition to protective effects, injection of liposomated miR-124 into the striatum of mice two days after transient MCAO promoted an anti-inflammatory state (M2 state) of microglia/macrophages and conversely reduced their pro-inflammatory state (M1 state), which correlated with a better functional outcome during the first week after stroke onset (Hamzei Taj et al. 2016b; Hamzei Taj et al. 2016a). In contrast, others have demonstrated that downregulation of miR-124 resulted in lower infarct volumes while no changes in terms of infarct volumes have been observed after overexpression of miR-124 (Liu et al. 2013; Zhu et al. 2014).

MicroRNAs are small molecules with short half-life and poor stability. To overcome this issue we have developed ~210 nm-size polymeric NPs with a fluorine compound that can be tracked by fluorine (^{19}F) magnetic resonance imaging (MRI) (Gomes et al. 2013). This system has already proven efficacy in miRNA delivery into cells both *in vitro* and *in vivo*. For example, we demonstrated, using this formulation, that intracerebroventricular delivery of miR-124-loaded NPs (miR-124 NPs) promotes SVZ neurogenesis in mice both in physiological conditions and after 6-hydroxydopamine (6-OHDA) lesions. We have also shown that administration of miR-124 NPs increased the number of new neurons in the lesioned area associated with amelioration of Parkinson's disease-related motor deficits (Chapter 3).

The present study has been conducted to evaluate if exposure of miR-124 NPs affects survival and differentiation of SVZ derived NSCs after exposure to oxygen and glucose deprivation (OGD). Positive results from these experiments prompted us to hypothesize that systemic administration of miR-124 affects stroke outcome measures, namely neurological functions during the first 14 days after photothrombotic stroke (PT). Moreover, we sought to identify the role of miR-124 on post-stroke inflammatory response and neurogenesis.

4.2. Results

4.2.1 miR-124 NPs protect SVZ cells and stimulate their differentiation after OGD

SVZ cells have been isolated and grown *in vitro* as neurospheres (cell suspensions) that are mostly stem/progenitors cells. A polymeric NP formulation was used as a carrier to deliver miR-124 into SVZ cells. These NPs have a MRI tracer (perfluoro-1,5-crown ether) in their core and are mainly constituted of a polymer – PLGA – that is coated with a cationic agent, protamine sulfate, to allow the complexation of negatively charged miRNA molecules. Based on our previous studies demonstrating that 1 µg/mL of NPs complexed with 200 nM (50 pmol) of miR-124 induced neuronal differentiation of SVZ cells *in vitro* without cytotoxic effects (Chapter 3), we applied these conditions to evaluate if miR-124 NPs have a beneficial effect on SVZ cells exposed to a combined oxygen and glucose deprivation. SVZ cultures obtained from post-natal C57BL/6 mice were exposed to OGD for 1 h followed by a reoxygenation period of 24 h with either fresh medium (non-treated cells) or fresh medium containing miR-124 NPs or scramble-miR NPs or void NPs. Control cells were not subjected to OGD (normoxic non-OGD control). Exposure to OGD for 1 h led to a significant 1.7-fold increase in the cell death of SVZ cultures, being this effect reverted in cultures transfected with miR-124 NPs after the OGD insult (Figure 4.1 B; non-control OGD 8.8 ± 0.8, non-treated cells 1 h OGD 15.4 ± 1.2, miR-124 NPs 1 h OGD 9.1 ± 0.7, ***P < 0.001, ###P < 0.001). To measure cell proliferation 5-bromo-2'-deoxyuridine (BrdU) was added to SVZ cells for the last 4 h of the 48 h post-OGD incubation period. BrdU is a thymidine analog that incorporates into the DNA of cells during the S phase of the mitotic process. The total levels of BrdU$^+$ cells were not altered by the exposure to OGD *per se* nor by the presence of miR-124 NPs after OGD (Figure 4.1 C). Finally, we studied the miR-124 NPs neurogenic potential after OGD by staining the cultures with the mature neuronal marker NeuN (neuronal nuclei; Figure 4.1 D, E). Surprisingly, OGD exposure did not alter the levels of neurons obtained from a SVZ cultures when compared with non-OGD basal conditions. Nevertheless, the presence of miR-124 NPs after the OGD insult resulted in a 1.6-fold increase in the NeuN$^+$ cells compared with non-OGD control (Figure 4.1 D, E; non-OGD control 23.0 ± 3.1, miR-124 NPs 1h OGD 37.7 ± 1.1, ***P < 0.001). These results indicate that miR-124 NPs may not only have a neurogenic potential but are also neuroprotective after OGD *in vitro*.
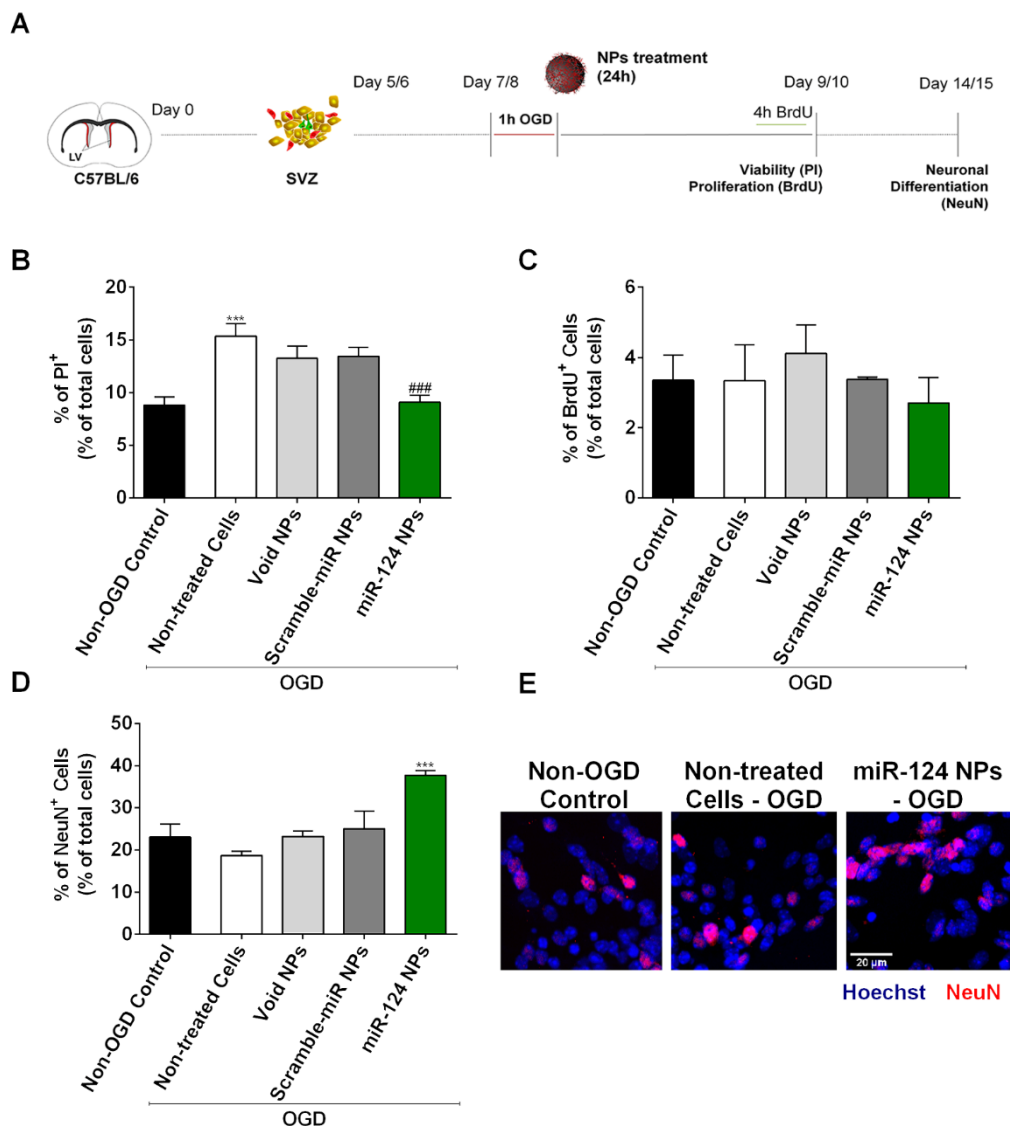
Figure 4.1   Effect of miR-124 NPs treatment on SVZ cell cultures after OGD.
(A) Experimental design of *in vitro* experiments. NSCs where isolated from the SVZ of C57BL/6 1 to 3 days-old pups and grown in suspension for 5 or 6 days to obtain neurospheres. Neurospheres were seeded and allowed to grow as monolayer for 2 days before being stimulated with OGD for 1 h. Cells were then incubated with void NPs, scramble-miR NPs or miR-124 NPs for 24 h. Cells were maintained in culture according to the parameters evaluated: 48 h for cell viability and proliferation assays and 7 days for neuronal differentiation. (B) Cell viability assessed by incorporation of propidium iodide (PI) into dead cells and presented as percentage of PI$^+$ cells in cultures stimulated with OGD and either non-treated or treated with void NPs, scramble-miR NPs or miR-124 NPs, respectively. PI$^+$ cells quantified in normoxic cultures (non-OGD control) served as controls. (C) Proliferation of SVZ cultures after OGD followed by different treatments. Graphs show the percentage of BrdU$^+$ cells of total cell counts. (D) Neuronal differentiation of the cultures measured by the percentage of NeuN$^+$ cells in NSC monolayer cultures. (E) Representative fluorescence photomicrographs of NeuN immunostainings in non-OGD control cultures, OGD non-treated and OGD miR-124 NPs treated cultures 7 days after treatment. Nuclei are shown in blue and NeuN in red. Scale bar: 20 μm. Data are expressed as means ± SEM (n = 3). Statistical analysis was performed using one-way ANOVA and Tukey multiple comparison. ***P < 0.001 versus non-OGD control; ###P < 0.001 versus 1h OGD non-treated cell condition. Abbreviations: NeuN, neuronal nuclei; NPs, nanoparticles; NSCs, neural stem cells; OGD, oxygen and glucose deprivation; SVZ, subventricular zone.

4.2.2 Treatment with miR-124 NPs does not affect lesion volume and functional outcome after photothrombosis

Next, we aimed at evaluating if administration of miR-124 NPs could modulate processes in the post-ischemic brain contributing to recovery of lost neurological function. For that, we evaluated sensorimotor function, the inflammatory response (pro-inflammatory cytokine levels in the ischemic territory and periphery) and neurogenesis (doublecortin (DCX) and BrdU cell number in SVZ and peri-infarcted area) in mice subjected to PT or sham operation. Behavioral tests were performed on day -1 and day 2, day 7 and day 14 after surgery. Following PT or sham surgery, the inflammatory response was studied on day 2 post-stroke while neurogenesis was evaluated on day 14 in mice that were intravenously injected with miR-124 NPs, scramble-miR NPs, void NPs or saline, respectively (Figure 4.2 A).

In pilot experiments, we observed that NPs were able to penetrate into the brain parenchyma by injecting 1 mg of fluorescein isothiocyanate (FITC)-NPs to mice immediately after PT. Co-staining of the FITC-NPs with the marker for endothelial cells CD31 clearly showed a wide distribution of FITC immunoreactivity throughout the brain parenchyma 4 h after intravenous injection. Signals were observed in brain microvessels as expected indicating that there was not a complete penetration of NPs (Figure 4.2 B). Importantly, FITC-NPs were found in the striatum and cortex, including the peri-infarcted area; in addition, significant accumulation of FITC-NPs was observed in white mater, namely the corpus callosum and taken up by astrocytes (Figure 4.2 C) and neurons (Figure 4.2 D). Administration of higher dosages (5 and 10 mg) of FITC-NPs showed similar results at 4 and 24 h following intravenous injection (data not shown).

Evaluation of infarct volumes revealed no differences between all treatment groups: PT saline 0.9 ± 0.1; PT void NPs 0.8 ± 0.2; PT scramble-miR NPs 0.7 ± 0.1; PT miR-124 NPs 0.8 ± 0.1 (Figure 4.2 E). As shown in Figure 4.2 F representative coronal sections show similar infarct areas in mice treated either with saline or miR-124 NPs, indicating that miR-124 NPs do not contribute to a reduction of the ischemic lesion. From these results, we can exclude that differences in lesion volumes did not influence outcome measures.

Neurological deficits and their recovery were assessed by two independent behavioral tests: the rotating pole test (Figure 4.3 A-F) and the grid test (Figure 4.3 G, H). After PT, mice showed neurological deficits that were not evident before PT. Prior to PT, all animals performed the rotating pole test with a median of 4 points (Figure 4.3 D). On day 2, the majority of the animals could not traverse the pole, the median throughout the groups was 2 (Figure 4.3 E). No difference was observed comparing the four treatment groups. A slight but non-significant recovery has been observed 14 days after PT due to spontaneous recovery. Similar to day 2, treatment with miR-124 NPs did not improve motor function in mice subjected to PT (Figure 4.3 F) compared to the non-treated (saline) mice subjected to PT. Likewise, mice subjected to PT made a significant higher number of foot faults in the grid test. Also here, treatment did not affect the performance at any timepoint measured (Figure 4.3 H). In both behavioral tests, sham-operated mice did not show deficits. They had a similar performance throughout the study (Figure 4.3 A-C, G).
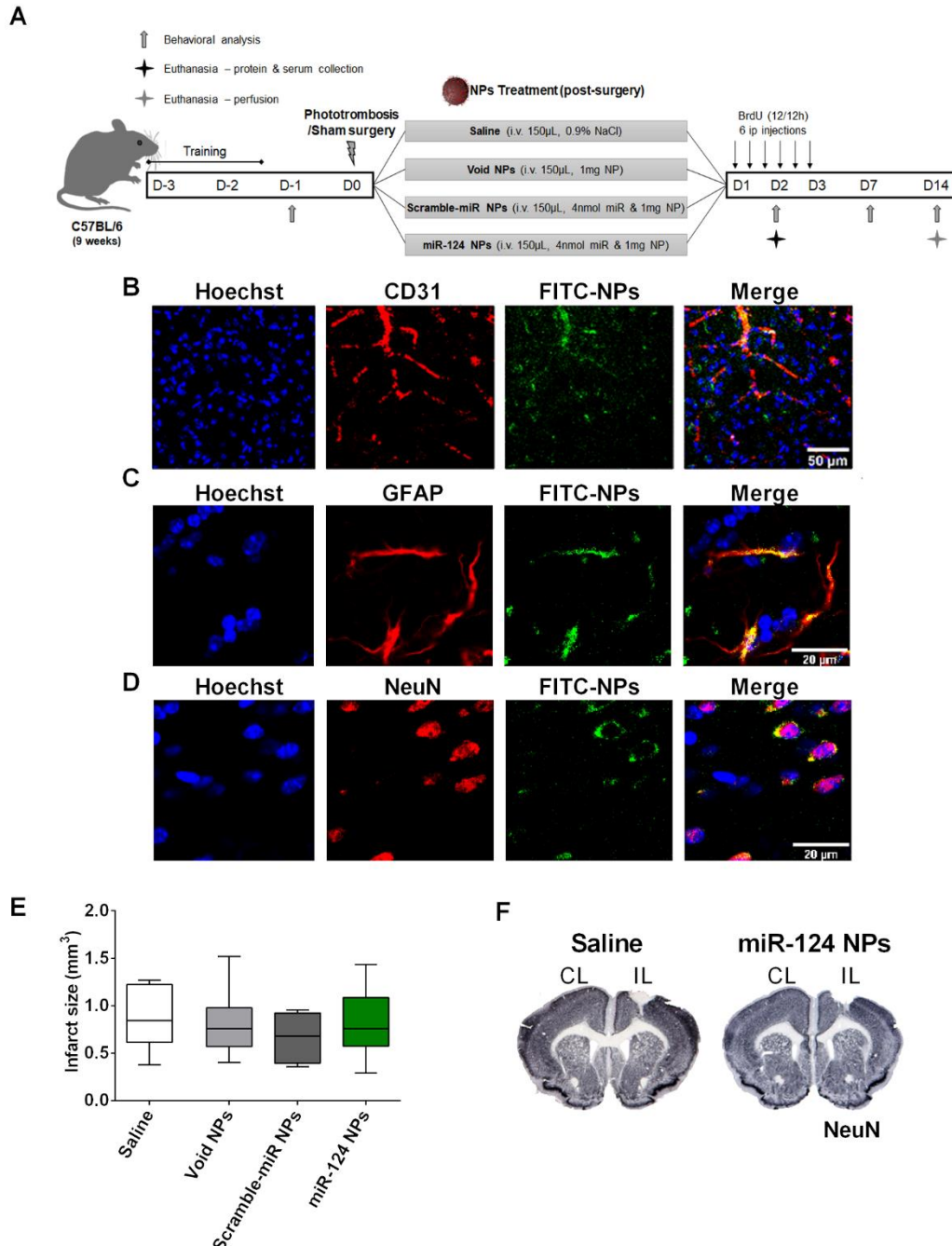
Figure 4.2   miR-124 NPs do not affect infarct volume of PT mice.
(A) Experimental design for the *in vivo* experiments. Before entering the study, mice were assigned to surgery and treatment groups subjecting them either to sham surgery or PT. Each group was then subdivided into 4 subgroups in which mice were treated with an intravenous injection in the tail vein of saline, void NPs, scramble-miR NPs or miR-124 NPs (total of 8 different groups) immediately after surgery. Pro-inflammatory cytokines from the ischemic territory (infarct core and adjacent peri-infarct tissue) and serum have been measured on day 2 after surgery. Infarct volume and neurogenesis have been studied 14 days after surgery. These mice received BrdU injections (every 12 h) during the first 3 days after surgery. After a training period, neurological function was tested on days -1, 2, 7 and 14, respectively. (B, C, D) Representative photomicrographs of the peri-infarct area 4 h after intravenous injection of 1 mg of FITC-NPs (green) and stained against the nuclear marker Hoechst (blue) and either the endothelial marker CD31 (red) (B), or the astrocyte marker GFAP (red) (C), or the neuronal marker NeuN (red) (D). Scale bar 50 µm (B) or 20 µm (C, D). (E) Infarct volume (in mm^3) in the 4 different groups following PT. Data are expressed as medians with the 1st and 3rd quartile with the following number of animals included in each experimental group: PT saline n = 6, PT void NPs n = 6, PT scramble-miR NPs n = 8, PT miR-124 NPs n = 8. F) Representative images of the infarct area (white) in coronal sections stained with NeuN of mice treated with saline (left) or miR-124 NPs (right). Abbreviations: BrdU, 5-bromo-2'-deoxyuridine; CL, contralateral hemisphere; FITC, fluorescein isothiocyanate; GFAP, glial fibrillary acidic protein; IL, ischemic hemisphere; NeuN, neuronal nuclei; NPs, nanoparticles; PT, photothrombosis.
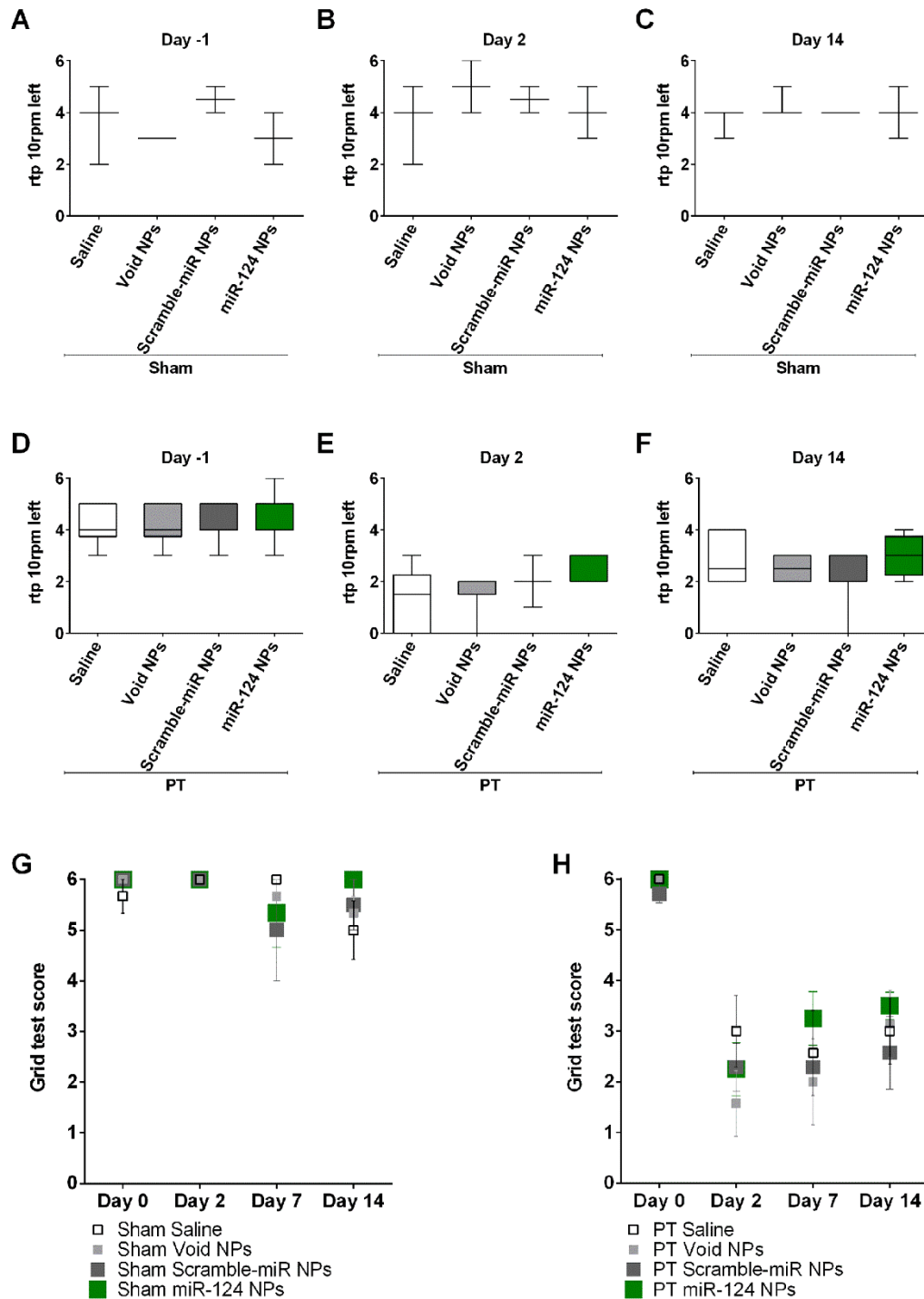
Figure 4.3   miR-124 does not affect neurological function after photothrombosis.
(A-C) Rotating pole test scores of mice subjected to sham surgery and treated either with saline, void NPs, scramble-miR NPs or miR-124 NPs administered intravenously immediately after PT. (D-F) Rotating pole test scores from mice subjected to PT and treated with saline, void NPs, scramble-miR NPs or miR-124 NPs administered intravenously immediately after PT. Results in (A-F) show the performance at 10 rotations of the pole to the left 2 days and 14 days after the insult, respectively. (G, H) Grid test presenting the number of foot faults of the left side paws traversing a 60 cm long grid as indicated in the Material and methods section (Chapter 2). Sham-operated mice (G) and mice subjected to PT (H) of the above-mentioned treatment groups were evaluated at days -1 or 0, 2, 7 and 14. All data are represented as medians with the 1st and 3rd quartile with 2 to 8 animals per group: sham saline n = 3, sham void NPs n = 3, sham scramble-miR NPs n = 2, sham miR-124 NPs n = 3, PT saline n = 6, PT void NPs n = 6, PT scramble-miR NPs n = 7, PT miR-124 NPs n = 8. Abbreviations: NPs, nanoparticles; PT, photothrombosis.

4.2.3 SVZ Neurogenesis after miR-124 NPs treatment in PT mice

To evaluate neurogenesis, mice were injected intraperitoneally with BrdU for 3 days after surgery (every 12 h, Figure 4.2 A) in order to assess dividing cells. The number of cells positive for DCX (DCX$^+$; marker of neuroblasts), BrdU$^+$ and double positive for DCX and BrdU (DCX$^+$/BrdU$^+$) were evaluated in the SVZ (Figure 4.4 A-E) and peri-infarct area (Figure 4.3 A, F-H). In the SVZ, two weeks after surgery and miR-124 NPs injection, we did not observe any differences between the number of DCX$^+$ cells in the PT animals when compared with sham-operated mice nor among the different treatment groups both in PT and sham animals (Figure 4.4 C). We observed that PT animals tend to have slightly higher numbers of BrdU$^+$ cells compared to sham-operated animals. Hence, treatment with miR-124 NPs did not change the total number of BrdU stained cells when compared with saline, void NPs or scramble-miR NPs, respectively (Figure 4.4 D). This increase, however, can be explained by higher levels of non-neuronal cells that may proliferate, as well as cell death in response to the damage caused by the PT. Likewise the number of DCX$^+$ cells and DCX$^+$/BrdU$^+$ cells were also not altered among the eight experimental groups (Figure 4.4 B, E). To investigate the number of cells that potentially migrated from the SVZ to the lesion area, a region of interest was created located above the SVZ and underneath the infarcted area (Figure 4.4 A), or the equivalent region in sham animals, was evaluated. Sham mice did not present any DCX$^+$ cells and the number of BrdU$^+$ cells was negligible (Sham saline 1.7 ± 0.9, Sham void NPs 1.3 ± 0.9, Sham scramble-miR NPs 2.0 ± 2.0, Sham miR-124 NPs 2.3 ± 2.3). Regarding the PT mice, the number of BrdU$^+$ cells was elevated in all the groups independent of the treatment (Figure 4.4 G; PT saline 91.3 ± 11.9, PT void NPs 94.2 ± 8.8, PT scramble-miR 95.3 ± 8.9, PT miR-124 NPs 94.8 ± 6.9). Despite some reports suggesting the migration of SVZ neuroblasts into the peri-infarcted area (Osman et al. 2011; Diederich et al. 2012) we found very few DCX$^+$ cells in this area (Figure 4.4 H; PT saline 0.0 ± 0.0, PT void NPs 1.2 ± 0.8, PT scramble-miR NPs 0.8 ± 0.5, PT miR-124 NPs 0.4 ± 0.4).

From these results, we conclude that stroke induced neurogenesis does not exist in our experimental conditions and that a single intravenous injection of miR-124 NPs was unable to elicit an increase in SVZ neurogenesis neither in the healthy nor in post-stroke brain.
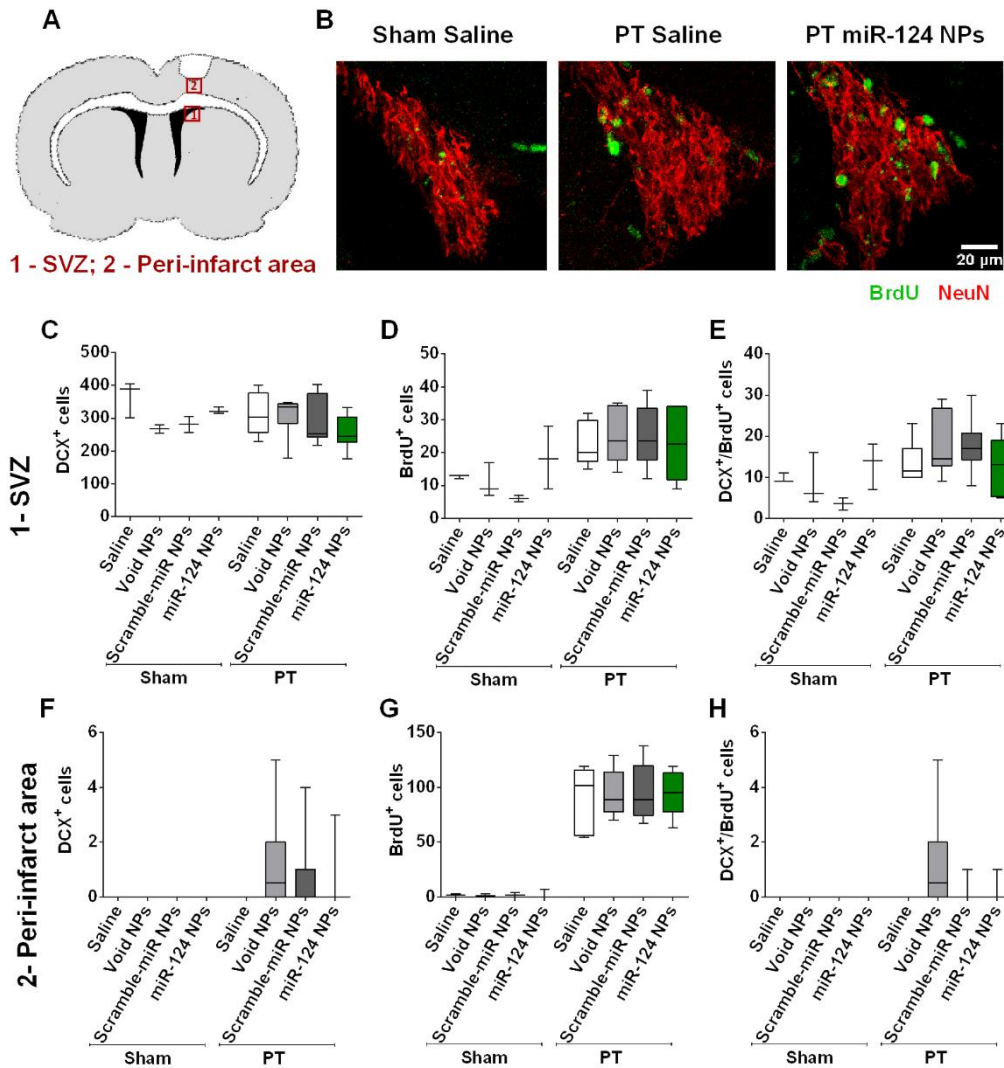
Figure 4.4   Neurogenesis is not affected by miR-124 NPs treatment.
(A) Illustration of a coronal slice of the mouse brain representing the areas used to evaluate neurogenesis in the SVZ (red rectangle 1) and the peri-infarct area (red rectangle 2). (B) Representative confocal images of BrdU (green) and DCX (red) staining observed in the SVZ of sham-operated and saline-treated animal, a mouse subjected to PT and saline-treated and a mouse subjected to PT miR-124 NPs-treated, respectively. Scale bar: 20 µm. Total number of (C, F) DCX$^+$ cells, (D, G) BrdU$^+$ cells and (E, H) DCX$^+$/BrdU$^+$ cells in the SVZ (C-E) and peri-infarct area (F-H) of mice after sham surgery or PT and indicated treatment conditions. All data are expressed as medians with the 1st and 3rd quartile values, with the following number of animals included in each experimental group: sham saline n = 3, sham void NPs n = 3, sham scramble-miR NPs n = 2, sham miR-124 NPs n = 3, PT saline n = 6, PT void NPs n = 6, PT scramble-miR NPs n = 8, PT miR-124 NPs n = 8. Abbreviations: BrdU, 5-bromo-2'-deoxyuridine; DCX, doublecortin; NPs, nanoparticles; PT, photothrombosis; SVZ, subventricular zone.

4.2.4 Effects of miR-124 NPs on the post-ischemic inflammatory response

miR-124 is predicted to attenuate inflammatory pathways, since a reduction in the miR-124 is needed to obtain a reactive microglial state (Freilich et al. 2013). We measured the levels of pro-inflammatory cytokines, namely interferon-gamma (IFNγ), interleukin-1beta (IL-1β), IL-6 and tumor necrosis factor-alpha (TNF-α) 48 h after PT (Figure 4.5). The levels of these four cytokines were measured in the ischemic territory (infarct core and peri-infarct area) to evaluate the local inflammatory response as well as in the serum of the same mice. In the brain, we found an elevation of all four

cytokines after PT compared to sham-operated mice, however, only IL-6 reached statistically significant levels. Animals subjected to PT treated with miR-124 NPs showed significantly higher levels of IL-6 compared to all experimental groups following sham surgery. In addition, the IL-6 levels of miR-124 NPs mice after PT were significantly higher compared to all other groups after PT (Figure 4.5 C). Regarding the peripheral response, there was no difference between any of the eight experimental groups (Figure 4.5 E-H), supporting previous studies that a peripheral immune response may be transient and limited to the first hours after stroke onset (Chapman et al. 2009; Ruscher et al. 2013). Once again, in contrary to our hypothesis treatment with miR-124 NPs did not reduce elevated levels of pro-inflammatory cytokines after PT.
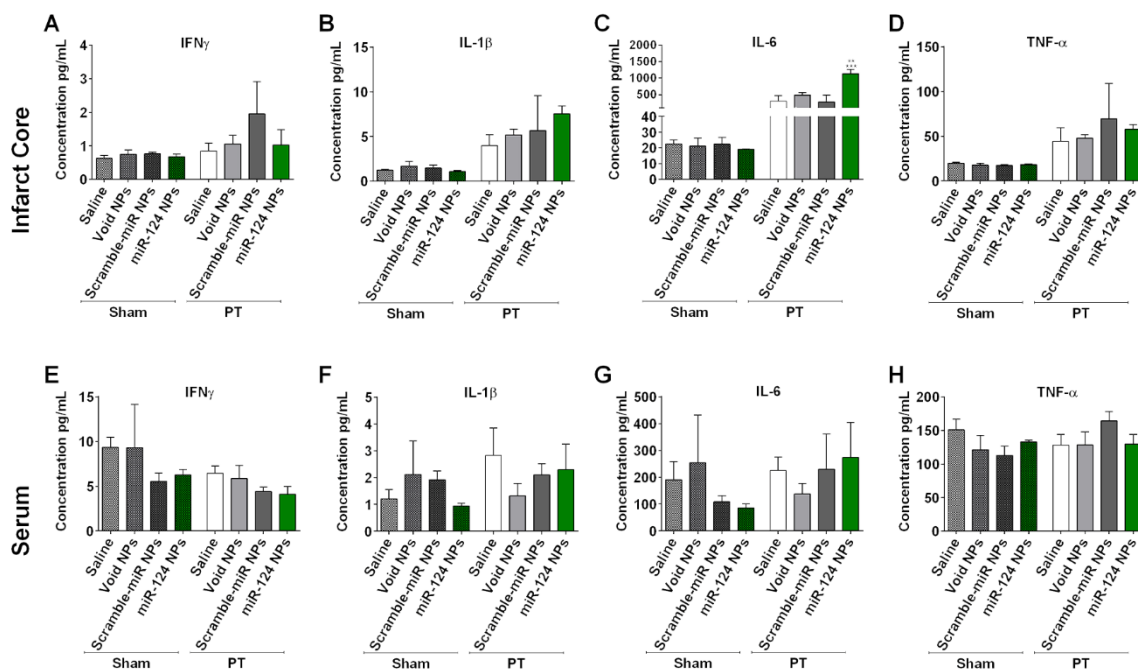
Figure 4.5   Effects of miR-124 NPs on levels of pro-inflammatory cytokines in the ischemic territory and serum.
(A-D) Levels of IFN-γ, IL-1β, IL-6 and TNF-α in the ischemic territory (infarct core and adjacent peri-infarct tissue) 2 days following PT. (E-H) Serum levels of the above-mentioned cytokines from the same animals. Data are shown as mean ± SEM with the following number of animals included in each experimental group: sham saline n = 3, sham void NPs n = 2, sham scramble-miR NPs n = 3, sham miR-124 NPs n = 2, PT saline n = 4, PT void NPs n = 4, PT scramble-miR NPs n = 3, PT miR-124 NPs n = 4. ***P < 0.001 versus all experimental groups subjected to sham surgery, **P < 0.01 versus all other experimental conditions after PT. Abbreviations: IFNγ interferon-gamma; IL, interleukin; NPs, nanoparticles; PT, photothrombosis; TNF-α, tumor necrosis factor-alpha.

4.3 Discussion

In this study, we investigated the effect of intravenous administration of miR-124 NPs as a possible therapeutic strategy to improve stroke outcome following permanent focal ischemia induced by photothrombosis. Experiments have been carried out based on *in vitro* studies showing an increased survival and differentiation of NSC following OGD. In contrast to *in vitro* experiments, administration of miR-124 NPs did not affect functional outcome following PT. In particular, we did not observe beneficial effects on lesion size, pro-inflammatory molecules or the number of neuronal progenitor cells in the SVZ and ischemic territory, respectively. Throughout the discussion, we will elaborate on our findings in the context of biological functions of miR-124 on mechanisms relevant for recovery of function after stroke.

NSCs are a self-renewing cell population that is also multipotent (Gage 2000). Endogenous NSCs participate in neural regeneration after injuries, namely in cerebral ischemia (Macas et al. 2006). However, NSCs have a limited repair potential due to low survival and neuronal differentiation. Strategies improving NSCs ability to contribute to repair lesioned areas can be seen as a promising tool to treat brain pathologies. miR-124 is the most abundant miRNA in the adult brain (Lagos-Quintana et al. 2002) and it is a well described inductor of SVZ neurogenesis with no effects on neuroblast migration capability (Cheng et al. 2009; Akerblom et al. 2012). More recently miR-124 has been associated with brain pathologies such as stroke, brain tumors and neurodegenerative disorders (Sun et al. 2015b). Indeed, we have recently shown that miR-124 might be a good candidate as a novel therapeutic molecule, since delivery of this miRNA using NPs led to amelioration of Parkinson's disease symptoms in mice lesioned with 6-OHDA. Treatment resulted in promotion of neurogenesis and the presence of new neurons in the lesioned striatum (Chapter 3). Here we showed that SVZ cells, which were exposed to OGD, and then treated with miR-124 NPs not only were protected but also more prone to differentiate towards a neuronal phenotype. In contrast, we observed a significant decrease of cell viability of control cultures exposed to OGD. Also, these cells did not show an alteration in terms of proliferation. This goes along with previous studies demonstrating that NSCs cultures exposed to long OGD intervals (> 4 h) show increased cell death and a reduction of cell proliferation (Park et al. 2012; Choi et al. 2014; Wang et al. 2015b; Bak et al. 2016) while shorter periods promoted NSCs survival (Wang et al. 2015b). Obviously, differences in NSCs culture sources and experimental conditions can explain these differences and lethal stimuli cause cell death. Importantly, we observed neuroprotection in SVZ cultures stimulated with miR-124 NPs after OGD. Moreover, treatment stimulated differentiation of progenitor cells. These results prompted us to test the efficacy of miR-124 NPs *in vivo* in a permanent focal photothrombosis mouse model for ischemia.

Stroke is the leading cause of disability worldwide. Current treatments are limited, only a narrow number of patients are eligible for the treatment and not all of these patients benefit from it. To date, for the majority of patients there is no and there will be no foreseeable treatment available in the near future. Development of new treatments, therefore, is timely. Hence, understanding the complex mechanisms contributing to tissue demise and recovery of function remains the first obligatory step in this process. We previously have shown that local administration of miR-124 NPs into the lateral ventricles were not only efficiently internalized by SVZ cells, but they also modulated SVZ neurogenic potential both in physiological and pathological conditions. Since intracerebroventricular injection of drugs is not a viable option for the majority of stroke patients, miR-124 NPs were administered systemically. This strategy is of higher clinical relevance. One of the major problems with this delivery route is the penetration into brain parenchyma through the blood brain barrier (BBB) (Saraiva et al. 2016). Nevertheless, here we show the internalization of NPs into brain resident cells. These proof-of-principle experiments unequivocally demonstrate the delivery of miR-124 NPs into the post-ischemic brain.

To reiterate we showed that a single intravenous injection of miR-124 NPs was not only able to reach the brain parenchyma of mice subjected to PT, but also was delivered into brain resident cells, namely astrocytes and neurons. However, miR-124 NPs did not improve functional outcome after the

insult. We observed similar infarct volumes between the experimental groups, which allow us to exclude infarct volume as a possible confounding variable for outcome measures, and the total number of DCX$^+$/BrdU$^+$ cells was also not altered in the SVZ. In addition, almost none of the DCX$^+$/BrdU$^+$ cells were detected in the ischemic core and peri-infarct tissue. Previously, it has been shown that viral administration of miR-124 for 21 days prior to MCAO resulted in a decrease of infarct volumes, reduced microglial activation and enhanced motor behavior (Doeppner et al. 2013). Neuroprotective effects were observed 4 and 8 weeks following transient MCAO being those a result of REST degradation mediated by USP-14, a miR-124 target. This study also showed increased neurogenesis in the SVZ (higher levels of DCX$^+$/BrdU$^+$ and NeuN$^+$/BrdU$^+$) in miR-124-treated mice (Doeppner et al. 2013). Moreover, local injection of miR-124 in the striatum of mice subjected to transient MCAO, two days after stroke, resulted in the reduction of the lesion, with higher neuronal survival within the first week after stroke, and was also associated with a better functional outcome (Hamzei Taj et al. 2016b).

On the other hand, infusion of an inhibitor of miR-124 (antagomiR) into the lateral ventricle of rats prior to transient MCAO resulted in smaller infarct volumes with a significant reduction of terminal deoxynucleotidyl transferase-mediated dUTP nick end labeling (TUNEL)$^+$ cells due to the upregulation of Ku70, a miR-124 target (Zhu et al. 2014). Another study even reports that intraventricular administration of miR-124 in mice immediately after MCAO resulted in a non-significant increase of infarct volumes 24 h after stroke. This study also shows that the administration of a miR-124 inhibitor reduced the ischemic lesion through upregulation of iASPP, the inhibitory member of the apoptosis-stimulating proteins of p53 family (Liu et al. 2013). Summarizing these studies in view of our results it seems that the route of administration of miR-124 is critical to achieve biological effects of miR-124 in the post-ischemic brain. Also, it needs to be considered that at an early time point following an ischemic insult the infarct has not been subsided. Therefore, effects of miR-124 on lesion volumes at an early stage following stroke i.e. 24 h might be due to effects on multiple processes i.e. brain edema without consequences for the final ischemic lesion and function (van der Maten et al. 2017). Also, differences in results might be due to different experimental stroke models. With some reservations, it seems that miR-124 is rather efficient in transient stroke models than in permanent models. Also, further studies need to elucidate the exact role of miR-124 antagonism in the post-ischemic brain. Our results do not support our initial hypothesis that miR-124 NPs could improve functional outcome following PT, with no changes in behavioral tests observed in this study.

Several processes have been discerned to contribute to brain tissue loss and reorganization of the post-ischemic brain including an inflammatory response but also cell genesis (Zhang et al. 2016b). The SVZ is the major neurogenic niche of rodents from where newborn neurons can migrate through the rostral migratory stream (RMS) towards the olfactory bulb where they differentiate into mature interneurons (Ming and Song 2011). DCX, a microtubule binding protein, is expressed in migrating neuroblasts and in adulthood it is mostly expressed in the neurogenic regions. Expression of DCX seems to be specific of newly generated neurons and does not occur during neuronal regeneration or gliogenesis (Nacher et al. 2001; Brown et al. 2003; Couillard-Despres et al. 2005). Moreover, DCX levels translate, in an accurate way, neurogenic changes in the SVZ and subgranular zone caused by external

cues and/or pathology (Couillard-Despres et al. 2005). The expression of DCX occurs for approximately 30 days with a maximum expression in the second week, thereafter reducing while NeuN expression increases (Brown et al. 2003). As so, DCX is widely accepted has a marker of neurogenesis *per se*. Strategies using expression of DCX and BrdU (administrated after the stimuli) allow a precise evaluation of the neurogenic response. Indeed, numerous studies using this strategy present the idea of migrating endogenous SVZ derived neurons reaching lesioned brain areas (Diederich et al., 2012; Osman et al., 2011; Lindvall and Kokaia, 2015). Hence, results have to be interpreted with caution. The actual migration process towards lesioned brain areas has not been unequivocally shown yet (Sullivan et al. 2015). In addition, BrdU incorporation also occurs in dying cells (Taupin 2007; Lehner et al. 2011). Cell death after ischemia is obvious and dying BrdU$^+$ cells in the ischemic territory should not be mistaken as newly formed neurons. We also found an increased number of BrdU$^+$ cells in the ischemic territory. However, almost none of these cells expressed DCX. Likewise, no differences in the number of differentiating cells have been found in the SVZ. On the other hand, lack of efficiency might be due to dosage, timing and route of administration of miR-124 important for its bioavailability and need. In fact, as mentioned before we have observed that a intracerebroventricular injection of miR-124 NPs results in enhancement of olfactory bulb neuroblasts under physiological conditions in mice four weeks after injection (Chapter 3).

The inflammatory response is a consequence of stroke and it contains well-orchestrated cascades involving resident and peripheral immune cells together with the expression and release of inflammatory molecules (Anrather and Iadecola 2016). miR-124 reduction is needed in order to shift the resting state of microglia to a reactive state (Freilich et al. 2013). miR-124 seems to be essential for the activation and maintenance of the M2 inflammatory state of microglia in the central nervous system, through downregulation of the C/EBP-α-PU.1 pathway (Ponomarev et al. 2007; Ponomarev et al. 2011; Ponomarev et al. 2013; Veremeyko et al. 2013). Overexpression of miR-124 in a macrophage cell line reduced the levels of TNF-α induced by lipopolysaccharide (LPS) *via* repression of the USP2 and USP14 (Sun et al. 2016). It may also modulate toll-like receptor (TLR) signaling by targeting proteins such as signal transducer and activator of transcription 3 (STAT3), TNF-α converting enzyme (TACE), necrosis factor (NF)-κB p65 and TNF receptor-associated factor 6 (TRAF6), culminating in reduction of pro-inflammatory cytokines (Sun et al. 2013b; Qiu et al. 2015). In addition, miR-124 can mediate the cholinergic anti-inflammatory pathway by targeting STAT3 and TACE reducing the release of IL-6 and TNF-α (Sun et al. 2013b).

Similar to other types of injury, injury induced by photothrombosis initiated an inflammatory response including the accumulation of immune cells and the release of inflammatory molecules in the ischemic territory. This is confirmed in the present study. Importantly, the only pro-inflammatory cytokine modulated by miR-124 NPs after PT was IL-6. Elevated levels were exclusively found in miR-124 NPs animals following PT suggesting a specific miR-124 mediated effect. This is in contrast to what has been observed before and may rather support a pro-inflammatory role of miR-124 as reported in models of epilepsy (Brennan et al. 2016). On the other hand, administration of miR-124 to mice subjected to PT did not affect the levels of IL-1β, IFNγ and TNF-α. Therefore, it is likely that miR-124 NPs were inefficient in modulating the central inflammatory response. Also, no significant peripheral inflammatory response

was seen among sham- and PT-operated animals nor among the different treatments. This goes along with previous studies questioning a prolonged upregulation of pro-inflammatory cytokines in rodents following stroke (Chapman et al. 2009; Ruscher et al. 2013).

Since miR-124 has a short half-life and poor stability *in vivo*, we developed a NP formulation that efficiently complexes and delivers miRNA into cells and that can be tracked non-invasively by ^{19}F MRI (Gomes et al. 2013). This overcomes safety issues, such as immunogenicity and oncogenic potential of viral vectors (Guzman-Villanueva et al. 2012). Our NP formulation was developed with components that had already been approved by the Food and Drug Administration (FDA) as biocompatible in other applications. The NPs were also optimized for *in vitro* delivery of miRNA and *in vivo* application based on local delivery of miRNA or tracking of injected cells previously transfected with NPs (Chapter 3)(Gomes et al. 2013). In fact, we showed previously that miRNA NPs were efficiently internalized by neural/progenitor cells, neuroblasts and endothelial cells. Internalization analysis showed that 24 h after transfection both miRNA and NPs could be found throughout the cytoplasm with about 50% of the miRNA co-localizing with NPs (Chapter 3)(Gomes et al. 2013). Interesting, at this timepoint around 35% of the miRNA were associated with early endosome vesicles, while only 5% were located in late endosome and lysosome vesicles. miRNA was also efficiently localized with the Argonaute 2 protein, an essential component of the microRNA-mediated silencing complex (miRISC) (Gomes et al. 2013), indicating that our formulation allows miRNA release inside the cells and avoids endolysosomal degradation. In non-viral delivery systems, such as polymeric NPs, endocytosis is the most common mechanism of internalization, with escape of the lysosomal degradation being a major concern in the design of these formulations (Liang and W. Lam 2012). It is also generally accepted that miRNA released into the cytoplasm is needed in order to be assembled into the miRISC. The mechanism behind miRNA escape from the endolysosomal pathway of our formulation was not addressed in this work. Nevertheless, we believed that cationic features of NPs helped the release into the cytoplasm, since they have the capacity to form transient holes in the membrane due to the proton sponge effect, therefore, escaping the endolysosomal pathway (Liang and W. Lam 2012). Another possibility is the Ago-chaperone heat shock proteins (HSPs) transportation, namely HSP90 and Hsc70 (important for loading miRNA in the miRISC). These proteins can interact with lipid membranes generating ATP-dependent pathways for cations (Arispe and De Maio 2000; Iwasaki et al. 2010). Notwithstanding, miR-124 NPs already showed the ability to deliver functional miR-124 into cells both *in vitro* and *in vivo* (Chapter 3).

Herein, we did not observe changes in terms of neurogenesis in the SVZ in either sham- or PT-operated mice treated with miR-124 NPs. This may suggest that only a suboptimal dose of miR-124 reached the brain parenchyma. Hence, immunofluorescence analysis of NPs and the increase of IL-6 levels in the post-ischemic brain strongly corroborate penetration of NPs and delivery of miRNA into brain cells. Therefore, modifications that improve the blood circulation time, increase cargo protection (mainly against RNases), reduce opsonization, decrease peripheral accumulation and enhance delivery of miRNA into the brain parenchyma, such as addiction of polyethylene glycol, surfactant agents or even a targeting molecule, may increase bioavailability of the miR-124 (Saraiva et al. 2016).

4.4. Conclusions

In the present study, we showed that a single intravenous injection of miR-124 NPs immediately after PT does not affect neurological deficits 14 days following the insult. In addition, no effects have been observed on the number of neuronal progenitor cells in the subventricular zone and ischemic territory despite positive results from *in vitro* experiments. Further evaluation studies will be required to investigate bioavailability of miR-124 NPs in brain parenchyma, the immunogenic role of miR-124 NPs and its effect in different rodent stroke models.

Chapter 5

GENERAL CONCLUSIONS

The discovery of neural stem cells (NSCs) in the adult mammalian brain opened new avenues in understanding brain plasticity. Adult neurogenesis seems to be mainly restricted to areas of the brain that display a specific microenvironment, being the major neurogenic niche the subventricular zone (SVZ). Studies on the composition and function of these neurogenic regions increased our understanding about adult neurogenesis and its involvement in brain functions. Remarkably, neurogenesis is enhanced in response to brain lesions. The multipotent and self-renewing abilities of NSCs together with their ability to integrate pre-established circuits make them good candidates for possible interventions in neurodegenerative disorders. Rrecruitment of endogenous NSCs sources to the site of lesion may be a good strategy to improve brain repair. Many pro-neurogenic factors have been implicated in controlling NSCs activity, including miR-124, extensively described as a pro-neurogenic molecule. Moreover, recent developments in the field of nanomedicine highlighted nanoparticles (NPs) as one of the best options not only to enhance the delivery of drugs into the brain, but also to act as scaffolds to improve survival and adaptation of new cells into damaged areas.

In this work, polymeric NPs to deliver miR-124 were used due to their ability to protect and increase miR-124 stability, as well as for their capability to deliver intracellularly higher concentrations of miR-124. The use of NPs to induce neuronal differentiation of endogenous adult NSCs is relatively recent and our laboratory was the first to establish it (Maia et al. 2011; Santos et al. 2012a). However, previous formulations could not be tracked in a temporal and spatial frame in living animals and were not used in a context of brain pathology. In Chapter 3 we used polymeric NPs that can be tracked non-invasively *in vivo*, by magnetic resonance imaging (MRI), due to the presence of perfluoro-1,5-crown ether (PFCE). These NPs have also in its composition poly(lactic acid-*co*-glycolic acid) (PLGA) and a cationic peptide, protamine sulfate that allows an efficient complexation of miRNA (Gomes et al. 2013). It is also important to notice that all NPs components were already approved by the Food and Drug Administration (FDA) in other applications. This NP formulation was able to efficiently deliver miR-132 into endothelial cells that afterwards exerted pro-survival and pro-angiogenic effects in an ischemic limb mouse model (Gomes et al. 2013). Herein, we showed that miR-124 NPs promote a robust enrichment in the number of mature neurons in SVZ NSCs cultures *in vitro*, while it decreases the number of astrocytic cells. miRNA-loaded NPs were efficiently internalized by cells able to differentiate in response to miR-124 overexpression such as stem/progenitor and immature cells. miR-124 NPs shift the profile of SVZ NSCs cultures from an undifferentiated and/or glial fate into a neuronal commitment fate by targeting Jagged1 and Sox9 (Nyfeler et al. 2005; Cheng et al. 2009; Åkerblom and Jakobsson 2014). It also enhanced axonogenesis a crucial process for the maturation and integration of newborn neurons. Accordingly, previous evidence showed that miR-124 overexpression not only promotes a neuronal commitment of progenitor cells (Cheng et al. 2009; Akerblom et al. 2012), but also controls cell fate either into neuronal or astrocytic differentiation (Neo et al. 2014). In addition, miR-124 enhances axonogenesis by regulating cytoskeleton proteins levels (Yu et al. 2008; Gu et al. 2014). *In vivo*, a single intracerebroventricular administration of miR-124 resulted in increased levels of migrating neuroblasts reaching the olfactory bulb (OB; the endpoint of SVZ-derived neurons) of healthy and 6-hydroxydopamine-challenged mice (6-OHDA; Parkinson's disease (PD) mouse model), where they fully differentiated into mature neurons. miR-124-induced neurogenesis at the SVZ-OB axis was most probably due to the division of

stem/progenitor cells into neuronal progenitors (doublecortin/5-bromo-2'-deoxyuridine-double positive cells; DCX$^+$/BrdU$^+$), but also from neuronal commitment of NSCs that have not undergone mitosis, or from late dividing cells generated after the BrdU pulse (total DCX$^+$ cells). Based on our *in vitro* and *in vivo* data, we may also speculate that miR-124 NPs triggered a shift from astrocytic-like cells to neurons without causing depletion in the NSCs pool, allowing the maintenance of the neurogenic niche and consequently, the continuous generation of new neurons. Nevertheless, others have shown that in physiological conditions miR-124 overexpression by viral vectors promotes neurogenesis in SVZ that does not interfere with migration nor OB integration, while it leads to a decrease in the levels of dividing precursor cells (Cheng et al. 2009; Akerblom et al. 2012). Therefore, additional studies are needed to address NSCs dynamics upon miR-124 treatment. Recent studies also showed that miR-124 upregulation is associated with protection of dopaminergic neurons by regulating apoptosis and autophagy processes (Wang et al. 2015a; Gong et al. 2016). Notably, in 6-OHDA-challenged mice, miR-124 NPs administration substantially enhanced maturation of SVZ-derived neurons into the lesioned striatum leading to amelioration of motor deficits. Nevertheless, it is essential to further study the underlying mechanisms in detail and/or cells involved in miR-124-induced motor recovery. Accordingly, besides neuronal differentiation, miR-124 seems to regulate cell death and inflammatory responses, resulting in neuroprotection in PD (Kanagaraj et al. 2014; Wang et al. 2015a; Gong et al. 2016) or reduction of infarct volume in stroke (Doeppner et al. 2013; Sun et al. 2013a). Therefore, broader applications of our formulation to other brain pathologies, such as ischemic stroke, are also anticipated.

Considering the previous work, in Chapter 4, we hypothesized that miR-124 NPs could be also of great value for recovery of lost function after stroke. First, we observed that miR-124 NPs protect SVZ cultures from oxygen and glucose deprivation (OGD; *in vitro* model of stroke). Moreover, even after OGD miR-124 NPs could trigger neuronal differentiation of SVZ NSCs. Based on these experiments we hypothesized that the *in vivo* administration unveils therapeutic effects of miR-124 NPs in a photothrombotic (PT) mouse model of stroke in terms of functional recovery, looking for possible effects on neurogenesis and neuroinflammation. Nevertheless, in contrary to our hypothesis a single intravenous injection of miR-124 NPs after PT stroke was unable to improve functional outcome of mice. Although we have observed FITC-NPs in the brain parenchyma of PT mice 4 h after intravenous administration of the NPs, we did not observe any differences in behavioral tests performed 14 days after the PT lesion. Also in terms of neurogenesis no alterations in the amount of newborn neurons were found in the SVZ nor in the ischemic territory of both PT and sham mice. Since we showed in Chapter 3 that miR-124 NPs increase SVZ-OB axis neurogenesis, we may speculate that lack of efficiency of miR-124 NPs in modulating neurogenesis might be due to low bioavailability caused either by dosage, route of administration or timing of the administration. Some studies showed that miR-124 downregulation were needed to decrease the infarct volume in middle cerebral arterial occlusion (MCAO) rodents, while miR-124 upregulation had no impact in the outcome (Liu et al. 2013; Zhu et al. 2014). Nevertheless, contrary to our findings others reported that overexpression of miR-124 previous (protective effect) or after a MCAO insult results in lower infarct volumes and functional improvement (Doeppner et al. 2013; Sun et al. 2013a; Hamzei Taj et al. 2016b). It is also important to consider that only a small portion of patients with ischemic stroke are treated with tissue plasminogen activator within

the first hours after symptom onset, showing the need for novel therapeutic strategies for stroke. As so, the study presented in Chapter 4 was performed to evaluate the effect of miRNA-124 NPs on the functional outcome as well as in the post-stroke neurogenesis and inflammation. Therefore, the PT stroke model has been chosen to assure low interindividual variability in infarct volumes and functional outcomes and low mortality. However, this model is not the most suitable to study acute processes of cell death and survival, since the brain supplying branches of the MCA are permanently occluded. Consequently, this model presents smaller penumbras preventing in this way reperfusion mechanisms observed in transient focal stroke models.

Regulation of inflammation through shifting the microglia reactivity from a pro-inflammatory state to an anti-inflammatory one was also achieved by miR-124 overexpression in MCAO mice (Hamzei Taj et al. 2016a). Changes in cytokines expression levels in the ischemic territory between sham- and PT-operated mice confirm the presence of an inflammatory response caused by the PT procedure. Nevertheless, we also did not find relevant differences among the different treatments (saline, void NPs, scramble-miR NPs or miR-124 NPs) within the PT mice, except for the increase of the levels of interleukin (IL)-6 in PT miR-124 NPs-treated mice. This result corroborate that miR-124 NPs are reaching the brain parenchyma and being uptaken. IL-6 is a pro-inflammatory cytokine indicating that in the experimental conditions tested miR-124 NPs appears to have a pro-inflammatory action rather than an anti-inflammatory one. Hence, an isolated increase of a cytokine suggests functions of this molecule beyond its involvement in post-stroke inflammation. Previous studies have demonstrated that elevated levels of the pro-inflammatory cytokine TNF-α is involved in mechanisms of neuronal plasticity (Stellwagen and Malenka 2006). Even though most of the data points to an anti-inflammatory role of miR-124 in microglia and monocytes/macrophages (Ponomarev et al. 2011; Jakus et al. 2013; Sun et al. 2013b), miR-124 was also reported as an activator of M1 state of microglia in epilepsy (Brennan et al. 2016). Furthermore, research on miR-124 NPs bioavailability in the brain, role of miR-124 NPs in the immune response, miR-124 NPs response in other models of stroke, such as transient MCAO, is still needed for a better understanding of the functions of miR-124 after stroke. In Chapter 4 we observed that miR-124 NPs are able to improve survival and increase neuronal differentiation of SVZ cultures after OGD insult, but they were unable to improve functional deficits of PT mice, reduce infarct volume, increase neurogenesis or decrease inflammation.

The ability of active molecules to cross the blood-brain barrier (BBB) into the brain parenchyma is a vital aspect for brain repair therapies. In Chapter 3, miR-124 NPs were delivered into the lateral ventricles by an intracerebral injection. This procedure, although highly invasive, permits to unveil the miR-124 NPs effect on SVZ neurogenesis without the biodistribution or bioavailability issues, allowing us to demonstrate the relevance of miR-124 NPs in brain repair strategies. Systemic delivery of miR-124 NPs by intravenous injections was then considered as a deliver strategy in Chapter 4 in order to circumvent the need of an invasive stereotaxic surgery and due to its higher clinical relevance. Overcoming the BBB is a great concern in delivering drugs to the brain; however, PT stroke causes BBB breakdown that could facilitate the passage of miR-124 NPs into the brain (Hoff et al. 2005; Piao et al.

2009; Nahirney et al. 2015). Although we found NPs in the brain parenchyma of PT mice, neither PT nor sham mice treated with miR-124 NPs were able to increase SVZ neurogenesis, indicative for a low bioavailability of the miR-124. We might also speculate that in sham-operated animals, since the BBB remain intact, lower amount of miR-124 NPs reached the NSCs explaining in part the lack of enhancement of SVZ neurogenesis, contrary to the increase of SVZ neurogenesis seen previously in healthy animals when miR-124 NPs were injected into the ventricle lumen. Nevertheless, improvement of our NP formulation is needed to increase efficacy of our treatment in systemic applications. The physicochemical characteristics of NPs make them versatile vehicles that can be easily modified in terms of size, charge, shape and surface ligands to better direct them across the BBB. As so, coating of NPs with ligands or antibodies that are recognized by receptors/transporters or epitopes on brain endothelial cells (Saraiva et al. 2016) to facilitate its passage to the brain parenchyma may be of great use to improve brain passage of NPs. Coating of NPs with lactoferrin (Hu et al. 2011) or transferrin antibodies (Yemisci et al. 2015) are examples of formulations that show increased brain accumulation in pathological situations. Blood clearance by the reticuloendothelial system may also limit the amount of NPs that reaches the brain. The use of poly(ethylene glycol) (PEG) increases NPs blood circulation time and consequently their brain accumulation (Saraiva et al. 2016). We anticipate that our polymeric NPs could be coated with PEG and specific ligands, such as transferrin, allowing us to improve efficacy in brain delivery after intravenous administration and reducing peripheral accumulation. The combination of the NP system with specific molecular cues to increase the targeting to specific sub-populations of the SVZ niche could also be beneficial to improve the neurogenic response and decrease off-target effects. For example, coating of NPs with epidermal growth factor receptor (EGFR)-binding peptides or Notch-1 ligands could trigger an increased uptake by proliferative progenitor cells forcing cell cycle exit and promoting subsequent neuronal differentiation. Yet, pharmacokinetics and biodistribution studies, central and peripheral toxicity analysis, mechanisms of BBB transport investigation and functional recovery evaluation *in vivo* are essential before conducting clinical studies.

Altogether, we showed that miR-124 NPs are able to modulate NSCs both *in vitro* and *in vivo*. Moreover, we prove that when delivered intracerebrally miR-124 NPs can ameliorate functional damage in a PD mouse model caused by 6-OHDA. miR-124 NPs also demonstrated efficacy in improving SVZ cultures survival and neuronal differentiation after OGD, despite intravenous injection of miR-124 NPs seemed to be incapable to improve stroke outcome in a PT mouse model. Notwithstanding, all these data evidence the fact that miR-124 NPs may represent a novel therapeutic approach for brain repair strategies based on the enhancement of the endogenous NSCs repair mechanisms.

Chapter 6

REFERENCES

Abdelfattah AM, Park C, Choi MY (2014) Update on non-canonical microRNAs. Biomol Concepts 5:275–87. doi: 10.1515/bmc-2014-0012

Agasse F, Bernardino L, Kristiansen H, et al (2008a) Neuropeptide Y promotes neurogenesis in murine subventricular zone. Stem Cells 26:1636–45. doi: 10.1634/stemcells.2008-0056

Agasse F, Bernardino L, Silva B, et al (2008b) Response to histamine allows the functional identification of neuronal progenitors, neurons, astrocytes, and immature cells in subventricular zone cell cultures. Rejuvenation Res 11:187–200. doi: 10.1089/rej.2007.0600

Åkerblom M, Jakobsson J (2014) MicroRNAs as Neuronal Fate Determinants. Neuroscientist 20:235–42. doi: 10.1177/1073858413497265

Akerblom M, Sachdeva R, Barde I, et al (2012) MicroRNA-124 Is a Subventricular Zone Neuronal Fate Determinant. J Neurosci 32:8879–8889. doi: 10.1523/JNEUROSCI.0558-12.2012

Almutairi MMA, Gong C, Xu YG, et al (2016) Factors controlling permeability of the blood–brain barrier. Cell Mol Life Sci 73:57–77. doi: 10.1007/s00018-015-2050-8

Alonso M, Viollet C, Gabellec M-M, et al (2006) Olfactory Discrimination Learning Increases the Survival of Adult-Born Neurons in the Olfactory Bulb. J Neurosci 26:10508–10513. doi: 10.1523/JNEUROSCI.2633-06.2006

Altman J (1962) Are New Neurons Formed in the Brains of Adult Mammals? Science (80-) 135:1127–1128. doi: 10.1126/science.135.3509.1127

Altman J (1969) Autoradiographic and histological studies of postnatal neurogenesis. IV. Cell proliferation and migration in the anterior forebrain, with special reference to persisting neurogenesis in the olfactory bulb. J Comp Neurol 137:433–57. doi: 10.1002/cne.901370404

Altman J (1963) Autoradiographic investigation of cell proliferation in the brains of rats and cats. Anat Rec 145:573–591. doi: 10.1002/ar.1091450409

Altman J, Das GD (1965) Autoradiographic and histological evidence of postnatal hippocampal neurogenesis in rats. J Comp Neurol 124:319–335. doi: 10.1002/cne.901240303

Altuvia Y, Landgraf P, Lithwick G, et al (2005) Clustering and conservation patterns of human microRNAs. Nucleic Acids Res 33:2697–706. doi: 10.1093/nar/gki567

Amura CR, Marek L, Winn RA, Heasley LE (2005) Inhibited neurogenesis in JNK1-deficient embryonic stem cells. Mol Cell Biol 25:10791–802. doi: 10.1128/MCB.25.24.10791-10802.2005

Anrather J, Iadecola C (2016) Inflammation and Stroke: An Overview. Neurotherapeutics 13:661–670. doi: 10.1007/s13311-016-0483-x

Aponso PM, Faull RLM, Connor B (2008) Increased progenitor cell proliferation and astrogenesis in the partial progressive 6-hydroxydopamine model of Parkinson's disease. Neuroscience 151:1142–53. doi: 10.1016/j.neuroscience.2007.11.036

Arias-Carrión O, Hernández-López S, Ibañez-Sandoval O, et al (2006) Neuronal precursors within the adult rat subventricular zone differentiate into dopaminergic neurons after substantia nigra lesion and chromaffin cell transplant. J Neurosci Res 84:1425–37. doi: 10.1002/jnr.21068

Arispe N, De Maio A (2000) ATP and ADP modulate a cation channel formed by Hsc70 in acidic phospholipid membranes. J Biol Chem 275:30839–43. doi: 10.1074/jbc.M005226200

Arvidsson A, Collin T, Kirik D, et al (2002) Neuronal replacement from endogenous precursors in the adult brain after stroke. Nat Med 8:963–970. doi: 10.1038/nm747

Bak SW, Choi H, Park H-H, et al (2016) Neuroprotective Effects of Acetyl-L-Carnitine Against Oxygen-Glucose Deprivation-Induced Neural Stem Cell Death. Mol Neurobiol 53:6644–6652. doi: 10.1007/s12035-015-9563-x

Baker S a, Baker KA, Hagg T (2004) Dopaminergic nigrostriatal projections regulate neural precursor proliferation in the adult mouse subventricular zone. Eur J Neurosci 20:575–9. doi: 10.1111/j.1460-9568.2004.03486.x

Baroukh NN, Van Obberghen E (2009) Function of microRNA-375 and microRNA-124a in pancreas and brain. FEBS J 276:6509–21. doi: 10.1111/j.1742-4658.2009.07353.x

Bartel DP (2004) MicroRNAs: genomics, biogenesis, mechanism, and function. Cell 116:281–297. doi: 10.1016/S0092-8674(04)00045-5

Bartel DP (2009) MicroRNAs: Target Recognition and Regulatory Functions. Cell 136:215–233. doi: 10.1016/j.cell.2009.01.002

Bédard A, Parent A (2004) Evidence of newly generated neurons in the human olfactory bulb. Dev Brain Res 151:159–168. doi: 10.1016/j.devbrainres.2004.03.021

Bennett L, Yang M, Enikolopov G, Iacovitti L (2009) Circumventricular organs: a novel site of neural stem cells in the adult brain. Mol Cell Neurosci 41:337–347. doi: 10.1016/j.mcn.2009.04.007

Berg DA, Yoon K-J, Will B, et al (2015) Tbr2-expressing intermediate progenitor cells in the adult mouse hippocampus are unipotent neuronal precursors with limited amplification capacity under homeostasis. Front Biol (Beijing) 10:262–271. doi: 10.1007/s11515-015-1364-0

REFERENCES

Bernardino L, Agasse F, Silva B, et al (2008) Tumor necrosis factor-alpha modulates survival, proliferation, and neuronal differentiation in neonatal subventricular zone cell cultures. Stem Cells 26:2361–71. doi: 10.1634/stemcells.2007-0914

Bernardino L, Eiriz MF, Santos T, et al (2012) Histamine stimulates neurogenesis in the rodent subventricular zone. Stem Cells 30:773–84. doi: 10.1002/stem.1042

Bernier PJ, Bedard A, Vinet J, et al (2002) Newly generated neurons in the amygdala and adjoining cortex of adult primates. Proc Natl Acad Sci U S A 99:11464–9. doi: 10.1073/pnas.172403999

Béthune J, Artus-Revel CG, Filipowicz W (2012) Kinetic analysis reveals successive steps leading to miRNA-mediated silencing in mammalian cells. EMBO Rep 13:716–23. doi: 10.1038/embor.2012.82

Bizzozero G (1894) Accrescimento e rigenerazione nell'organismo. In: Arch. Sci. Medi. Torino, Minerva Medica, pp 1101–1137

Bode AM, Dong Z (2007) The functional contrariety of JNK. Mol Carcinog 46:591–8. doi: 10.1002/mc.20348

Boekhoorn K, Joels M, Lucassen PJ (2006) Increased proliferation reflects glial and vascular-associated changes, but not neurogenesis in the presenile Alzheimer hippocampus. Neurobiol Dis 24:1–14. doi: 10.1016/j.nbd.2006.04.017

Bonaguidi MA, Song J, Ming GL, Song H (2012) A unifying hypothesis on mammalian neural stem cell properties in the adult hippocampus. Curr Opin Neurobiol 22:754–761. doi: 10.1016/j.conb.2012.03.013

Bonaguidi MA, Wheeler MA, Shapiro JS, et al (2011) In vivo clonal analysis reveals self-renewing and multipotent adult neural stem cell characteristics. Cell 145:1142–55. doi: 10.1016/j.cell.2011.05.024

Brennan GP, Dey D, Chen Y, et al (2016) Dual and Opposing Roles of MicroRNA-124 in Epilepsy Are Mediated through Inflammatory and NRSF-Dependent Gene Networks. Cell Rep 14:2402–12. doi: 10.1016/j.celrep.2016.02.042

Brill MS, Ninkovic J, Winpenny E, et al (2009) Adult generation of glutamatergic olfactory bulb interneurons. Nat Neurosci 12:1524–33. doi: 10.1038/nn.2416

Brown JP, Couillard-Després S, Cooper-Kuhn CM, et al (2003) Transient expression of doublecortin during adult neurogenesis. J Comp Neurol 467:1–10. doi: 10.1002/cne.10874

Cai X, Hagedorn CH, Cullen BR (2004) Human microRNAs are processed from capped, polyadenylated transcripts that can also function as mRNAs. RNA 10:1957–66. doi: 10.1261/rna.7135204

Chapman KZ, Dale VQ, Dénes Á, et al (2009) A Rapid and Transient Peripheral Inflammatory Response Precedes Brain Inflammation after Experimental Stroke. J Cereb Blood Flow Metab 29:1764–1768. doi: 10.1038/jcbfm.2009.113

Chen Y, Zhao H, Tan Z, et al (2015) Bottleneck limitations for microRNA-based therapeutics from bench to the bedside. Pharmazie 70:147–54. doi: 91/ph.2015.4774

Chendrimada TP, Gregory RI, Kumaraswamy E, et al (2005) TRBP recruits the Dicer complex to Ago2 for microRNA processing and gene silencing. Nature 436:740–744. doi: 10.1038/nature03868

Cheng L-C, Pastrana E, Tavazoie M, Doetsch F (2009) miR-124 regulates adult neurogenesis in the subventricular zone stem cell niche. Nat Neurosci 12:399–408. doi: 10.1038/nn.2294

Choi N-Y, Choi H, Park H-H, et al (2014) Neuroprotective effects of amlodipine besylate and benidipine hydrochloride on oxidative stress-injured neural stem cells. Brain Res 1551:1–12. doi: 10.1016/j.brainres.2014.01.016

Christie KJ, Turnley AM (2012) Regulation of endogenous neural stem/progenitor cells for neural repair-factors that promote neurogenesis and gliogenesis in the normal and damaged brain. Front Cell Neurosci 6:70. doi: 10.3389/fncel.2012.00070

Codega P, Silva-Vargas V, Paul A, et al (2014) Prospective identification and purification of quiescent adult neural stem cells from their in vivo niche. Neuron 82:545–59. doi: 10.1016/j.neuron.2014.02.039

Conaco C, Otto S, Han J-J, Mandel G (2006) Reciprocal actions of REST and a microRNA promote neuronal identity. Proc Natl Acad Sci U S A 103:2422–7. doi: 10.1073/pnas.0511041103

Coronas V, Bantubungi K, Fombonne J, et al (2004) Dopamine D3 receptor stimulation promotes the proliferation of cells derived from the post-natal subventricular zone. J Neurochem 91:1292–301. doi: 10.1111/j.1471-4159.2004.02823.x

Coronas V, Srivastava LK, Liang J-J, et al (1997) Identification and localization of dopamine receptor subtypes in rat olfactory mucosa and bulb: a combined in situ hybridization and ligand binding radioautographic approach. J Chem Neuroanat 12:243–257. doi: 10.1016/S0891-0618(97)00215-9

Couillard-Despres S, Winner B, Schaubeck S, et al (2005) Doublecortin expression levels in adult brain reflect neurogenesis. Eur J Neurosci 21:1–14. doi: 10.1111/j.1460-9568.2004.03813.x

Crews L, Mizuno H, Desplats P, et al (2008) Alpha-synuclein alters Notch-1 expression and neurogenesis in mouse embryonic stem cells and in the hippocampus of transgenic mice. J Neurosci 28:4250–60. doi: 10.1523/JNEUROSCI.0066-08.2008

Curtis MA, Kam M, Nannmark U, et al (2007) Human neuroblasts migrate to the olfactory bulb via a lateral ventricular extension. Science (80-) 315:1243–1249. doi: 10.1126/science.1136281

Curtis MA, Low VF, Faull RLM (2012) Neurogenesis and progenitor cells in the adult human brain: A comparison between hippocampal and subventricular progenitor proliferation. Dev Neurobiol 72:990–1005. doi: 10.1002/dneu.22028

Curtis MA, Penney EB, Pearson AG, et al (2003) Increased cell proliferation and neurogenesis in the adult human Huntington's disease brain. Proc Natl Acad Sci U S A 100:9023–9027. doi: 10.1073/pnas.1532244100

Damier P (1999) The substantia nigra of the human brain: II. Patterns of loss of dopamine-containing neurons in Parkinson's disease. Brain 122:1437–1448. doi: 10.1093/brain/122.8.1437

Dauer W, Przedborski S (2003) Parkinson's Disease. Neuron 39:889–909. doi: 10.1016/S0896-6273(03)00568-3

Daugaard I, Hansen TB (2017) Biogenesis and Function of Ago-Associated RNAs. Trends Genet. doi: 10.1016/j.tig.2017.01.003

De Marchis S, Temoney S, Erdelyi F, et al (2004) GABAergic phenotypic differentiation of a subpopulation of subventricular derived migrating progenitors. Eur J Neurosci 20:1307–1317. doi: 10.1111/j.1460-9568.2004.03584.x

Decimo I, Bifari F, Rodriguez FJ, et al (2011) Nestin- and doublecortin-positive cells reside in adult spinal cord meninges and participate in injury-induced parenchymal reaction. Stem Cells 29:2062–76. doi: 10.1002/stem.766

del Zoppo GJ, Milner R, Mabuchi T, et al (2007) Microglial activation and matrix protease generation during focal cerebral ischemia. Stroke 38:646–651. doi: 10.1161/01.STR.0000254477.34231.cb

Dempsey RJ, Sailor KA, Bowen KK, et al (2003) Stroke-induced progenitor cell proliferation in adult spontaneously hypertensive rat brain: effect of exogenous IGF-1 and GDNF. J Neurochem 87:586–597. doi: 10.1046/j.1471-4159.2003.02022.x

Deng W, Aimone JB, Gage FH (2010) New neurons and new memories: how does adult hippocampal neurogenesis affect learning and memory? Nat Rev Neurosci 11:339–350. doi: 10.1038/nrn2822

Desplats P, Spencer B, Crews L, et al (2012) α-Synuclein induces alterations in adult neurogenesis in Parkinson disease models via p53-mediated repression of Notch1. J Biol Chem 287:31691–702. doi: 10.1074/jbc.M112.354522

Diederich K, Frauenknecht K, Minnerup J, et al (2012) Citicoline Enhances Neuroregenerative Processes After Experimental Stroke in Rats. Stroke 43:1931–1940. doi: 10.1161/STROKEAHA.112.654806

Djuranovic S, Nahvi A, Green R (2012) miRNA-Mediated Gene Silencing by Translational Repression Followed by mRNA Deadenylation and Decay. Science (80-) 336:237–240. doi: 10.1126/science.1215691

Doeppner TR, Doehring M, Bretschneider E, et al (2013) MicroRNA-124 protects against focal cerebral ischemia via mechanisms involving Usp14-dependent REST degradation. Acta Neuropathol 126:251–65. doi: 10.1007/s00401-013-1142-5

Doetsch F, Alvarez-Buylla A (1996) Network of tangential pathways for neuronal migration in adult mammalian brain. Proc Natl Acad Sci 93:14895–14900. doi: 10.1073/pnas.93.25.14895

Doetsch F, Caillé I, Lim DA, et al (1999) Subventricular Zone Astrocytes Are Neural Stem Cells in the Adult Mammalian Brain. Cell 97:703–716. doi: 10.1016/S0092-8674(00)80783-7

Doetsch F, García-Verdugo JM, Alvarez-Buylla A (1997) Cellular composition and three-dimensional organization of the subventricular germinal zone in the adult mammalian brain. J Neurosci 17:5046–61.

Doetsch F, Petreanu L, Caille I, et al (2002) EGF Converts Transit-Amplifying Neurogenic Precursors in the Adult Brain into Multipotent Stem Cells. Neuron 36:1021–1034. doi: 10.1016/S0896-6273(02)01133-9

Eichhorn SW, Guo H, McGeary SE, et al (2014) mRNA Destabilization Is the Dominant Effect of Mammalian MicroRNAs by the Time Substantial Repression Ensues. Mol Cell 56:104–115. doi: 10.1016/j.molcel.2014.08.028

Eiriz MF, Valero J, Malva JO, Bernardino L (2014) New insights into the role of histamine in subventricular zone-olfactory bulb neurogenesis. Front Neurosci 8:1–7. doi: 10.3389/fnins.2014.00142

Eriksson PS, Perfilieva E, Björk-Eriksson T, et al (1998) Neurogenesis in the adult human hippocampus. Nat Med 4:1313–1317. doi: 10.1038/3305

Ernst A, Alkass K, Bernard S, et al (2014) Neurogenesis in the striatum of the adult human brain. Cell 156:1072–83. doi: 10.1016/j.cell.2014.01.044

Faigle R, Song H (2013) Signaling mechanisms regulating adult neural stem cells and neurogenesis. Biochim Biophys Acta 1830:2435–48. doi: 10.1016/j.bbagen.2012.09.002

Fang M, Wang J, Zhang X, et al (2012) The miR-124 regulates the expression of BACE1/β-secretase correlated with cell death in Alzheimer's disease. Toxicol Lett 209:94–105. doi: 10.1016/j.toxlet.2011.11.032

Filippov V, Kronenberg G, Pivneva T, et al (2003) Subpopulation of nestin-expressing progenitor cells in the adult murine hippocampus shows electrophysiological and morphological characteristics of astrocytes. Mol Cell

REFERENCES

Neurosci 23:373–382. doi: 10.1016/S1044-7431(03)00060-5

Franke K, Otto W, Johannes S, et al (2012) miR-124-regulated RhoG reduces neuronal process complexity via ELMO/Dock180/Rac1 and Cdc42 signalling. EMBO J 31:2908–2921. doi: 10.1038/emboj.2012.130

Freilich RW, Woodbury ME, Ikezu T (2013) Integrated expression profiles of mRNA and miRNA in polarized primary murine microglia. PLoS One 8:e79416. doi: 10.1371/journal.pone.0079416

Fricke IB, Viel T, Worlitzer MM, et al (2016) 6-hydroxydopamine-induced Parkinson's disease-like degeneration generates acute microgliosis and astrogliosis in the nigrostriatal system but no bioluminescence imaging-detectable alteration in adult neurogenesis. Eur J Neurosci 43:1352–65. doi: 10.1111/ejn.13232

Friedman RC, Farh KK-H, Burge CB, Bartel DP (2009) Most mammalian mRNAs are conserved targets of microRNAs. Genome Res 19:92–105. doi: 10.1101/gr.082701.108

Fröhlich E (2012) The role of surface charge in cellular uptake and cytotoxicity of medical nanoparticles. Int J Nanomedicine 7:5577–91. doi: 10.2147/IJN.S36111

Gage FH (2000) Mammalian neural stem cells. Science 287:1433–8. doi: 10.1126/science.287.5457.1433

Gao X, Qian J, Zheng S, et al (2014) Overcoming the blood-brain barrier for delivering drugs into the brain by using adenosine receptor nanoagonist. ACS Nano 8:3678–3689. doi: 10.1021/nn5003375

Garcia AD, Doan NB, Imura T, et al (2004) GFAP-expressing progenitors are the principal source of constitutive neurogenesis in adult mouse forebrain. Nat Neurosci 7:1233–1241. doi: 10.1038/nn1340

Gil-Perotín S, Duran-Moreno M, Cebrián-Silla A, et al (2013) Adult Neural Stem Cells From the Subventricular Zone: A Review of the Neurosphere Assay. Anat Rec 296:1435–1452. doi: 10.1002/ar.22746

Godnic I, Zorc M, Jevsinek Skok D, et al (2013) Genome-wide and species-wide in silico screening for intragenic MicroRNAs in human, mouse and chicken. PLoS One 8:e65165. doi: 10.1371/journal.pone.0065165

Goings GE, Sahni V, Szele FG (2004) Migration patterns of subventricular zone cells in adult mice change after cerebral cortex injury. Brain Res 996:213–226. doi: 10.1016/j.brainres.2003.10.034

Gomes RSM, Neves RP Das, Cochlin L, et al (2013) Efficient Pro-survival/angiogenic miRNA Delivery by an MRI-Detectable Nanomaterial. ACS Nano 7:3362–72. doi: 10.1021/nn400171w

Gong X, Wang H, Ye Y, et al (2016) miR-124 regulates cell apoptosis and autophagy in dopaminergic neurons and protects them by regulating AMPK/mTOR pathway in Parkinson's disease. Am J Transl Res 8:2127–37.

González-González E, López-Casas PP, del Mazo J (2008) The expression patterns of genes involved in the RNAi pathways are tissue-dependent and differ in the germ and somatic cells of mouse testis. Biochim Biophys Acta - Gene Regul Mech 1779:306–311. doi: 10.1016/j.bbagrm.2008.01.007

Gonzalez-Perez O, Chavez-Casillas O, Jauregui-Huerta F, et al (2011) Stress by noise produces differential effects on the proliferation rate of radial astrocytes and survival of neuroblasts in the adult subgranular zone. Neurosci Res 70:243–250. doi: 10.1016/j.neures.2011.03.013

Goodman CM, McCusker CD, Yilmaz T, Rotello VM (2004) Toxicity of Gold Nanoparticles Functionalized with Cationic and Anionic Side Chains. Bioconjug Chem 15:897–900. doi: 10.1021/bc049951i

Gromnicova R, Davies HA, Sreekanthreddy P, et al (2013) Glucose-coated gold nanoparticles transfer across human brain endothelium and enter astrocytes in vitro. PLoS One 8:e81043. doi: 10.1371/journal.pone.0081043

Gu X, Meng S, Liu S, et al (2014) MiR-124 Represses ROCK1 Expression to Promote Neurite Elongation Through Activation of the PI3K/Akt Signal Pathway. J Mol Neurosci 52:156–165. doi: 10.1007/s12031-013-0190-6

Guerrero-Cazares H, Gonzalez-Perez O, Soriano-Navarro M, et al (2011) Cytoarchitecture of the lateral ganglionic eminence and rostral extension of the lateral ventricle in the human fetal brain. J Comp Neurol 519:1165–1180. doi: 10.1002/cne.22566

Guerrero S, Araya E, Fiedler JL, et al (2010) Improving the brain delivery of gold nanoparticles by conjugation with an amphipathic peptide. Nanomedicine (Lond) 5:897–913. doi: 10.2217/nnm.10.74

Guzman-Villanueva D, El-Sherbiny IM, Herrera-Ruiz D, et al (2012) Formulation approaches to short interfering RNA and MicroRNA: Challenges and implications. J Pharm Sci 101:4046–4066. doi: 10.1002/jps.23300

Hamzei Taj S, Kho W, Aswendt M, et al (2016a) Dynamic Modulation of Microglia/Macrophage Polarization by miR-124 after Focal Cerebral Ischemia. J Neuroimmune Pharmacol 11:733–748. doi: 10.1007/s11481-016-9700-y

Hamzei Taj S, Kho W, Riou A, et al (2016b) MiRNA-124 induces neuroprotection and functional improvement after focal cerebral ischemia. Biomaterials 91:151–65. doi: 10.1016/j.biomaterials.2016.03.025

Hermanns M (2011) Weathering the storm: living with Parkinson's disease. J Christ Nurs 28:76-82–4. doi: 10.1097/CNJ.0b013e31820b8d9f

Hertel J, Lindemeyer M, Missal K, et al (2006) The expansion of the metazoan microRNA repertoire. BMC Genomics 7:25. doi: 10.1186/1471-2164-7-25

Hoff EI, oude Egbrink MGA, Heijnen VVT, et al (2005) In vivo visualization of vascular leakage in photochemically induced cortical infarction. J Neurosci Methods 141:135–141. doi: 10.1016/j.jneumeth.2004.06.004

Höglinger GU, Arias-Carrión O, Ipach B, Oertel WH (2014) Origin of the dopaminergic innervation of adult neurogenic areas. J Comp Neurol. doi: 10.1002/cne.23537

Höglinger GU, Rizk P, Muriel MP, et al (2004) Dopamine depletion impairs precursor cell proliferation in Parkinson disease. Nat Neurosci 7:726–35. doi: 10.1038/nn1265

Hou Q, Ruan H, Gilbert J, et al (2015) MicroRNA miR124 is required for the expression of homeostatic synaptic plasticity. Nat Commun 6:10045. doi: 10.1038/ncomms10045

Hu K, Shi Y, Jiang W, et al (2011) Lactoferrin conjugated PEG-PLGA nanoparticles for brain delivery: Preparation, characterization and efficacy in Parkinsons disease. Int J Pharm 415:273–283. doi: 10.1016/j.ijpharm.2011.05.062

Huntzinger E, Izaurralde E (2011) Gene silencing by microRNAs: contributions of translational repression and mRNA decay. Nat Rev Genet 12:99–110. doi: 10.1038/nrg2936

Iancu R, Mohapel P, Brundin P, Paul G (2005) Behavioral characterization of a unilateral 6-OHDA-lesion model of Parkinson's disease in mice. Behav Brain Res 162:1–10. doi: 10.1016/j.bbr.2005.02.023

Itokazu Y, Kitada M, Dezawa M, et al (2006) Choroid plexus ependymal cells host neural progenitor cells in the rat. Glia 53:32–42. doi: 10.1002/glia.20255

Iwakura Y, Piao Y-S, Mizuno M, et al (2005) Influences of dopaminergic lesion on epidermal growth factor-ErbB signals in Parkinson's disease and its model: neurotrophic implication in nigrostriatal neurons. J Neurochem 93:974–83. doi: 10.1111/j.1471-4159.2005.03073.x

Iwasaki S, Kobayashi M, Yoda M, et al (2010) Hsc70/Hsp90 Chaperone Machinery Mediates ATP-Dependent RISC Loading of Small RNA Duplexes. Mol Cell 39:292–299. doi: 10.1016/j.molcel.2010.05.015

Jagmag SA, Tripathi N, Shukla SD, et al (2015) Evaluation of Models of Parkinson's Disease. Front Neurosci 9:503. doi: 10.3389/fnins.2015.00503

Jakus PB, Kalman N, Antus C, et al (2013) TRAF6 is functional in inhibition of TLR4-mediated NF-κB activation by resveratrol. J Nutr Biochem 24:819–23. doi: 10.1016/j.jnutbio.2012.04.017

Jallouli Y, Paillard A, Chang J, et al (2007) Influence of surface charge and inner composition of porous nanoparticles to cross blood-brain barrier in vitro. Int J Pharm 344:103–109. doi: 10.1016/j.ijpharm.2007.06.023

Ji Q, Ji Y, Peng J, et al (2016) Increased Brain-Specific MiR-9 and MiR-124 in the Serum Exosomes of Acute Ischemic Stroke Patients. PLoS One 11:e0163645. doi: 10.1371/journal.pone.0163645

Jiang Q, Wang Y, Hao Y, et al (2009) miR2Disease: a manually curated database for microRNA deregulation in human disease. Nucleic Acids Res 37:D98–D104. doi: 10.1093/nar/gkn714

Jiang W, Gu W, Brannstrom T, et al (2001) Cortical Neurogenesis in Adult Rats After Transient Middle Cerebral Artery Occlusion. Stroke 32:1201–1207. doi: 10.1161/01.STR.32.5.1201

Jiang W, Kim BYS, Rutka JT, Chan WCW (2008) Nanoparticle-mediated cellular response is size-dependent. Nat Nanotechnol 3:145–50. doi: 10.1038/nnano.2008.30

Jin K, Sun Y, Xie L, et al (2003) Directed migration of neuronal precursors into the ischemic cerebral cortex and striatum. Mol Cell Neurosci 24:171–189. doi: 10.1016/S1044-7431(03)00159-3

Jin K, Wang X, Xie L, et al (2006) Evidence for stroke-induced neurogenesis in the human brain. Proc Natl Acad Sci U S A 103:13198–13202. doi: 10.1073/pnas.0603512103

Jing X, Miwa H, Sawada T, et al (2012) Ephrin-A1-mediated dopaminergic neurogenesis and angiogenesis in a rat model of Parkinson's disease. PLoS One 7:e32019. doi: 10.1371/journal.pone.0032019

Kadota T, Shingo T, Yasuhara T, et al (2009) Continuous intraventricular infusion of erythropoietin exerts neuroprotective/rescue effects upon Parkinson's disease model of rats with enhanced neurogenesis. Brain Res 1254:120–7. doi: 10.1016/j.brainres.2008.11.094

Kam M, Curtis MA, McGlashan SR, et al (2009) The cellular composition and morphological organization of the rostral migratory stream in the adult human brain. J Chem Neuroanat 37:196–205. doi: 10.1016/j.jchemneu.2008.12.009

Kanagaraj N, Beiping H, Dheen ST, Tay SSW (2014) Downregulation of miR-124 in MPTP-treated mouse model of Parkinson's disease and MPP iodide-treated MN9D cells modulates the expression of the calpain/cdk5 pathway proteins. Neuroscience 272:167–79. doi: 10.1016/j.neuroscience.2014.04.039

Kaplan M, Hinds J (1977) Neurogenesis in the adult rat: electron microscopic analysis of light radioautographs. Science (80-) 197:1092–1094. doi: 10.1126/science.887941

Karginov F V, Cheloufi S, Chong MMW, et al (2010) Diverse endonucleolytic cleavage sites in the mammalian transcriptome depend upon microRNAs, Drosha, and additional nucleases. Mol Cell 38:781–8. doi: 10.1016/j.molcel.2010.06.001

Kempermann G, Kuhn HG, Gage FH (1997) More hippocampal neurons in adult mice living in an enriched environment. Nature 386:493–5. doi: 10.1038/386493a0

Kilpatrick TJ, Bartlett PF (1993) Cloning and growth of multipotential neural precursors: Requirements for

REFERENCES

proliferation and differentiation. Neuron 10:255–265. doi: 10.1016/0896-6273(93)90316-J

Kim Y, Yeo J, Lee JH, et al (2014) Deletion of Human tarbp2 Reveals Cellular MicroRNA Targets and Cell-Cycle Function of TRBP. Cell Rep 9:1061–1074. doi: 10.1016/j.celrep.2014.09.039

Kippin TE, Kapur S, van der Kooy D (2005) Dopamine specifically inhibits forebrain neural stem cell proliferation, suggesting a novel effect of antipsychotic drugs. J Neurosci 25:5815–23. doi: 10.1523/JNEUROSCI.1120-05.2005

Klein C, Butt SJB, Machold RP, et al (2005) Cerebellum- and forebrain-derived stem cells possess intrinsic regional character. Development 132:4497–508. doi: 10.1242/dev.02037

Kobayashi T, Ahlenius H, Thored P, et al (2006) Intracerebral infusion of glial cell line-derived neurotrophic factor promotes striatal neurogenesis after stroke in adult rats. Stroke 37:2361–7. doi: 10.1161/01.STR.0000236025.44089.e1

Kotan D, Tatar A, Aygul R, Ulvi H (2013) Assessment of nasal parameters in determination of olfactory dysfunction in Parkinson's disease. J Int Med Res 41:334–9. doi: 10.1177/0300060513476433

Kreuzberg M, Kanov E, Timofeev O, et al (2010) Increased subventricular zone-derived cortical neurogenesis after ischemic lesion. Exp Neurol 226:90–9. doi: 10.1016/j.expneurol.2010.08.006

Krichevsky AM, King KS, Donahue CP, et al (2003) A microRNA array reveals extensive regulation of microRNAs during brain development. RNA 9:1274–81. doi: 10.1261/rna.5980303

Krichevsky AM, Sonntag K-C, Isacson O, Kosik KS (2006) Specific microRNAs modulate embryonic stem cell-derived neurogenesis. Stem Cells 24:857–64. doi: 10.1634/stemcells.2005-0441

Krupinski J, Kaluza J, Kumar P, et al (1994) Role of angiogenesis in patients with cerebral ischemic stroke. Stroke 25:1794–1798. doi: 10.1161/01.STR.25.9.1794

Krutfeldt J, Rajewsky N, Braich R, et al (2005) Silencing of microRNAs in vivo with "antagomirs." Nature 438:685–689. doi: 10.1038/nature04303

Kuhn HG, Dickinson-Anson H, Gage FH (1996) Neurogenesis in the dentate gyrus of the adult rat: age-related decrease of neuronal progenitor proliferation. J Neurosci 16:2027–33.

Kukekov VG, Laywell ED, Suslov O, et al (1999) Multipotent stem/progenitor cells with similar properties arise from two neurogenic regions of adult human brain. Exp Neurol 156:333–44. doi: 10.1006/exnr.1999.7028

Kumar A, Aakriti, Gupta V (2016) A review on animal models of stroke: An update. Brain Res Bull 122:35–44. doi: 10.1016/j.brainresbull.2016.02.016

Kuric E, Ruscher K (2014) Dynamics of major histocompatibility complex class II-positive cells in the postischemic brain--influence of levodopa treatment. J Neuroinflammation 11:145. doi: 10.1186/s12974-014-0145-z

Kwak PB, Tomari Y (2012) The N domain of Argonaute drives duplex unwinding during RISC assembly. Nat Struct Mol Biol 19:145–151. doi: 10.1038/nsmb.2232

Kyle S, Saha S (2014) Nanotechnology for the detection and therapy of stroke. Adv Heal Mater 3:1703–1720. doi: 10.1002/adhm.201400009

Lafenêtre P, Leske O, Ma-Högemeie Z, et al (2010) Exercise can rescue recognition memory impairment in a model with reduced adult hippocampal neurogenesis. Front Behav Neurosci 3:34. doi: 10.3389/neuro.08.034.2009

Lagace DC (2012) Does the endogenous neurogenic response alter behavioral recovery following stroke? Behav Brain Res 227:426–432. doi: 10.1016/j.bbr.2011.08.045

Lagos-Quintana M, Rauhut R, Yalcin A, et al (2002) Identification of Tissue-Specific MicroRNAs from Mouse. Curr Biol 12:735–739. doi: 10.1016/S0960-9822(02)00809-6

Lakhan SE, Kirchgessner A, Hofer M (2009) Inflammatory mechanisms in ischemic stroke: therapeutic approaches. J Transl Med 7:97. doi: 10.1186/1479-5876-7-97

Lao CL, Lu C-S, Chen J-C (2013) Dopamine D 3 receptor activation promotes neural stem/progenitor cell proliferation through AKT and ERK1/2 pathways and expands type-B and -C cells in adult subventricular zone. Glia 61:475–489. doi: 10.1002/glia.22449

Larsson O, Nadon R (2013) Re-analysis of genome wide data on mammalian microRNA-mediated suppression of gene expression. Transl (Austin, Tex) 1:e24557. doi: 10.4161/trla.24557

Laterza OF, Lim L, Garrett-Engele PW, et al (2009) Plasma MicroRNAs as sensitive and specific biomarkers of tissue injury. Clin Chem 55:1977–83. doi: 10.1373/clinchem.2009.131797

Lee SY, Ferrari M, Decuzzi P (2009) Shaping nano-/micro-particles for enhanced vascular interaction in laminar flows. Nanotechnology 20:495101. doi: 10.1088/0957-4484/20/49/495101

Lee Y, Ahn C, Han J, et al (2003) The nuclear RNase III Drosha initiates microRNA processing. Nature 425:415–419. doi: 10.1038/nature01957

Lee Y, Hur I, Park S-Y, et al (2006) The role of PACT in the RNA silencing pathway. EMBO J 25:522–32. doi: 10.1038/sj.emboj.7600942

Lee Y, Kim M, Han J, et al (2004) MicroRNA genes are transcribed by RNA polymerase II. EMBO J 23:4051–60. doi: 10.1038/sj.emboj.7600385

Lehner B, Sandner B, Marschallinger J, et al (2011) The dark side of BrdU in neural stem cell biology: detrimental effects on cell cycle, differentiation and survival. Cell Tissue Res 345:313–328. doi: 10.1007/s00441-011-1213-7

Leuner B, Mendolia-Loffredo S, Kozorovitskiy Y, et al (2004) Learning enhances the survival of new neurons beyond the time when the hippocampus is required for memory. J Neurosci 24:7477–81. doi: 10.1523/JNEUROSCI.0204-04.2004

Li SD, Huang L (2009) Nanoparticles evading the reticuloendothelial system: role of the supported bilayer. Biochim Biophys Acta 1788:2259–2266. doi: 10.1016/j.bbamem.2009.06.022

Li W, Luo R, Lin X, et al (2015) Remote modulation of neural activities via near-infrared triggered release of biomolecules. Biomaterials 65:76–85. doi: 10.1016/j.biomaterials.2015.06.041

Li Z, Rana TM (2014) Therapeutic targeting of microRNAs: current status and future challenges. Nat Rev Drug Discov 13:622–638. doi: 10.1038/nrd4359

Liang W, W. Lam JK (2012) Endosomal Escape Pathways for Non-Viral Nucleic Acid Delivery Systems. In: Molecular Regulation of Endocytosis. InTech. doi: 10.5772/46006

Lie DC, Dziewczapolski G, Willhoite AR, et al (2002) The adult substantia nigra contains progenitor cells with neurogenic potential. J Neurosci 22:6639–49. doi: 20026700

Lim LP, Lau NC, Garrett-Engele P, et al (2005) Microarray analysis shows that some microRNAs downregulate large numbers of target mRNAs. Nature 433:769–773. doi: 10.1038/nature03315

Lin R (2015) Classic and novel stem cell niches in brain homeostasis and repair. Brain Res 1628:327–342. doi: 10.1016/j.brainres.2015.04.029

Lin R, Cai J, Nathan C, et al (2015) Neurogenesis is enhanced by stroke in multiple new stem cell niches along the ventricular system at sites of high BBB permeability. Neurobiol Dis 74:229–239. doi: 10.1016/j.nbd.2014.11.016

Lindow M, Kauppinen S (2012) Discovering the first microRNA-targeted drug. J Cell Biol 199:407–412. doi: 10.1083/jcb.201208082

Lindqvist D, Kaufman E, Brundin L, et al (2012) Non-motor symptoms in patients with Parkinson's disease - correlations with inflammatory cytokines in serum. PLoS One 7:e47387. doi: 10.1371/journal.pone.0047387

Lindvall O, Kokaia Z (2015) Neurogenesis following Stroke Affecting the Adult Brain. Cold Spring Harb Perspect Biol 7:a019034. doi: 10.1101/cshperspect.a019034

Lindvall O, Kokaia Z (2010) Stem cells in human neurodegenerative disorders--time for clinical translation? J Clin Invest 120:29–40. doi: 10.1172/JCI40543

Liu BF, Gao EJ, Zeng XZ, et al (2006) Proliferation of neural precursors in the subventricular zone after chemical lesions of the nigrostriatal pathway in rat brain. Brain Res 1106:30–9. doi: 10.1016/j.brainres.2006.05.111

Liu H, Jablonska A, Li Y, et al (2016) Label-free CEST MRI Detection of Citicoline-Liposome Drug Delivery in Ischemic Stroke. Theranostics 6:1588–1600. doi: 10.7150/thno.15492

Liu X, Li F, Zhao S, et al (2013) MicroRNA-124-Mediated Regulation of Inhibitory Member of Apoptosis-Stimulating Protein of p53 Family in Experimental Stroke. Stroke 44:1973–1980. doi: 10.1161/STROKEAHA.111.000613

Liu XS, Chopp M, Zhang RL, et al (2011) MicroRNA Profiling in Subventricular Zone after Stroke : MiR-124a Regulates Proliferation of Neural Progenitor Cells through Notch Signaling Pathway. PLoS One 6:1–11. doi: 10.1371/journal.pone.0023461

Liu Y, Zhang J, Han R, et al (2015) Downregulation of serum brain specific microRNA is associated with inflammation and infarct volume in acute ischemic stroke. J Clin Neurosci 22:291–5. doi: 10.1016/j.jocn.2014.05.042

Lledo P-M, Alonso M, Grubb MS (2006) Adult neurogenesis and functional plasticity in neuronal circuits. Nat Rev Neurosci 7:179–193. doi: 10.1038/nrn1867

Lockman PR, Koziara JM, Mumper RJ, Allen DD (2004) Nanoparticle surface charges alter blood-brain barrier integrity and permeability. J Drug Target 12:635–41. doi: 10.1080/10611860400015936

Lois C, Alvarez-Buylla A (1994) Long-distance neuronal migration in the adult mammalian brain. Science (80-) 264:1145–1148. doi: 10.1126/science.8178174

Lois C, Alvarez-Buylla A (1993) Proliferating subventricular zone cells in the adult mammalian forebrain can differentiate into neurons and glia. Proc Natl Acad Sci 90:2074–2077. doi: 10.1073/pnas.90.5.2074

Lois C, Garc a-Verdugo J-M, Alvarez-Buylla A (1996) Chain Migration of Neuronal Precursors. Science (80-) 271:978–981. doi: 10.1126/science.271.5251.978

Lorenz MR, Holzapfel V, Musyanovych A, et al (2006) Uptake of functionalized, fluorescent-labeled polymeric particles in different cell lines and stem cells. Biomaterials 27:2820–8. doi: 10.1016/j.biomaterials.2005.12.022

Low VF, Dragunow M, Tippett LJ, et al (2011) No change in progenitor cell proliferation in the hippocampus in Huntington's disease. Neuroscience 199:577–588. doi: 10.1016/j.neuroscience.2011.09.010

REFERENCES

Lucassen PJ, Stumpel MW, Wang Q, Aronica E (2010) Decreased numbers of progenitor cells but no response to antidepressant drugs in the hippocampus of elderly depressed patients. Neuropharmacology 58:940–9. doi: 10.1016/j.neuropharm.2010.01.012

Lund E (2004) Nuclear Export of MicroRNA Precursors. Science (80-) 303:95–98. doi: 10.1126/science.1090599

Ma DK, Bonaguidi MA, Ming G-L, Song H (2009) Adult neural stem cells in the mammalian central nervous system. Cell Res 19:672–82. doi: 10.1038/cr.2009.56

Ma DK, Marchetto MC, Guo JU, et al (2010) Epigenetic choreographers of neurogenesis in the adult mammalian brain. Nat Neurosci 13:1338–44. doi: 10.1038/nn.2672

Macas J, Nern C, Plate KH, Momma S (2006) Increased generation of neuronal progenitors after ischemic injury in the aged adult human forebrain. J Neurosci 26:13114–9. doi: 10.1523/JNEUROSCI.4667-06.2006

MacRae IJ, Zhou K, Doudna JA (2007) Structural determinants of RNA recognition and cleavage by Dicer. Nat Struct Mol Biol 14:934–940. doi: 10.1038/nsmb1293

Maia J, Santos T, Aday S, et al (2011) Controlling the neuronal differentiation of stem cells by the intracellular delivery of retinoic acid-loaded nanoparticles. ACS Nano 5:97–106. doi: 10.1021/nn101724r

Makeyev E V, Zhang J, Carrasco MA, Maniatis T (2007) The MicroRNA miR-124 promotes neuronal differentiation by triggering brain-specific alternative pre-mRNA splicing. Mol Cell 27:435–48. doi: 10.1016/j.molcel.2007.07.015

Marlier Q, Verteneuil S, Vandenbosch R, Malgrange B (2015) Mechanisms and Functional Significance of Stroke-Induced Neurogenesis. Front Neurosci. doi: 10.3389/fnins.2015.00458

Marti-Fabregas J, Romaguera-Ros M, Gomez-Pinedo U, et al (2010) Proliferation in the human ipsilateral subventricular zone after ischemic stroke. Neurology 74:357–365. doi: 10.1212/WNL.0b013e3181cbccec

Martinez-Veracoechea FJ, Frenkel D (2011) Designing super selectivity in multivalent nano-particle binding. Proc Natl Acad Sci U S A 108:10963–8. doi: 10.1073/pnas.1105351108

Meijer HA, Kong YW, Lu WT, et al (2013) Translational repression and eIF4A2 activity are critical for microRNA-mediated gene regulation. Science 340:82–5. doi: 10.1126/science.1231197

Meijer HA, Smith EM, Bushell M (2014) Regulation of miRNA strand selection: follow the leader? Biochem Soc Trans 42:1135–1140. doi: 10.1042/BST20140142

Menn B, Garcia-Verdugo JM, Yaschine C, et al (2006) Origin of Oligodendrocytes in the Subventricular Zone of the Adult Brain. J Neurosci 26:7907–7918. doi: 10.1523/JNEUROSCI.1299-06.2006

Millan MJ, Maiofiss L, Cussac D, et al (2002) Differential actions of antiparkinson agents at multiple classes of monoaminergic receptor. I. A multivariate analysis of the binding profiles of 14 drugs at 21 native and cloned human receptor subtypes. J Pharmacol Exp Ther 303:791–804. doi: 10.1124/jpet.102.039867

Ming G-L, Song H (2011) Adult Neurogenesis in the Mammalian Brain: Significant Answers and Significant Questions. Neuron 70:687–702. doi: 10.1016/j.neuron.2011.05.001

Ming G, Song H (2005) Adult Neurogenesis in the Mammalian Central Nervous System. Annu Rev Neurosci 28:223–250. doi: 10.1146/annurev.neuro.28.051804.101459

Minger SL, Ekonomou A, Carta EM, et al (2007) Endogenous neurogenesis in the human brain following cerebral infarction. Regen Med 2:69–74. doi: 10.2217/17460751.2.1.69

Mishima T, Mizuguchi Y, Kawahigashi Y, et al (2007) RT-PCR-based analysis of microRNA (miR-1 and -124) expression in mouse CNS. Brain Res 1131:37–43. doi: 10.1016/j.brainres.2006.11.035

Monteys AM, Spengler RM, Wan J, et al (2010) Structure and activity of putative intronic miRNA promoters. RNA 16:495–505. doi: 10.1261/rna.1731910

Morshead CM, Reynolds BA, Craig CG, et al (1994) Neural stem cells in the adult mammalian forebrain: A relatively quiescent subpopulation of subependymal cells. Neuron 13:1071–1082. doi: 10.1016/0896-6273(94)90046-9

Mozaffarian D, Benjamin EJ, Go AS, et al (2015) Heart disease and stroke statistics--2015 update: a report from the American Heart Association. Circulation 131:e29-322. doi: 10.1161/cir.0000000000000152

Mu Y, Zhao C, Gage FH (2011) Dopaminergic modulation of cortical inputs during maturation of adult-born dentate granule cells. J Neurosci 31:4113–23. doi: 10.1523/JNEUROSCI.4913-10.2011

Nacher J, Crespo C, McEwen BS (2001) Doublecortin expression in the adult rat telencephalon. Eur J Neurosci 14:629–644. doi: 10.1046/j.0953-816x.2001.01683.x

Nahirney PC, Reeson P, Brown CE (2015) Ultrastructural analysis of blood–brain barrier breakdown in the peri-infarct zone in young adult and aged mice. J Cereb Blood Flow Metab 0271678X15608396. doi: 10.1177/0271678X15608396

Nakayama D, Matsuyama T, Ishibashi-Ueda H, et al (2010) Injury-induced neural stem/progenitor cells in post-stroke human cerebral cortex. Eur J Neurosci 31:90–98. doi: 10.1111/j.1460-9568.2009.07043.x

Nance EA, Woodworth GF, Sailor KA, et al (2012) A dense poly(ethylene glycol) coating improves penetration of large polymeric nanoparticles within brain tissue. Sci Transl Med 4:149ra119. doi:

10.1126/scitranslmed.3003594

Neo WH, Yap K, Lee SH, et al (2014) MicroRNA miR-124 controls the choice between neuronal and astrocyte differentiation by fine-tuning Ezh2 expression. J Biol Chem 289:20788–20801. doi: 10.1074/jbc.M113.525493

Niewoehner J, Bohrmann B, Collin L, et al (2014) Increased brain penetration and potency of a therapeutic antibody using a monovalent molecular shuttle. Neuron 81:49–60. doi: 10.1016/j.neuron.2013.10.061

Ninkovic J, Götz M (2007) Signaling in adult neurogenesis: from stem cell niche to neuronal networks. Curr Opin Neurobiol 17:338–344. doi: 10.1016/j.conb.2007.04.006

Noland CL, Doudna JA (2013) Multiple sensors ensure guide strand selection in human RNAi pathways. RNA 19:639–48. doi: 10.1261/rna.037424.112

Nottebohm F (2002) Why are some neurons replaced in adult brain? J Neurosci 22:624–8.

Nyfeler Y, Kirch RD, Mantei N, et al (2005) Jagged1 signals in the postnatal subventricular zone are required for neural stem cell self-renewal. EMBO J 24:3504–15. doi: 10.1038/sj.emboj.7600816

O'Keeffe GC, Tyers P, Aarsland D, et al (2009) Dopamine-induced proliferation of adult neural precursor cells in the mammalian subventricular zone is mediated through EGF. Proc Natl Acad Sci U S A 106:8754–9. doi: 10.1073/pnas.0803955106

O'Sullivan SS, Johnson M, Williams DR, et al (2011) The effect of drug treatment on neurogenesis in Parkinson's disease. Mov Disord 26:45–50. doi: 10.1002/mds.23340

Oliva A a, Atkins CM, Copenagle L, Banker G a (2006) Activated c-Jun N-terminal kinase is required for axon formation. J Neurosci 26:9462–9470. doi: 10.1523/JNEUROSCI.2625-06.2006

Oliveira LMA, Falomir-Lockhart LJ, Botelho MG, et al (2015) Elevated α-synuclein caused by SNCA gene triplication impairs neuronal differentiation and maturation in Parkinson's patient-derived induced pluripotent stem cells. Cell Death Dis 6:e1994. doi: 10.1038/cddis.2015.318

Ortega F, Berninger B, Costa MR (2013) Primary culture and live imaging of adult neural stem cells and their progeny. Methods Mol Biol 1052:1–11. doi: 10.1007/7651_2013_22

Osman AM, Porritt MJ, Nilsson M, Kuhn HG (2011) Long-term stimulation of neural progenitor cell migration after cortical ischemia in mice. Stroke 42:3559–3565. doi: 10.1161/STROKEAHA.111.627802

Paez-Gonzalez P, Abdi K, Luciano D, et al (2011) Ank3-Dependent SVZ Niche Assembly Is Required for the Continued Production of New Neurons. Neuron 71:61–75. doi: 10.1016/j.neuron.2011.05.029

Palmer TD, Takahashi J, Gage FH (1997) The adult rat hippocampus contains primordial neural stem cells. Mol Cell Neurosci 8:389–404. doi: 10.1006/mcne.1996.0595

Palmer TD, Willhoite AR, Gage FH (2000) Vascular niche for adult hippocampal neurogenesis. J Comp Neurol 425:479–494. doi: 10.1002/1096-9861(20001002)425:4<479::AID-CNE2>3.0.CO;2-3

Parent JM, Vexler ZS, Gong C, et al (2002) Rat forebrain neurogenesis and striatal neuron replacement after focal stroke. Ann Neurol 52:802–13. doi: 10.1002/ana.10393

Park J, Park H-H, Choi H, et al (2012) Coenzyme Q10 protects neural stem cells against hypoxia by enhancing survival signals. Brain Res 1478:64–73. doi: 10.1016/j.brainres.2012.08.025

Pearson BJ, Doe CQ (2004) Specification of temporal identity in the developing nervous system. Annu Rev Cell Dev Biol 20:619–647. doi: 10.1146/annurev.cellbio.19.111301.115142

Petricevic J, Forempoher G, Ostojic L, et al (2011) Expression of nestin, mesothelin and epithelial membrane antigen (EMA) in developing and adult human meninges and meningiomas. Acta Histochem 113:703–11. doi: 10.1016/j.acthis.2010.09.005

Piao M-S, Lee J-K, Park C-S, et al (2009) Early activation of matrix metalloproteinase-9 is associated with blood–brain barrier disruption after photothrombotic cerebral ischemia in rats. Acta Neurochir (Wien) 151:1649–1653. doi: 10.1007/s00701-009-0431-1

Plane JM, Andjelkovic A V, Keep RF, Parent JM (2010) Intact and injured endothelial cells differentially modulate postnatal murine forebrain neural stem cells. Neurobiol Dis 37:218–227. doi: 10.1016/j.nbd.2009.10.008

Pluchino S, Quattrini A, Brambilla E, et al (2003) Injection of adult neurospheres induces recovery in a chronic model of multiple sclerosis. Nature 422:688–94. doi: 10.1038/nature01552

Ponomarev ED, Maresz K, Tan Y, Dittel BN (2007) CNS-derived interleukin-4 is essential for the regulation of autoimmune inflammation and induces a state of alternative activation in microglial cells. J Neurosci 27:10714–21. doi: 10.1523/JNEUROSCI.1922-07.2007

Ponomarev ED, Veremeyko T, Barteneva N, et al (2011) MicroRNA-124 promotes microglia quiescence and suppresses EAE by deactivating macrophages via the C/EBP-α–PU.1 pathway. Nat Med 17:64–70. doi: 10.1038/nm.2266

Ponomarev ED, Veremeyko T, Weiner HL (2013) MicroRNAs are universal regulators of differentiation, activation, and polarization of microglia and macrophages in normal and diseased CNS. Glia 61:91–103. doi: 10.1002/glia.22363

Ponti G, Obernier K, Alvarez-Buylla A (2013) Lineage progression from stem cells to new neurons in the adult brain

REFERENCES

ventricular-subventricular zone. Cell Cycle 12:1649–1650. doi: 10.4161/cc.24984

Qiu S, Feng Y, LeSage G, et al (2015) Chronic Morphine-Induced MicroRNA-124 Promotes Microglial Immunosuppression by Modulating P65 and TRAF6. J Immunol 194:1021–1030. doi: 10.4049/jimmunol.1400106

Quiñones-Hinojosa A, Sanai N, Soriano-Navarro M, et al (2006) Cellular composition and cytoarchitecture of the adult human subventricular zone: A niche of neural stem cells. J Comp Neurol 494:415–434. doi: 10.1002/cne.20798

Rainer TH, Leung LY, Chan CPY, et al (2016) Plasma miR-124-3p and miR-16 concentrations as prognostic markers in acute stroke. Clin Biochem 49:663–668. doi: 10.1016/j.clinbiochem.2016.02.016

Ramalingam P, Palanichamy JK, Singh A, et al (2014) Biogenesis of intronic miRNAs located in clusters by independent transcription and alternative splicing. RNA 20:76–87. doi: 10.1261/rna.041814.113

Ramon y Cajal S (1913) Estudios sobre la degeneración y regeneración del sistema nervioso. In: Madrid, Moya.

Reale M, Iarlori C, Thomas A, et al (2009) Peripheral cytokines profile in Parkinson's disease. Brain Behav Immun 23:55–63. doi: 10.1016/j.bbi.2008.07.003

Revest J-M, Dupret D, Koehl M, et al (2009) Adult hippocampal neurogenesis is involved in anxiety-related behaviors. Mol Psychiatry 14:959–967. doi: 10.1038/mp.2009.15

Reynolds B, Weiss S (1992) Generation of neurons and astrocytes from isolated cells of the adult mammalian central nervous system. Science (80-) 255:1707–1710. doi: 10.1126/science.1553558

Rodriguez A, Griffiths-Jones S, Ashurst JL, Bradley A (2004) Identification of mammalian microRNA host genes and transcription units. Genome Res 14:1902–10. doi: 10.1101/gr.2722704

Ruiz-Cabello J, Barnett BP, Bottomley PA, Bulte JWM (2011) Fluorine (19F) MRS and MRI in biomedicine. NMR Biomed 24:114–29. doi: 10.1002/nbm.1570

Ruscher K, Johannesson E, Brugiere E, et al (2009) Enriched environment reduces apolipoprotein E (ApoE) in reactive astrocytes and attenuates inflammation of the peri-infarct tissue after experimental stroke. J Cereb Blood Flow Metab 29:1796–805. doi: 10.1038/jcbfm.2009.96

Ruscher K, Kuric E, Liu Y, et al (2013) Inhibition of CXCL12 signaling attenuates the postischemic immune response and improves functional recovery after stroke. J Cereb Blood Flow Metab 33:1225–34. doi: 10.1038/jcbfm.2013.71

Sanai N, Nguyen T, Ihrie RA, et al (2011) Corridors of Migrating Neurons in the Human Brain and Their Decline During Infancy. Nature 478:382–386. doi: 10.1038/nature10487

Sanai N, Tramontin AD, Quiñones-Hinojosa A, et al (2004) Unique astrocyte ribbon in adult human brain contains neural stem cells but lacks chain migration. Nature 427:740–4. doi: 10.1038/nature02301

Santos T, Ferreira R, Maia J, et al (2012a) Polymeric nanoparticles to control the differentiation of neural stem cells in the subventricular zone of the brain. ACS Nano 6:10463–74. doi: 10.1021/nn304541h

Santos T, Maia J, Agasse F, et al (2012b) Nanomedicine boosts neurogenesis: new strategies for brain repair. Integr Biol 4:973–981. doi: 10.1039/c2ib20129a

Sanuki R, Onishi A, Koike C, et al (2011) miR-124a is required for hippocampal axogenesis and retinal cone survival through Lhx2 suppression. Nat Neurosci 14:1125–34. doi: 10.1038/nn.2897

Saraiva C, Praça C, Ferreira R, et al (2016) Nanoparticle-mediated brain drug delivery: Overcoming blood–brain barrier to treat neurodegenerative diseases. J Control Release 235:34–47. doi: 10.1016/j.jconrel.2016.05.044

Schaeublin NM, Braydich-Stolle LK, Schrand AM, et al (2011) Surface charge of gold nanoparticles mediates mechanism of toxicity. Nanoscale 3:410. doi: 10.1039/c0nr00478b

Schapira AH V (2009) Neurobiology and treatment of Parkinson's disease. Trends Pharmacol Sci 30:41–7. doi: 10.1016/j.tips.2008.10.005

Schmidt-Hieber C, Jonas P, Bischofberger J (2004) Enhanced synaptic plasticity in newly generated granule cells of the adult hippocampus. Nature 429:184–187. doi: 10.1038/nature02553

Seri B, García-Verdugo JM, McEwen BS, Alvarez-Buylla A (2001) Astrocytes Give Rise to New Neurons in the Adult Mammalian Hippocampus. J Neurosci 21:7158–7160.

Shilo M, Motiei M, Hana P, Popovtzer R (2014) Transport of nanoparticles through the blood-brain barrier for imaging and therapeutic applications. Nanoscale 6:2146–52. doi: 10.1039/c3nr04878k

Shors TJ, Miesegaes G, Beylin A, et al (2001) Neurogenesis in the adult is involved in the formation of trace memories. Nature 410:372–376. doi: 10.1038/35066584

Simats A, Garcia-Berrocoso T, Montaner J (2016) Natalizumab: a new therapy for acute ischemic stroke? Expert Rev Neurother 16:1013–1021. doi: 10.1080/14737175.2016.1219252

Sohel MH (2016) Extracellular/Circulating MicroRNAs: Release Mechanisms, Functions and Challenges. Achiev Life Sci 10:175–186. doi: 10.1016/j.als.2016.11.007

Sonavane G, Tomoda K, Makino K (2008) Biodistribution of colloidal gold nanoparticles after intravenous administration: effect of particle size. Colloids Surf B Biointerfaces 66:274–280. doi:

10.1016/j.colsurfb.2008.07.004

Sonntag K-C (2010) MicroRNAs and deregulated gene expression networks in neurodegeneration. Brain Res 1338:48–57. doi: 10.1016/j.brainres.2010.03.106

Spalding KLL, Bergmann O, Alkass K, et al (2013) Dynamics of hippocampal neurogenesis in adult humans. Cell 153:1219–1227. doi: 10.1016/j.cell.2013.05.002

Spillantini MG, Schmidt ML, Lee VM-Y, et al (1997) Alpha-synuclein in Lewy bodies. Nature 388:839–40. doi: 10.1038/42166

Stellwagen D, Malenka RC (2006) Synaptic scaling mediated by glial TNF-α. Nature 440:1054–1059. doi: 10.1038/nature04671

Stolt CC, Lommes P, Sock E, et al (2003) The Sox9 transcription factor determines glial fate choice in the developing spinal cord. Genes Dev 17:1677–89. doi: 10.1101/gad.259003

Sui Y, Horne MK, Stanić D (2012) Reduced proliferation in the adult mouse subventricular zone increases survival of olfactory bulb interneurons. PLoS One 7:e31549. doi: 10.1371/journal.pone.0031549

Sullivan R, Duncan K, Dailey T, et al (2015) A possible new focus for stroke treatment - migrating stem cells. Expert Opin Biol Ther 15:949–958. doi: 10.1517/14712598.2015.1043264

Sun GJ, Zhou Y, Stadel RP, et al (2015a) Tangential migration of neuronal precursors of glutamatergic neurons in the adult mammalian brain. Proc Natl Acad Sci 112:9484–9489. doi: 10.1073/pnas.1508545112

Sun Y, Gui H, Li Q, et al (2013a) MicroRNA-124 protects neurons against apoptosis in cerebral ischemic stroke. CNS Neurosci Ther 19:813–9. doi: 10.1111/cns.12142

Sun Y, Li Q, Gui H, et al (2013b) MicroRNA-124 mediates the cholinergic anti-inflammatory action through inhibiting the production of pro-inflammatory cytokines. Cell Res 23:1270–1283. doi: 10.1038/cr.2013.116

Sun Y, Luo Z-M, Guo X-M, et al (2015b) An updated role of microRNA-124 in central nervous system disorders: a review. Front Cell Neurosci 9:1–8. doi: 10.3389/fncel.2015.00193

Sun Y, Qin Z, Li Q, et al (2016) MicroRNA-124 negatively regulates LPS-induced TNF-α production in mouse macrophages by decreasing protein stability. Acta Pharmacol Sin 37:889–97. doi: 10.1038/aps.2016.16

Taupin P (2007) BrdU immunohistochemistry for studying adult neurogenesis: paradigms, pitfalls, limitations, and validation. Brain Res Rev 53:198–214. doi: 10.1016/j.brainresrev.2006.08.002

Tennant KA, Adkins DL, Donlan NA, et al (2011) The organization of the forelimb representation of the C57BL/6 mouse motor cortex as defined by intracortical microstimulation and cytoarchitecture. Cereb Cortex 21:865–876. doi: 10.1093/cercor/bhq159

Thored P, Arvidsson A, Cacci E, et al (2006) Persistent production of neurons from adult brain stem cells during recovery after stroke. Stem Cells 24:739–47. doi: 10.1634/stemcells.2005-0281

Towler BP, Jones CI, Newbury SF (2015) Mechanisms of regulation of mature miRNAs. Biochem Soc Trans 43:1208–14. doi: 10.1042/BST20150157

Ungerstedt U, Arbuthnott GW (1970) Quantitative recording of rotational behavior in rats after 6-hydroxy-dopamine lesions of the nigrostriatal dopamine system. Brain Res 24:485–493. doi: 10.1016/0006-8993(70)90187-3

Valdmanis PN, Gu S, Schuermann N, et al (2012) Expression determinants of mammalian argonaute proteins in mediating gene silencing. Nucleic Acids Res 40:3704–3713. doi: 10.1093/nar/gkr1274

van den Berge S a, van Strien ME, Hol EM (2013) Resident adult neural stem cells in Parkinson′s disease—The brain′s own repair system? Eur J Pharmacol 719:117–127. doi: 10.1016/j.ejphar.2013.04.058

van den Berge SA, Middeldorp J, Zhang CE, et al (2010) Longterm quiescent cells in the aged human subventricular neurogenic system specifically express GFAP-δ. Aging Cell 9:313–326. doi: 10.1111/j.1474-9726.2010.00556.x

van den Berge SA, van Strien ME, Korecka JA, et al (2011) The proliferative capacity of the subventricular zone is maintained in the parkinsonian brain. Brain 134:3249–3263. doi: 10.1093/brain/awr256

van der Maten G, Henck V, Wieloch T, Ruscher K (2017) CX3C chemokine receptor 1 deficiency modulates microglia morphology but does not affect lesion size and short-term deficits after experimental stroke. BMC Neurosci 18:11. doi: 10.1186/s12868-016-0325-0

Varfolomeev EE, Ashkenazi A (2004) Tumor Necrosis Factor. Cell 116:491–497. doi: 10.1016/S0092-8674(04)00166-7

Veremeyko T, Siddiqui S, Sotnikov I, et al (2013) IL-4/IL-13-dependent and independent expression of miR-124 and its contribution to M2 phenotype of monocytic cells in normal conditions and during allergic inflammation. PLoS One 8:e81774. doi: 10.1371/journal.pone.0081774

Virgone-Carlotta A, Uhlrich J, Akram MN, et al (2013) Mapping and kinetics of microglia/neuron cell-to-cell contacts in the 6-OHDA murine model of Parkinson's disease. Glia 61:1645–1658. doi: 10.1002/glia.22546

Visvanathan J, Lee S, Lee B, et al (2007) The microRNA miR-124 antagonizes the anti-neural REST/SCP1 pathway during embryonic CNS development. Genes Dev 21:744–9. doi: 10.1101/gad.1519107

Wahid F, Khan T, Kim YY (2014) MicroRNA and diseases: Therapeutic potential as new generation of drugs.

REFERENCES

Biochimie 104:12–26. doi: 10.1016/j.biochi.2014.05.004

Walker TL, White A, Black DM, et al (2008) Latent stem and progenitor cells in the hippocampus are activated by neural excitation. J Neurosci 28:5240–7. doi: 10.1523/JNEUROSCI.0344-08.2008

Walkey CD, Olsen JB, Guo H, et al (2012) Nanoparticle size and surface chemistry determine serum protein adsorption and macrophage uptake. J Am Chem Soc 134:2139–2147. doi: 10.1021/ja2084338

Walter HL, van der Maten G, Antunes AR, et al (2015) Treatment with AMD3100 attenuates the microglial response and improves outcome after experimental stroke. J Neuroinflammation 12:24. doi: 10.1186/s12974-014-0232-1

Wang D, Zhang Z, O'Loughlin E, et al (2012a) Quantitative functions of Argonaute proteins in mammalian development. Genes Dev 26:693–704. doi: 10.1101/gad.182758.111

Wang H, Ye Y, Zhu Z, et al (2015a) MiR-124 Regulates Apoptosis and Autophagy Process in MPTP Model of Parkinson's Disease by Targeting to Bim. Brain Pathol. doi: 10.1111/bpa.12267

Wang Q, Yang L, Wang Y (2015b) Enhanced differentiation of neural stem cells to neurons and promotion of neurite outgrowth by oxygen–glucose deprivation. Int J Dev Neurosci 43:50–57. doi: 10.1016/j.ijdevneu.2015.04.009

Wang S, Okun MS, Suslov O, et al (2012b) Neurogenic potential of progenitor cells isolated from postmortem human Parkinsonian brains. Brain Res 1464:61–72. doi: 10.1016/j.brainres.2012.04.039

Wang X (2014) Composition of seed sequence is a major determinant of microRNA targeting patterns. Bioinformatics 30:1377–1383. doi: 10.1093/bioinformatics/btu045

Wang Z (2009) miRNA Mimic Technology. In: MicroRNA Interference Technologies. Springer Berlin Heidelberg, Berlin, Heidelberg, pp 93–100. doi: 10.1007/978-3-642-00489-6_4

Weng H, Shen C, Hirokawa G, et al (2011) Plasma miR-124 as a biomarker for cerebral infarction. Biomed Res 32:135–141. doi: 10.2220/biomedres.32.135

Weston C (2002) The JNK signal transduction pathway. Curr Opin Genet Dev 12:14–21. doi: 10.1016/S0959-437X(01)00258-1

Wiley DT, Webster P, Gale A, Davis ME (2013) Transcytosis and brain uptake of transferrin-containing nanoparticles by tuning avidity to transferrin receptor. Proc Natl Acad Sci U S A 110:8662–8667. doi: 10.1073/pnas.1307152110

Wilson RC, Tambe A, Kidwell MA, et al (2015) Dicer-TRBP Complex Formation Ensures Accurate Mammalian MicroRNA Biogenesis. Mol Cell 57:397–407. doi: 10.1016/j.molcel.2014.11.030

Winner B, Desplats P, Hagl C, et al (2009) Dopamine receptor activation promotes adult neurogenesis in an acute Parkinson model. Exp Neurol 219:543–52. doi: 10.1016/j.expneurol.2009.07.013

Winner B, Geyer M, Couillard-Despres S, et al (2006) Striatal deafferentation increases dopaminergic neurogenesis in the adult olfactory bulb. Exp Neurol 197:113–21. doi: 10.1016/j.expneurol.2005.08.028

Witwer KW, Halushka MK (2016) Toward the promise of microRNAs – Enhancing reproducibility and rigor in microRNA research. RNA Biol 13:1103–1116. doi: 10.1080/15476286.2016.1236172

Wojtowicz JM, Kee N (2006) BrdU assay for neurogenesis in rodents. Nat Protoc 1:1399–1405. doi: 10.1038/nprot.2006.224

Wu J, Xie X (2006) Comparative sequence analysis reveals an intricate network among REST, CREB and miRNA in mediating neuronal gene expression. Genome Biol 7:R85. doi: 10.1186/gb-2006-7-9-r85

Xie J, Lee S, Chen X (2010) Nanoparticle-based theranostic agents. Adv Drug Deliv Rev 62:1064–79. doi: 10.1016/j.addr.2010.07.009

Xu P, Yoshioka K, Yoshimura D, et al (2003) In vitro development of mouse embryonic stem cells lacking JNK/stress-activated protein kinase-associated protein 1 (JSAP1) scaffold protein revealed its requirement during early embryonic neurogenesis. J Biol Chem 278:48422–33. doi: 10.1074/jbc.M307888200

Xue Y, Ouyang K, Huang J, et al (2013) Direct conversion of fibroblasts to neurons by reprogramming PTB-regulated microRNA circuits. Cell 152:82–96. doi: 10.1016/j.cell.2012.11.045

Yamashita T, Ninomiya M, Hernandez Acosta P, et al (2006) Subventricular Zone-Derived Neuroblasts Migrate and Differentiate into Mature Neurons in the Post-Stroke Adult Striatum. J Neurosci 26:6627–6636. doi: 10.1523/JNEUROSCI.0149-06.2006

Yekta S, Shih I-H, Bartel DP (2004) MicroRNA-directed cleavage of HOXB8 mRNA. Science 304:594–6. doi: 10.1126/science.1097434

Yemisci M, Caban S, Gursoy-Ozdemir Y, et al (2015) Systemically administered brain-targeted nanoparticles transport peptides across the blood-brain barrier and provide neuroprotection. J Cereb Blood Flow Metab 35:469–75. doi: 10.1038/jcbfm.2014.220

Yi R, Qin Y, Macara IG, Cullen BR (2003) Exportin-5 mediates the nuclear export of pre-microRNAs and short hairpin RNAs. Genes Dev 17:3011–6. doi: 10.1101/gad.1158803

Yoo AS, Staahl BT, Chen L, Crabtree GR (2009) MicroRNA-mediated switching of chromatin-remodelling complexes in neural development. Nature 460:642–6. doi: 10.1038/nature08139

Yoo AS, Sun AX, Li L, et al (2011) MicroRNA-mediated conversion of human fibroblasts to neurons. Nature 476:228–31. doi: 10.1038/nature10323

Yoshida H, Hastie CJ, McLauchlan H, et al (2004) Phosphorylation of microtubule-associated protein tau by isoforms of c-Jun N-terminal kinase (JNK). J Neurochem 90:352–8. doi: 10.1111/j.1471-4159.2004.02479.x

Yu J, Chung K, Deo M, et al (2008) MicroRNA miR-124 regulates neurite outgrowth during neuronal differentiation. Exp Cell Res 314:2618–2633. doi: 10.1016/j.yexcr.2008.06.002

Yu YJ, Zhang Y, Kenrick M, et al (2011) Boosting brain uptake of a therapeutic antibody by reducing its affinity for a transcytosis target. Sci Transl Med 3:84ra44. doi: 10.1126/scitranslmed.3002230

Zeng L, He X, Wang Y, et al (2014) MicroRNA-210 overexpression induces angiogenesis and neurogenesis in the normal adult mouse brain. Gene Ther 21:37–43. doi: 10.1038/gt.2013.55

Zeng Y, Cullen BR (2005) Efficient Processing of Primary microRNA Hairpins by Drosha Requires Flanking Nonstructured RNA Sequences. J Biol Chem 280:27595–27603. doi: 10.1074/jbc.M504714200

Zhang L, Deng J, Pan Q, et al (2016a) Targeted methylation sequencing reveals dysregulated Wnt signaling in Parkinson disease. J Genet Genomics 43:587–592. doi: 10.1016/j.jgg.2016.05.002

Zhang R, Zhang Z, Chopp M (2016b) Function of neural stem cells in ischemic brain repair processes. J Cereb Blood Flow Metab 36:2034–2043. doi: 10.1177/0271678X16674487

Zhang T-T, Li W, Meng G, et al (2016c) Strategies for transporting nanoparticles across the blood-brain barrier. Biomater Sci 4:219–29. doi: 10.1039/c5bm00383k

Zhao C, Deng W, Gage FH (2008) Mechanisms and functional implications of adult neurogenesis. Cell 132:645–60. doi: 10.1016/j.cell.2008.01.033

Zhao C, Sun G, Li S, et al (2010) MicroRNA let-7b regulates neural stem cell proliferation and differentiation by targeting nuclear receptor TLX signaling. Proc Natl Acad Sci U S A 107:1876–81. doi: 10.1073/pnas.0908750107

Zhou Q-H, Fu A, Boado RJ, et al (2011) Receptor-mediated abeta amyloid antibody targeting to Alzheimer's disease mouse brain. Mol Pharm 8:280–5. doi: 10.1021/mp1003515

Zhu F, Liu J-L, Li J-P, et al (2014) MicroRNA-124 (miR-124) Regulates Ku70 Expression and is Correlated with Neuronal Death Induced by Ischemia/Reperfusion. J Mol Neurosci 52:148–155. doi: 10.1007/s12031-013-0155-9